DOKUZ EYLÜL UNIVERSITY

GRADUATE SCHOOL OF NATURAL AND APPLIED SCIENCES

INVESTIGATION OF ARSENIC ADSORPTION PERFORMANCE OF THE MODIFIED NATURAL MATERIALS

by

Sedef ARIKAN

September, 2016

İZMİR

INVESTIGATION OF ARSENIC ADSORPTION PERFORMANCE OF THE MODIFIED NATURAL MATERIALS

A Thesis Submitted to the
Graduate School of Natural and Applied Sciences of Dokuz Eylül University
In Partial Fulfillment of the Requirements for the Degree of Doctor of Philosophy in Environmental Engineering, Environmental Engineering Program

by
Sedef ARIKAN

September, 2016
İZMİR

Ph.D. THESIS EXAMINATION RESULT FORM

We have read the thesis entitled **"INVESTIGATION OF ARSENIC ADSORPTION PERFORMANCE OF THE MODIFIED NATURAL MATERIALS"** completed by **SEDEF ARIKAN** under supervision of **PROF. DR. DENİZ DÖLGEN** and we certify that in our opinion it is fully adequate, in scope and in quality, as a thesis for the degree of Doctor of Philosophy.

Prof. Dr. Deniz DÖLGEN

Supervisor

Prof. Dr. Mehmet Necdet ALPASLAN	Prof. Dr. Ali Aydın GÖKTAŞ
Thesis Committee Member	Thesis Committee Member
Prof. Dr. Alper BABA	Doc. Dr. N. Altınay PERENDECİ
Examining Committee Member	Examining Committee Member

Prof.Dr. Ayşe OKUR
Director
Graduate School of Natural and Applied Sciences

ACKNOWLEDGEMENTS

I would like to express my deepest gratitude to my thesis advisor, Prof. Dr. Deniz DÖLGEN, for her academic supervision, supports and encouragement throughout my PhD study.

I am deeply grateful to my thesis committee members, Prof. Dr. Mehmet Necdet ALPASLAN and Prof. Dr. Ali Aydın GÖKTAŞ, for their guidance, suggestions and valuable comments.

I would like to acknowledge Dokuz Eylül University Environmental Engineering Department in order to give the opportunity for laboratory use. I would like to thank İZSU and Duman Madencilik for providing materials I used in experimental studies.

This thesis study was funded by Dokuz Eylül University, Scientific Research Project Program (Project no: BAP 2013KBFEN030). I would like to acknowledge Dokuz Eylül University for this financial support.

Sedef ARIKAN

INVESTIGATION OF ARSENIC ADSORPTION PERFORMANCE OF THE MODIFIED NATURAL MATERIALS

ABSTRACT

In this study, arsenic adsorption capacities of modified sand and modified sepiolite were investigated. Modification process was accomplished by mixing materials in iron solution and then drying. Surface morphologies and elemental analysis were done by scanning electron microscope (SEM) and energy dispersive X-ray spectroscopy (EDX) for both raw and modified materials to evaluate effect of modification. Pore volume and surface area of materials were analyzed by Brauner-Emmer-Teller method (BET) and phase compositions were determined by X-ray diffraction (XRD). Batch experiments were performed to determine adsorption parameters (pH, contact time, adsorbent dose, initial concentration, particle size and competing anions). Results showed that iron was successfully impregnated onto surface of materials. Adsorption mechanisms were described by Freundlich isotherm for modified sand and Langmuir isotherm for modified sepiolite. Adsorption kinetics followed pseudo second order reaction kinetics. In order to determine design parameters of modified materials, column studies were performed and kinetic models were applied. Column studies were performed as a function of bed height, initial concentration and flow rate. The study showed that modified sepiolite would be a more effective material compared to modified sand to remove arsenic from solution. Regeneration studies and reuse potential of materials were evaluated. Modified sand column was regenerated and used efficiently after the first regeneration. However, regeneration of modified sepiolite caused clogging of the column due to destruction of media. The results revealed that, modified sand of and modified sepiolite are effective and cost efficient materials especially for rural areas to remove arsenic from water by adsorption.

Keywords: Arsenic, adsorption, modified materials

MODİFİYE EDİLMİŞ DOĞAL MALZEMELERİN ARSENİK ADSORPSİYON VERİMİNİN ARAŞTIRILMASI

ÖZ

Bu çalışmada, modifiye kum ve modifiye sepiyolit malzemelerinin arsenik adsorpsiyon kapasiteleri araştırılmıştır. Modifikasyon prosesi malzemelerin demir çözeltisi ile karıştırılması ve ardından fırında kurutulması ile gerçekleştirilmiştir. Modifikasyonun etkisini inceleyebilmek için ham ve modifiye malzemelerin yüzey morfolojileri ve elementel analizleri taramalı elektron mikroskobu ve enerji dağılımlı X ışını spektroskopisi (EDX) ile yapılmıştır. Malzemelerin boşluk hacmi ve yüzey alanları Brauner-Emmer-Teller (BET) metodu ile ve faz bileşimleri X ışını dağılım (XRD) cihazı ile belirlenmiştir. Kesikli deneylerle önemli adsorpsiyon parametrelerinden olan pH, temas süresi, adsorban dozu, başlangıç arsenik konsantrasyonu, partikül büyüklüğü ve yarışan anyonların etkisi araştırılmıştır. Sonuçlar demirin başarılı bir şekilde kum ve sepiyolit üzerine tutunduğunu göstermiştir. Adsorpsiyon mekanizması modifiye kum için Freundlich izotermi ve modifiye sepiyolit için Langmuir izotermi ile uyumlu olarak açıklanmıştır. Adsorpsiyon kinetikleri yalancı ikinci derece reaksiyon modeline uymuştur. Modifiye malzemelerin tasarım parametrelerini belirleyebilmek için kolon çalışmaları yapılmış ve kinetik modeller uygulanmıştır. Kolon çalışmaları yatak derinliği, giriş konsantrasyonu ve debiye bağlı olarak gerçekleştirilmiştir. Sonuçlar modifiye kum ile karşılaştırıldığında, arsenik giderimi bakımından, modifiye sepiyolitin daha verimli olduğunu göstermiştir. Kolonların rejenerasyonu ve ardından yeniden kullanım potansiyeli değerlendirilmiştir. Modifiye kum kolonu rejenere edilebilmiş ve ilk rejenerasyondan sonra tekrar etkin olarak kullanılabilmiştir. Modifiye sepiyolitin rejenerasyonu materyalin yapısının bozulması sonucu kolonun tıkanmasına neden olmuştur. Sonuçlar, modifiye kum ve sepiyolitin özelllikle kırsal kesimler için adsorpsiyon ile sudan arseniği gidermede etkili ve düşük maliyetli malzemeler olduğunu ortaya koymuştur.

Anahtar kelimeler: Arsenik, adsorpsiyon, modifiye malzemeler

CONTENTS

Pages

LIST OF FIGURES

Pages

LIST OF TABLES

Pages

CHAPTER ONE
INTRODUCTION

1.1 The Problem Statement

Arsenic contamination in drinking water is a worldwide problem in recent years. Arsenic is a heavy metal and can cause toxic effects and even be fatal depending on its dose and exposure time. Because of the proven and widespread negative health impacts on humans, in 1993, the World Health Organization (WHO) reduced the health-based provisional guideline for arsenic concentration in drinking water from 50 to 10 µg/L. Naturally-occurring and human-induced arsenic pollution in drinking water has also been discovered in many places in Turkey. Therefore, control of elevated arsenic concentrations in water sources has become a major concern. Particularly, western parts of central Anatolia (e.g. Kütahya, Emet, Simav, Uşak, Balıkesir, İzmir) have high risk due to their geological and geothermal properties which pose suitable conditions for arsenic contamination of water resources (Baba & Sozbilir, 2012).

In literature, there are several arsenic treatment methods, e.g. coagulation/filtration, oxidation/filtration, ion exchange, adsorption and membrane process. Effectiveness of these methods depend on quantity of water, concentration and form of arsenic (As(III)/As(V)) in water and the other parameters such as pH, organic matter and existing ions in water. Among the methods, adsorption is emerged as efficient and a cost effective technique if the adsorbent is cheap and easily accessible.

In Turkey, arsenic contaminated groundwater is the only viable source of drinking water in many villages, and thus has to be treated. Most of them are rural and small scale remote villages; therefore both economic considerations and labor requirements are important in appropriate technology selection. Wellhead treatment systems are proposed as a typical solution for these areas; and filtration or adsorption processes are often used as treatment methods. Adsorption is a clean technology with low/no sludge production. The most important problem is the availability of the appropriate adsorbent material. Because, imported patented adsorbent materials have been used in those systems and resulted with high operational costs. However, adsorption process would be high efficient, easily operated and low cost treatment alternative for arsenic removal if these adsorbent materials can be produced with own sources.

1.2 Objectives and Scope of This Study

There are a lot of imported commercial product (G2, SMI III, GFH, etc.) but they are costly and foreign depended. The principal aim of this study is to develop efficient and economically competitive adsorbent for arsenic removal by using puzzolonic materials available in Turkey. In this framework, sand and sepiolite which are abundant natural materials in Turkey were utilized.

Improvement of adsorptive characteristics of these materials was other purpose of the study and thus materials were modified by iron coating process to improve their adsorption capacity. Characterization of these materials was done for both raw and coated materials in order to compare and analyze the effect of coating.

Exploring the optimal operational parameters and adsorption capacity of the materials was also aimed in this study. Batch studies were performed by using both modified sand and modified sepiolite and two different commercial products (I1and I2) to investigate and compare adsorption mechanism.

In order to design of a column, performance of fixed bed columns packed with modified sand and modified sepiolite were investigated for arsenic removal. The lab scale column experiments were provided important parameters such as column breakthrough curves, that is useful for the determination of the life span of the adsorbent.

Finally, in many cases, spent adsorbents are considered as hazardous waste; hence regeneration is an important issue for adsorption practices. Therefore, regeneration and reuse capacity of modified sand and modified sepiolite were also investigated in this study.

1.3 Thesis Structure

This thesis consists of six chapters; i.e. Introduction, Arsenic Pollution and Treatment Methods, Adsorption of Arsenic Compounds, Material & Methods, Results & Discussions, and Conclusions parts.

In the first chapter, i.e. introduction part, problem statement was defined and objectives of the study were explained.

In the next step, i.e. chapter two, literature of arsenic pollution focusing to properties and sources of arsenic compounds, and health impacts were reviewed. Treatment methods for arsenic removal were classified as conventional and well-head methods and explained briefly considering their advantages and disadvantages.

Since adsorption process was specifically studied as a typical treatment alternative for well head systems, detailed explanations were presented in chapter three. Mechanism of adsorption was discussed via isotherm and kinetic studies. Adsorbents used for arsenic treatment were surveyed from literature, and a table containing the information on the adsorbents and coating methods derived from various studies in literature was introduced.

Materials and methods used in this thesis were explained in chapter four. Reagents, preparation of modified materials as an adsorbent, characterization of these materials, arsenic measurement and batch and column studies were explained in detail. Experimental study containing information regarding to experimental procedure and parameters investigated in the study were explained in this section.

Experimental outcomes were discussed in chapter five, i.e. Results and discussion part. Here, data regarding to material characterization were presented to explain the treatment mechanisms. Results from batch studies were given, and isotherms and kinetics were evaluated. Later on, column studies were explained. The effects of various factors such as bed depth, initial arsenic concentration and flow rate were illustrated separately. Data derived from those studies were processed to form breakthrough curve. Finally, mathematical models, such as Bohart-Adams and Thomas models, were applied to the experimental data to simulate breakthrough curves.

In the last chapter, i.e. chapter six, findings of the study were summarized together with the recommendations for further researches.

CHAPTER TWO
ARSENIC POLLUTION AND TREATMENT METHODS

2.1 Arsenic in Water: Sources and Speciation

Arsenic is released to the aquatic environment from both natural and man-made sources. Naturally, arsenic in water is caused by the weathering and dissolution of arsenic-bearing rocks, volcanic actions, geothermal activities, forest fire, etc. Mining, smelting of non-ferrous metals, glass manufacturing, cement manufacturing, and coal-fired power plants are major industrial processes that contribute to anthropogenic (man-made) arsenic contamination in water, soil and air. The contribution of agriculture is due to the use of arsenic compounds as pesticides, herbicides, and wood preservatives (ATSDR, 2007).

Arsenic bonds with various elements such as oxygen, sulfur, and chlorine to form inorganic arsenic compounds and with carbon and hydrogen to form organic arsenic compounds (World Bank Group, 1998). Arsenobetaine, arsenocholine, tetramethylarsonium salts, arsenosugars and arsenic-containing lipids are typical organic arsenic compounds and mainly found in terrestrial species as well as marine organisms. Hence, organic arsenic species are abundant in seafood, but they are less harmful to health, and are readily eliminated by the body.

Inorganic arsenic compounds are mainly of geological origin and is generally more toxic than organic arsenic. Inorganic arsenic can occur in the environment in four valency states: –3 (arsin), 0 (arsenic), +3 (arsenite) and +5 (arsenate); however in natural waters, trivalent arsenite (As^{+3}) or pentavalent arsenate (As^{+5}) forms are most dominant forms. Arsenic acid (H_3AsO_4, $H_2AsO_4^-$, $HAsO_4^{2-}$), arsenious acids (H_3AsO_3,$H_2AsO_3^-$,$HAsO_3^{2-}$), arsenic trioxide (As_2O_3), arsenic pentoxide (As_2O_5), Arsenic sulfide (As_2S_3) are typical inorganic arsenic compounds (IARC, n.d.).

Elemental arsenic is produced by reduction of arsenic trioxide (As_2O_3) with charcoal. As_2O_3 is produced as a by-product of metal smelting operations. It has been estimated that 70% of the world arsenic production is used in timber treatment as copper chrome arsenate (CCA), 22% in agricultural chemicals, and the remainder in glass, pharmaceuticals and non-ferrous alloys (WHO, 2001).

The valency and species of inorganic arsenic are dependent on both redox conditions and pH of the water (Thakur et al., 2011). In general, arsenite is normally found in groundwater under reducing conditions (<200 mV)(WHO, 2011) and in five forms: $H_4AsO_3^+$, H_3AsO_3, $H_2AsO_3^-$, $HAsO_3^{2-}$, and AsO_3^{3-} (Feenstra et al., 2007). Similarly, under oxidizing conditions, arsenate compounds are expected to be dominant in water. As(V) exists in four forms in aqueous solution based on pH, i.e. H_3AsO_4, $H_2AsO_4^-$, $HAsO_4^{2-}$; and AsO_4^{3-}.

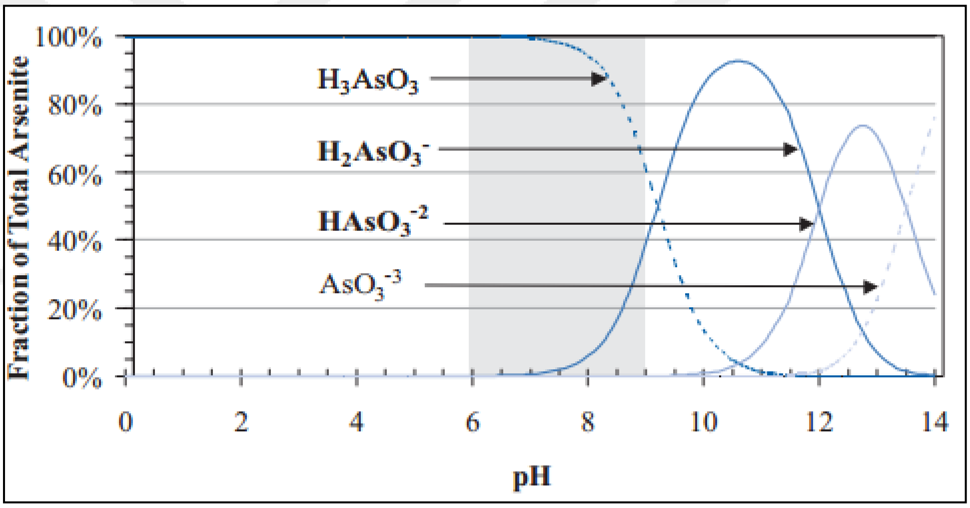

Figure 2.1 Dissociation of arsenite [As(III)](EPA, 2003)

The pH dependencies of arsenite and arsenate are depicted in Figure 2.1 and Figure 2.2, respectively. In case of oxygenated waters, arsenic acid predominates only at extremely low pH (< 2). In the pH range of 2 to 11, it is in the form of $H_2AsO_4^-$ and $HAsO_4^{2-}$. In slightly reduced conditions and low pH values, arsenious acid converted to $H_2AsO_3^-$ as the pH increases. When the pH exceeds 12, $HAsO_3^{2-}$ does appear. The ionic forms of As(V) dominate at pH >3, and As(III) is neutral at pH <9 and ionic at pH >9. H_3AsO_4 may be present for strongly acidic pH values and AsO_4^{3-} in extremely alkaline conditions. Under reducing conditions H_3AsO_3 predominates for pH values below 9.

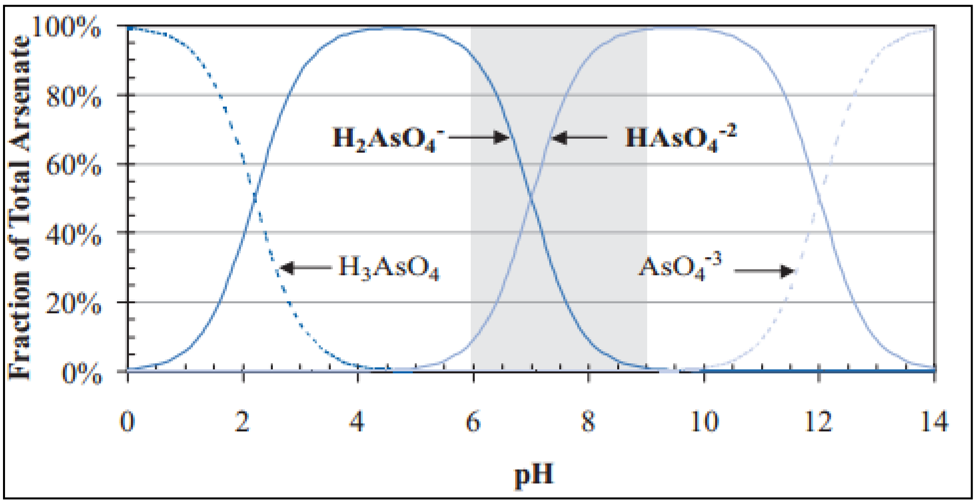

Figure 2.2 Dissociation of arsenate [As(V)] (EPA, 2003)

The toxicity and mobility of arsenic varies with its valency state and chemical form. As(III) is generally more toxic to humans and four to ten times more soluble in water than As(V) (US EPA. 1997; US OSHA, 2001). Elemental arsenic is not soluble in water whereas arsenic compounds may readily dissolve. In aqueous systems, arsenic exhibits anionic behavior.

Arsenic speciation is a critical issue and has to be known for the removal of arsenic. Negative surface charges provide efficient adsorption, anion exchange, and co-precipitation processes. Since the net charge of As(III) is neutral at natural pH levels (6-9), this form is not easily removed. However, net molecular charge of As(V) is negative (-1 or -2) at natural pH levels, enabling it to be removed with greater efficiency. Conversion of As(III) to As(V) is crucial for any arsenic treatment process (Feenstra et al., 2007). This conversion can be accomplished by adding an oxidizing agent such as chlorine or permanganate.

2.2 Health Impacts of Arsenic and Related Regulations

Arsenic can have both acute and chronic toxic effects on humans. Soluble inorganic arsenic is acutely toxic. Intake of inorganic arsenic during long period can cause to chronic arsenic poisoning (arsenicosis) (WHO, 2010). Organic arsenic compounds, which are abundant in seafood, are less harmful to health and are rapidly eliminated by the body (WHO, 2001). The symptoms of acute arsenic poisoning are vomiting, abdominal pain and diarrhea. Muscle cramping and even death can be seen due to quantity of dosage. During long-term exposure to high levels of inorganic arsenic (e.g. through drinking water), the first changes are usually seen in the skin as pigmentation changes and then skin lesions and hard patches on the palms of the hands and soles of the feet. Moreover, peripheral neuropathy, gastrointestinal symptoms, conjunctivitis, diabetes, renal system effects, enlarged liver, bone marrow depression, destruction of erythrocytes, high blood pressure and cardiovascular disease can occur. Beside these, arsenic can cause cancers of the skin, bladder and lungs. Arsenic can pass through the placenta. Pregnant women chronically exposed to arsenic-contaminated drinking-water are at increased risk for spontaneous abortion, stillbirth and preterm birth. In utero and early-life exposures to arsenic have been linked to the development of lung cancer and bronchiectasia later in life (WHO, 2010). The International Agency for Research on Cancer (IARC) has classified arsenic and arsenic compounds as carcinogenic to humans, and has also stated that arsenic in drinking-water is carcinogenic to humans.

Standards and guidelines for arsenic are aimed at protecting the human health. Because of the proven and widespread negative health effects on humans, in 1993, the WHO lowered the health-based provisional guideline for a "safe" limit for arsenic concentration in drinking water from 50 μg/L to 10 μg/L (i.e. from 0.05 mg/l to 0.01 mg/l). WHO retained this provisional guideline level in the latest edition of its standards (WHO 1993; WHO 2004). The WHO provisional guideline of 10 μg/L has been adopted as a national standard by most countries, including Japan, Jordan, Laos, Mongolia, Namibia, Syria and the USA, and by the European Union (EU). The US EPA has set 10 μg/L as the allowable level for arsenic in drinking water (maximum contaminant level) (EPA, 2001) and is proposing to change the arsenic standard in drinking water to 5 ppb (0.005 mg/L) to more adequately protect public health. Similarly to those countries, Turkey reduced arsenic limits from 50 μg/L to 10 μg/L in 2005. The new standard has been enforced since 2008.

2.3 Treatment Methods of Arsenic

Both in the literature and full-scale applications, various arsenic treatment methods are available. These methods are different from each other due to i) quantity of water , ii) initial arsenic concentration and its form (As(III) or As(V) and iii) other existing ions in water (Alpaslan et al., 2010). The most common methods are chemical precipitation/coagulation, ion exchange, membrane process, and adsorption. Those methods can preferably used in conventional (or centralized), well-head or point of use (POU) treatment systems.

Conventional (or centralized) systems are economical solutions, and in areas of high population density, capital costs can be distributed over a large number of consumers, therefore treatment cost is not high (Johnston et al., 2001). However, in centralized plants, all of the water even though only a small fraction will eventually be consumed through drinking purpose is treated by arsenic removal techniques, that may increase the treatment costs. Generation of significant amounts of arsenic-rich wastes is another issue that should be considered as the disadvantages of such systems. On the other hand, in small communities, water supply conditions are different from in urban settings. The population served is smaller and qualified staff to operate plants is less. Hence wellhead or POU treatment (household systems) is recommended for small towns or rural remote areas.

2.3.1 Conventional Arsenic Treatment For Large Public Water Treatment

Conventional coagulation-separation process is mostly used in centralized removal systems both in industrialized and developing countries (Feenstra, 2007). Removal efficiencies are quite higher for As(V) (up to greater than 99 percent removal) than for As(III) (US EPA, n.d.). Conventional treatment plant may contain coagulation, flocculation, sedimentation, and filtration, and finally by disinfection processes at full-scale. The typical flow scheme of the plant is presented in Figure 2.3.

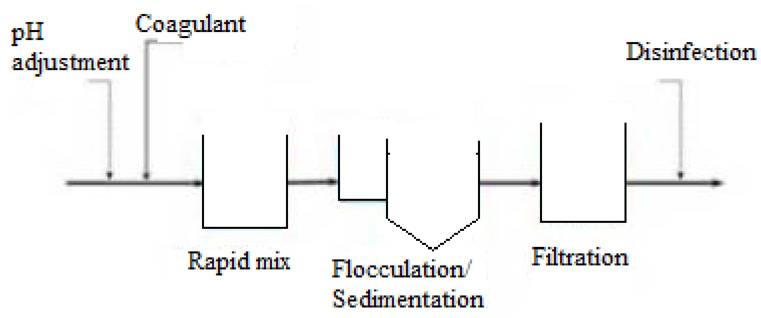

Figure 2.3 Flow diagram of conventional (centralized) arsenic treatment plant

Coagulation is rapid mixing process of a positively charged coagulant (aluminum or iron salt) is added to raw water in order to destabilize the negatively charged particulate and colloidal matters. Coagulant aid polymers may also be added to enhance the coagulation efficiency. In the next step, flocs are formed in the flocculation unit by gentle mixing. After flocculation, flocs are separated in a separation unit, usually using sedimentation and rapid sand filtration. Performance of the process is depend on pH of water and ratio of Fe:As (that should be > 20) in water (US EPA, n.d.).

Lime-soda softening is a precipitative process using lime or soda to reduce hardness in source waters. Hardness is occurred in the water when multivalent ions, especially calcium (Ca^{2+}) and magnesium (Mg^{2+}) found in water. A typical softening process includes rapid mixing, flocculation, sedimentation, recarbonation, and filtration stages. Pre-treatment by aeration and pre-sedimentation may also be used to oxidize arsenic compounds (if required). The flow scheme of lime-soda softening process is given in Figure 2.4.

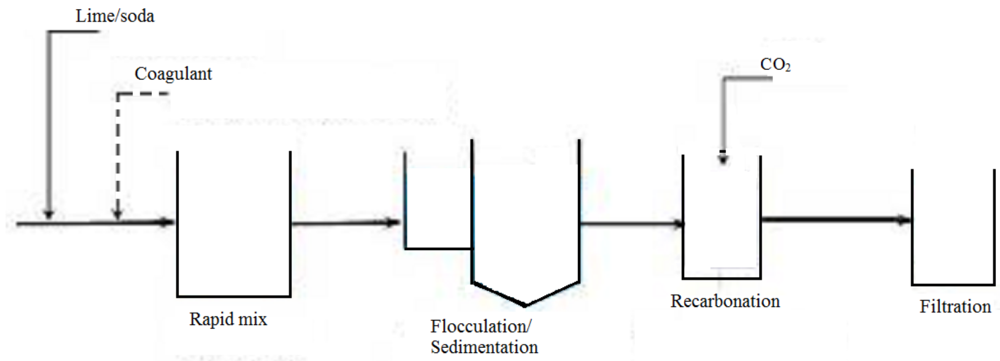

Figure 2.4 Typical lime-soda softening process flow diagram

pH is the most important parameter for effective precipitative softening. For calcium carbonate precipitation the pH is raised to approximately 10 and for magnesium hydroxide precipitation the pH is raised above 11.

Arsenic can be removed simultaneously while softening. For optimal performance to remove both As(III) and As(V), the pH range used in softening experiments varied between 9 and 12. When softening is performed with lime at pHs higher than 10.5, magnesium hydroxide is formed and As(V) is removed by co-precipitation with magnesium hydroxide. Arsenic removal is greatly increased at pH greater than 10.5 and (US EPA, n.d.).

2.3.2 Well Head Arsenic Treatment Systems For Rural Remote Areas

Conventional system may have operational difficulties due to waste generation, trained operator, and high costs especially for small scale applications, e.g. in villages. Therefore, well head treatment plants including ion exchange, membrane systems, adsorption or oxidation/filtration techniques are recommended by United States Environmental Protection Agency (US EPA) as Best Available Technologies (BAT). Table 2.1 gives the comparison of arsenic treatment processes for well head treatment.

Table 2.1 Comparision of arsenic treatment methods

TREATMENT METHOD	ADVANTAGE	DISADVANTAGE
Ion Exchange	pH insensitive (in the range of pH 6.5-9)	Other ions transit to water
Membrane Process	High arsenic removal	As contaminated water formation Membrane fouling Expensive systems
Adsorption	Low-cost by using natural materials Suitable for large pH interval High arsenic removal	Used adsorbant should be considered as solid or hazardous waste
Oxidation-Filtration	For Fe /Mn treatment Simultaneous As removal occurs by adsorption or coprecipitation	Oxidizing agent and iron addition Need backwashing Sludge formation 50-85% arsenic removal (additonal treatment can be required)

Ion exchange is a physical-chemical process in which ions are swapped between a solution phase and solid resin phase (US EPA, 2003). It can hold arsenic very efficiently, and as a result of the ion exchange process gives another ion into the water. The removal efficiency depends on the resin type, regeneration frequency, initial arsenic concentration, and competing ions in the water. Ion exchange processes can remove arsenic from water very effectively (greater than 99 percent removal), when arsenic is in the As(V) oxidation state. As(V) can be removed through the use of strong-base anion exchange resin (SBA) in either chloride or hydroxide form. These resins are insensitive to pH in the range 6.5 to 9.0 (US EPA, 2000). The flow diagram of typical ion exchange process is presented in Figure 2.5.

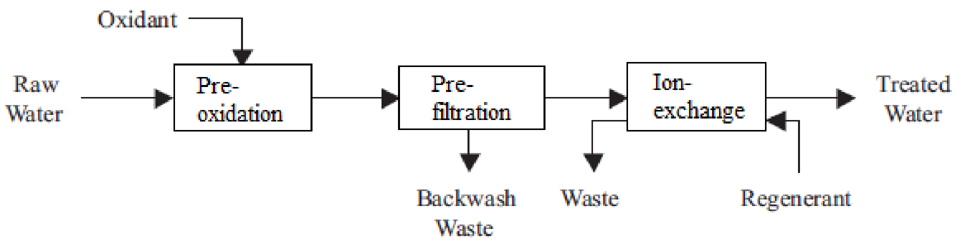

Figure 2.5 Ion exchange process flow diagram

Membrane processes work under pressure and can remove arsenic by using selective membranes. Two classes of membrane filtration can be considered: low-pressure membranes, such as microfiltration and ultrafiltration; and high-pressure membranes such as nanofiltration and reverse osmosis (Johnston et al., 2001). The use of microfiltration (MF) and ultrafiltration (UF) membranes is dependent on the size of arsenic particles removed from water. To increase removal efficiency, coagulation process can be applied in order to increase the size of the particles previous to the membrane unit. Nano-filtration and reverse osmosis membranes are efficient to remove dissolved arsenic compounds.

In general, membrane filtration is more effective for removal As(V) than for As(III). Removal efficiency of As(V) from water by membrane processes varies between 50 -90 percent. However, removal of As(III) by membrane separation is not effective and efficiency changes between 20 to 75 percent removal. Membrane filtration requires a relatively high-quality influent water to control fouling. To prevent fouling, reverse osmosis filters are almost always preceded by a pretreatment (i.e.filtration) step. These processes are relatively expensive systems from the other removal methods due to both operation and initial investment costs. Especially, high-pressure membrane methods, i.e. NF, RO, are currently more expensive than other arsenic removal methods, and are only used when very low arsenic levels are essential. On the other hand, recent advances particularly in operating low pressure systems at high recovery rates, could become membrane methods a feasible and cost effective systems for arsenic treatment (Johnston et al., 2001).

Typical flow scheme of membrane based systems for arsenic removal is illustrated in Figure 2.6.

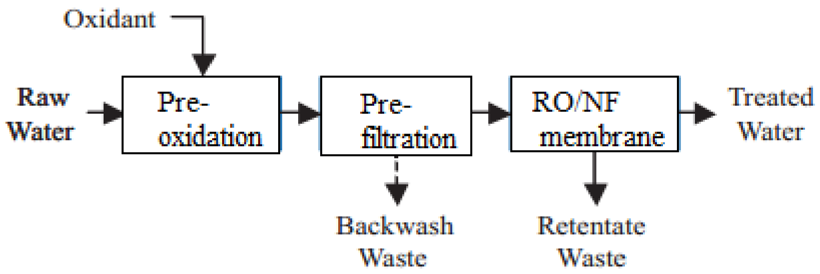

Figure 2.6 Flow diagram of a high pressure membrane systems for arsenic removal

Adsorption is very effective and a commonly used treatment option for arsenic removal due to ease of operation and low/no sludge production. This process changes phase of arsenic from large water volumes into solid phase. Figure 2.7 describes flow diagram of adsorptive treatment method. Arsenic removal by adsorptive media depends on the initial concentration, oxidation state, adsorbent type, pH and competing anions.

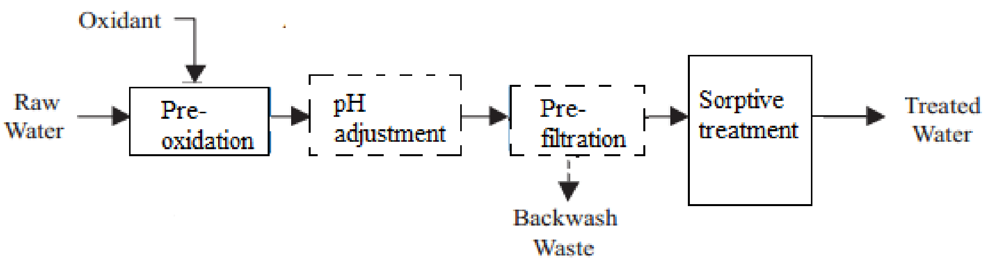

Figure 2.7 Adsorption process flow diagram

Oxidation/filtration is normally used for iron/manganese removal from water. The common iron/manganese methods consist of air oxidation or chemical oxidation followed by media filtration. Arsenic can also be removed by this process simultaneously by adsorption and coprecipitation mechanisms. Suitable Fe:As ratio in water is important in order to remove arsenic efficiently (US EPA, n.d.). Flow scheme of oxidation/filtration is given in Figure 2.8.

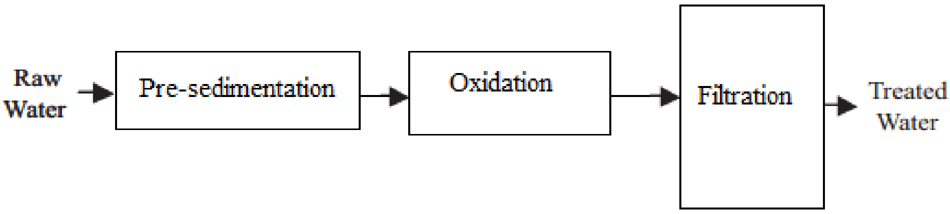

Figure 2.8 Oxidation/filtration process flow diagram

CHAPTER THREE
ADSORPTION OF ARSENIC COMPOUNDS

3.1 Definition and Mechanisms of Adsorption

Adsorption is the seperation process of collecting soluble substances that are in solution on a suitable interface. The interface can be between the liquid and a gas, a solid or another liquid (Tchobanoglous & Burton,1991). Adsorption processes can be classified as either physical adsorption or chemisorption depending on the type of forces between the adsorbate and the adsorbent. If the force of attraction between adsorbate and adsorbent are Vander Waal's forces, the adsorption is named as physical adsorption. In physical adsorption, the pulling effect between the adsorbate and adsorbent are weak, therefore this type of adsorption can be easily reversed (desorption) by thermal ways or by decreasing the pressure. If the forces of attraction are chemically bonding, the adsorption is called chemisorption. In chemisorptions, the force of attraction is so strong, so adsorption can not be easily reversed (Odesola &Adebayo , 2010).

When the adsorbent and adsorbate are contacted for enough time, equilibrium will be obtained between the amount of adsorbate adsorbed and the amount of adsorbate in solution. The equilibrium relationship is described by adsorption isotherms. The adsorption capacity is defined as the amount of adsorbed material and determined as a function of the concentration at a constant temperature, and the resulting function is called an adsorption isotherm (Tchobanoglous & Burton, 1991).

There are many different types of isotherms used for determining capacity of adsorbents, e.g. Freundlich, Langmuir and Brunauer-Emmett-Teller isotherms. However, in this study, Langmuir adsorption isotherms and Freundlich adsorption isotherms which are the most widely used isotherms in water treatment, were eveluated.

3.2 Adsorption Isotherms

Adsorption isotherms are important to calculate adsorption capacity of an adsorbent. The amount of arsenic uptake by adsorbants was calculated from the following equation:

$$q = \frac{(C_0 - C_e)V}{m} \tag{3.1}$$

Where q is the adsorption capacity (mg/g), C_0 is the initial arsenic concentration (mg/ L), C_e is the equilibrium concentration of arsenic in solution (mg/ L), V is the solution volume (L), and m is the mass of adsorbant (g).

3.2.1 Freundlich Isotherm

Herbert Max Finley Freundlich, a German physical chemist, presented an empirical adsorption isotherm for non-ideal systems in 1906. Freundlich isotherm gives an empirical expression representing the isothermal variation of adsorption of a quantity of adsorbate by unit mass of solid adsorbent. Both the monolayer (chemisorption) and multilayer adsorption (physisorption) are relevant to the Freundlich isotherm (Yang, 1998).

Freundlich isotherm can be given as:

$$q_e = k_f C_e^{\frac{1}{n}} \tag{3.2}$$

Where k_f is the adsorption capacity (mg/g), q_e is amount tof adsorbate adsorbed per unit mass of adsorbent (mg/g) at equilibrum and C_e is equilibrum concentration and 1/n is affinity coefficient and linearilized form is:

$$lnq_e = lnk_f + \frac{1}{n}(lnC_e) \tag{3.3}$$

3.2.2 Langmuir Isotherm

Irving Langmuir, an American chemist developed a relationship between amount of gas adsorbed on the surface and the pressure of that gas. Such equations are now referred to as Langmuir adsorption isotherms. It is a semi-empirical isotherm derived from a proposed kinetic mechanism. Langmuir isotherm gives the relationship for adsorption capacity and concentration based on some assumptions regard to uniform surface, a single layer of adsorbed material, and constant temperature.

$$q_e = \frac{q_m b C_e}{1+bC_e} \tag{3.4}$$

Where q_e is the amount of arsenic adsorbed at equilibrum (mg/g), C_e is the equilibrum concentration(mg/L), q_m is the adsorption capacity (mg/g), b is the adsorption energy (L/mg) and linearized form is:

$$\frac{1}{q_e} = \frac{1}{q_m} + \frac{1}{bq_m}\left(\frac{1}{C_e}\right) \tag{3.5}$$

3.3 Adsorption Kinetics

Adsorption kinetics is used to determine the rate of adsorption by using concentration of adsorbate at a specific time. Adsorption kinetics indicates how fast the reaction occurs towards equilibrium and define the rate constant or adsorption coefficient. In this study, first order reaction model, pseudo-first order reaction model, second order reaction model and pseudo-second-order reaction model are used to evaluate kinetic coefficients.

3.3.1 First-Order Reaction Model

First-order reaction model based on the solution concentration can be given as:

$$-\frac{dC_t}{dt} = kC_t \tag{3.6}$$

Where C_t is the concentration at a contact time (mg/L), C_o is the initial concentration (mg/L)and k is the first order adsorption rate constant. Reaarranging equation (3.6):

$$-\frac{dC_t}{C_t} = kdt \tag{3.7}$$

Integrating equation (3.7) for the boundary conditions t =0 to t=t and C_t=C_o to C_t=C_t gives the linearized form of model.

$$lnC_t = lnC_o - kt \tag{3.8}$$

By plotting the graph for (lnC_t) versus (t), k is found from slope of line.

3.3.2 Pseudo-First Order Reaction Model

Pseudo-first order reaction model is based on the adsorption capacity and can be represented as:

$$\frac{dq_t}{dt} = k_1(q_e - q_t) \tag{3.9}$$

Where q_e is adsorption capacity at equilibrium time,q_t is the adsorption capacity of any time and k_1 is the pseudo first order adsorption rate constant.

Integrating equation (3.9), the boundary conditions t =0 to t=t and q_t=0 to q_t=q_t gives the linearized form of model as shown below.

$$\ln(q_e - q_t) = lnq_e - k_1 t \quad (3.10)$$

By plotting graph for $\ln(q_e$-$q_t)$ versus (t), k_1 is obtained from slope of line.

3.3.3 Second Order Reaction Model

Second order reaction model fits adsorption process in general and it is expressed as:

$$-\frac{dC_t}{dt} = k_2 C_t^2 \quad (3.11)$$

Where C_t is the concentration at a contact time(mg/L), and C_o the initial concentration (mg/L) and k_2 is the second order adsorption rate constant.

Rearranging equation (3.11) and integrating the boundary conditions t =0 to t=t and C_t=0 to C_t=C_t:

$$\frac{1}{C_t} - \frac{1}{C_o} = k_2 t \quad (3.12)$$

k_2 is found from slope of line by plotting the graph for ($1/C_t$) versus (t).

3.3.4 Pseudo-Second Order Reaction Model

Pseudo-second order reaction model is based on the adsorption capacity and can be formed as:

$$\frac{dq_t}{dt} = k_{p2}(q_e - q_t)^2 \quad (3.13)$$

Where q_t is the adsorption capacity of any time (mg/g), q_e is the adsorption capacity at equilibrium time (mg/g) and k_{p2} is the pseudo second order adsorption rate constant.

Rearranging equation (3.13) and integrating for the boundary conditions t =0 to t=t and q_t=0 to q_t=q_t gives the linearized form of model:

$$\frac{1}{q_e-q_t} = \frac{1}{q_e} + k_{p2}t \tag{3.14}$$

Reaarranging equation (3.14), it is obtained:

$$\frac{t}{q_t} = \frac{1}{k_{p2}q_e^2} + \frac{1}{q_e}t \tag{3.15}$$

The graph for (t/q_t) versus (t), k_{p2} is found from slope of line.

3.4 Adsorbents Used For Arsenic Treatment

Sorption with low cost materials arises as an alternative removal technology for arsenic treatment. Adsorption has outstanding features like high removal performance and low/no sludge production. Adsorbent choice is very important to obtain maximum efficiency from adsorption process. The properties e.g. large surface area, adsorption capacity, low cost and regeneration capacity of an adsorbent are criteria for optimum adsorbent choice. Activated carbon, activated alumina, and iron based materials are commonly used adsorbents for arsenic treatment in adsorption processes, and thus explained in the following sections by emphasizing on iron based materials.

3.4.1 Activated Alumina

Activated alumina (AA) is a porous and granular material. The media, aluminum trioxide, is prepared through the dehydration of aluminum hydroxide at high temperatures. Average diameter of AA grains are 0.3 to 0.6 mm and have high surface area for adsorption. The removal of As(V) by AA sorption can be accomplished by continuously passing water under pressure through one or several beds filled with AA media. The selectivity of AA towards As(III) is poor, due to the overall neutral molecular charge at pH levels below 9.2. Therefore, pre-oxidation of As(III) to As(V) is important stage. Several different studies have established the optimum pH range as 5.5-6.0, and showed taht greater than 98% arsenic removal under these conditions. AA column operated under acidic pH conditions runs 5 to 20 times longer than under natural pH conditions (6.0-9.0) (EPA, 2003).

3.4.2 Activated Carbon

Activated carbon (AC), both in powdered or granulated forms can be used for As(III) and As(V) removal from aqueous solutions. Activated carbon can be produced from carbonaceous material, including coal (bituminous, subbituminous, and lignite), peat, wood, or nutshells (i.e., coconut). Arsenic sorption by AC is greatly dependent on pH and its oxidation state (Ansari and Sadegh, 2006). Adsorption capacity of AC depends on its characteristics, adsorbate chemical properties, temperature, pH, ionic strength, etc. Commercial activated carbons have been extensively used for As(III) and As(V) adsorption from water (Mohan and Pitman, 2007). AC media is normally regenerated by using thermal processes. However, AC regeneration used for arsenic removal from water might not be feasible. Because, arsenic might not volatilize at the temperatures typically used in AC regeneration and off-gas containing arsenic from the regeneration process may be difficult or costly to manage, as well (EPA, 2002).

3.4.3 Iron Based Adsorbents

It is well known that natural affinity of arsenic for iron (hydro)oxides (Wilkie and Hering,1996; Goldberg and Johnston, 2001; Dixit and Hering, 2003), however small surface area of ironhydroxides via agglomeration through adsorption process is a disadvantage for arsenic removal. However, when the iron(hyro)oxides supported by natural materials (e.g. clay minerals) it can prevent agglomeration; and in contrast to ironhydroxides, iron modificated material generates continously FeOH, FeOOH or HFO (hydrous ferric oxide) in water medium (Maji et al., 2011). These oxides have much more active surface than simple ironoxides so arsenite and arsenate can adsorb easily. Therefore it is more effective and cheaper using iron-modified natural porous materials than iron oxides. It is also cost-efficient method when using easily available materials as adsorbent. Several studies were done with respect to natural affinity of arsenic for iron (hydro)oxides by using iron based materials such as ferrous based red mud sludge (Li et al., 2010), bead cellulose loaded with iron oxyhydroxide (Guo et al., 2007), iron-loaded activated carbon, ,iron based biomass-silica gel composites (Martínez-Cabanas et al., 2015), iron-oxide coated sponge (Nguyen et al., 2010), iron-oxide-coated natural rock (Maji et al., 2012), iron oxide coated cement (Kundu & Gupta, 2007), Fe-exchanged natural zeolite (Li et al.,2011), iron oxide-coated perlite (Mostafa et al., 2011), modified activated carbons with iron hydro(oxide) nanoparticles (Vitela-Rodriguez & Rangel-Mendez, 2013).

Various methods were carried out in order to prepare these materials. Material coating methods in these studies were given in Table 3.1.

Table 3.1 Material coating methods in the literature

Modified material	Preperation for coating	Coating with	Contact time	After coating process	Reference
Ironoxide coated sand (200g)	Washing and drying in oven	80 ml 2M $FeNO_3$ (pH 11)	2 min	110˚C drying for 14 h, rinsing with distilled water, 105˚C drying	Gupta et al., 2005
Ironoxide coated sand (0.6-0.8 mm)	Acid washing (pH 1,24 h) Rinsing with distilled water, 110˚C drying for 20h	FeNO3	-	-	Thirunavukkarasu et al., 2001
Ironoxide coated rock (100g)(0.148mm)	Washing and drying 140˚C	50g $FeNO_3$ in 150 ml water	30 min	140˚C drying rinsing and 140˚C drying	Maji et al., 2011
Fe exchanged natural zeolit (2 mm) (120 g)	-	360 ml 20 mmol/L Fe(III) solution (pH 9)	20 h 150 rpm	Rinsing ,allow to dry naturally	Li et al., 2011
Iron coated zeolite	-	2000g zeolite+ 1L 10% $FeCl_3$(pH10)	Agitated 50˚C for 1 h	drying	Jeon et al., 2009
Iron oxide coated perlite	Soaked in H_2SO_4 sol. (pH 1) for 24 h then rinse 3 times with DIW dried 105˚C C 24 h	FeCl3 sol. 200 rpm until pH(9.5)+ 100 g perlite	60˚C 200 rpm for 24 h	dried 105˚C 24 h washed 6 times with DIW, dried at 60˚C	Mostafa et al., 2011

Quartz is very poor to remove arsenic, because the mineral surface is negatively charged at pH > 2. However, quartz sand can be used as support material and can be made highly sorptive by coating the grains with metal oxides. Iron-oxide coated sand was first used to treat metal-bearing wastewaters and succesfully operated in fixed beds (Edwards & Benjamin 1989; Bailey et al. 1992; Satpathy and Chaudhuri 1995). In 1996, Joshi & Chaudhuri studied arsenic removal by ironoxide coated with groundwater sand first time. They achieved app. 80% removal with 1mg/L of inital arsenic concentration and 10 g/L adsorbant dose at a pH 7.5 and for 3-4 hours contact time. Thirunavukkarasu et al., 2001 reported 325 µg/L initial As containing syntetic water 92% removal for 5 hours contact time. Gupta et al. 2005, studied with initial As(III) concentration of 100 µg/l syntetic water in batch systems and obtained maximum As(III) removal efficiency 99% for coated sand at an adsorbent dose of 20 g/l. Devi et al., 2014 investigated the effect of limestone addition on removal efficiency of arsenic. They obtained arsenic (III) removal efficiency increased with the increased dose of coated sand and was best removed at pH 7. Limestone addition had no significant effect and 97.5 % arsenic removal was obtained at a coated sand dosage of 5 g/100 ml with or without limestone.

Beside batch studies, column studies by using iron coated materials in the literature are quite limited. Whereas, it is very important to perform these studies in order to apply them to real plant design.Kundu and Gupta (2007), studied iron oxide coated cement for arsenic removal and found it an effective adsorbent .In another study, iron-oxide coated natural rock was used in fixed bed and quality of the effluent water was sufficient for the use of practical purposes (Maji et al., 2012).

Regeneration of adsorbent and its reuse is also very important for a more cost effective treatment. Chen et al., 2015 reported, iron media replacement cost accounts for around 80% of systems total operational costs. They studied batch and column regeneration tests and showed up to 80% of the arsenic can be stripped from exhausted media products. The authors also obtained in pilot tests that the regenerated media can achieve arsenic removals similar to virgin media. Gosh & Gupta (2012) also reported that a 2% caustic solution is effective for the regeneration of exhausted activated alumina used in very small arsenic removal systems in West Bengal.

A brief summary for batch and column studies in the literature are given below in Table 3.2 and Table 3.3, respectively.

Table 3.2 Performances of iron coated materials in the literature (Batch experiments)

Adsorbent-adsorbent dose	**pH-Temperature**	**Initial Arsenic Consentration (µg/l)**	**As(III) removal (%)**	**As(V) removal (%)**	**Contact time**	**Adsorption Capacity (mg/g)**	**Source**
Ironoxide coated rock (IOCR) (15g/l) (Groundwater)	7.5- 25°	40	75 (As_T)		6 h	0.36	Maji et al.,2011
Cliptilolite zeolite (20 g/l) (Syntetic water)	7-8	500			24h	0.1 As(III) 0.05 As(V)	Li et al.,2011
Iron impregnated chitosan (0.2 g/L) (Syntetic water)	8	1007	60		30 min	6.48	Gang et al., 2010
Ironoxide coated sand (20g/l) (Syntetic water)	7.5	100	99		2h	0.02857	Gupta et al., 2005

Table 3.2 Performances of iron coated materials in the literature (Batch experiments)(Cont.)

Adsorbent-adsorbent dose	**pH-Temperature**	**Initial Arsenic Concentration (μg/l)**	**As(III) removal (%)**	**As(V) removal (%)**	**Contact time**	**Adsorption Capacity (mg/g)**	**Source**
Iron coated zeolite (33g/L) (Syntetic water)	3-10	20120		99.9	30 min	0.68 As5	Jeon et al., 2009
GAc Fe (8g/l) (Syntetic water)	7-30°	200	92.4	97.6	15 h	0.231 As(III) 0.248 As(V)	Mondal et al, 2008
Iron-oxide coated perlite (10 g/l) (Syntetic water)	6.5-7	1000 As(V)		100%	5min	0.39	Mostafa et al.,2011
Modified sepiolite (5g/l) (Syntetic water)	7	538	91.6 As_T		4h	0.501	**This study**
Modified sand (5g/l) (Syntetic water)	7	100	91.2 As_T		4 h	0.142	**This study**

Table 3.3 Performances of iron coated materials in the literature (Column studies)

Material	**As influent (mg/L)**	**Flow rate (ml/min)**	**Height (cm)**	**Diameter (cm)**	**Breakthrough volume (L)**	**Breakthrough point (mg/L)**	**Exhaust Volume (L)**	**Source**
Ironoxide coated zeolite	2 As(V)	0.5	17	1,1	4.8	0.01		Jeon et al.,2009
Ironoxide coated cement	1.35	8.5	20	2	5.61	0.01		Kundu et al.,2007
Ironoxide coated rock	0.6 As(III)	8	20	2	30.24	0.01	52.8	Maji et al., 2012
Ironoxide coated sand	0.62	3	20	1,1	5.3	0.01	13	**This study**
Ironoxide coated sepiolite	0.514	3	20	1.1	23	0.01	46	**This study**

3.5 Evaluation of the Arsenic Adsorption and Desorption Mechanism on Iron Oxide Coated Materials

As(V) in aqueous solution exists in anionic forms ($H_2AsO_4^-$, $HAsO_4^{2-}$, AsO_4^{3-}) above pH 3 and so it can be effectively removed by iron hydroxide attached to the surface of the modified materials. As(III) is present as an anion only above pH 9 ($H_2AsO_3^-$, $HAsO_3^{2-,}$ AsO_3^{3-}), conversely. Only a small percentage of H_3AsO_3 is dissociated in the pH interval 6–9. Thus for effective treatment of As(III) the solution pH must above 7.

The responsible mechanism for the removal of arsenic by adsorption on iron-modified adsorbents, which refers to the formation of surface complexes between soluble arsenic species and the surface hydroxyl groups, as arsenic connects with the iron sites of the material (Edwards, 1994). Iron coated material generates continously FeOH, FeOOH or HFO (hydrous ferric oxide) in water medium (Maji et al., 2011). These oxides have much more active surface than simple ironoxides so arsenite and arsenate can adsorb easily. Therefore it is more effective and cheaper using iron coated natural porous materials than iron oxides.

According to Clifford et al., 2011, “ligand exchange” is a more appropriate term than adsorption for the highly specific surface reactions involved due to the arsenic removal mechanism of the adsorptive media process is usually an exchange of anions, such as arsenic, for surface hydroxides of the media. Adsorption processes are also exchange processes and occurrs at specific locations between adsorbent and adsorbate interface (Mercado-Borrayo et al., 2014).

The pH of solution caused protonation or deprotanation of surface hydroxyl groups of adsorbent (≡FeOH represents the groups on the surface). Depending on pH, surface functional group can be negative, positive or netral charged as in formulations (3.15) and (3.16) (Essington, 2015).

$$\equiv FeOH^0 + H^+ \rightarrow \equiv FeOH_2^+ \quad (3.16)$$
$$\equiv FeOH^0 \rightarrow \equiv FeO^- + H^+ \quad (3.17)$$

A ligand from the aqueous phase displaces surface bound water resulting with formation of surface complex expressed as ligand exchange process (Essington, 2015). Arsenic adsorption by iron oxide occurs in that way: First, iron oxide in aquoeus solution hydrolizes and oxyhydroxides are produced on the iron surface over the active adsorption sites. Arsenite or arsenate ions react with these active sites and adsorption occurs by reaction of OH^- ions on the adsorbent surface and arsenite or arsenate ions as shown in Figure 3.1(Mercado-Borrayo et al., 2014).

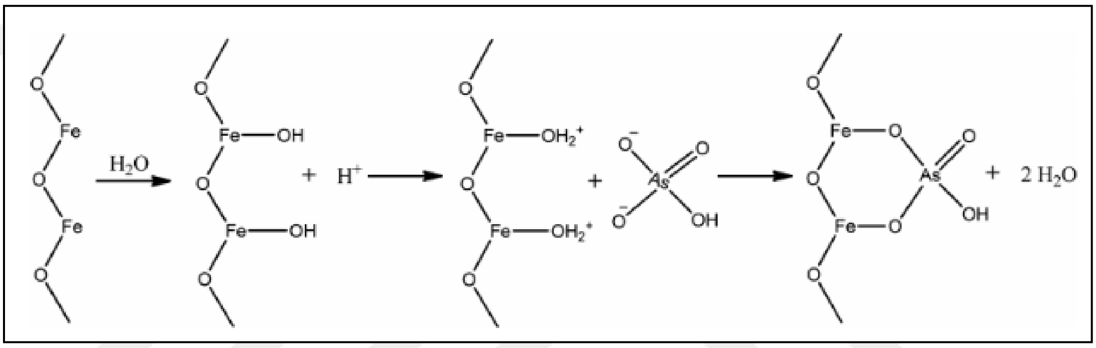

Figure 3.1. Mechanism of arsenic removal (Mercado-Borrayo et al., 2014)

The mechanism of arsenic adsorption by ligand exchange process depend on the solution pH can be illusrated as (Maji et al., 2011):

For arsenate:

$$\equiv FeOH + H_2AsO_4^- \rightarrow \equiv FeHAsO_4^- + H_2O \quad (3.18)$$
$$\equiv FeOH + HAsO_4^{2-} \rightarrow \equiv FeAsO_4^{2-} + H_2O \quad (3.19)$$

For arsenite:

$$\equiv FeOH + H_2AsO_3^- \rightarrow \equiv FeHAsO_3^- + H_2O \quad (3.20)$$
$$\equiv FeOH + HAsO_3^{2-} \rightarrow \equiv FeAsO_3^{2-} + H_2O \quad (3.21)$$

Fendorf et al., 1997 studied to deduce the local coordination environment of arsenate on the mineral goethite (R-FeOOH) by Extended X-ray absorption fine structure (EXAFS) spectroscopy. They obtained three different surface complexes exist on goethite for both oxyanions: a monodentate complex, a bidentate-binuclear complex, and a bidentate-mononuclear complex based on the oxyanion-Fe distances. Later EXAFS studies also proved that the arsenic removal mechanisms using Fe(III) oxides involved in both mono- and bidentate complex formation with ferric oxyhydroxides as given in Figure 3.2 (Goldberg, 2002; Li,2011; Maji et al., 2011; Watts et al., 2014).

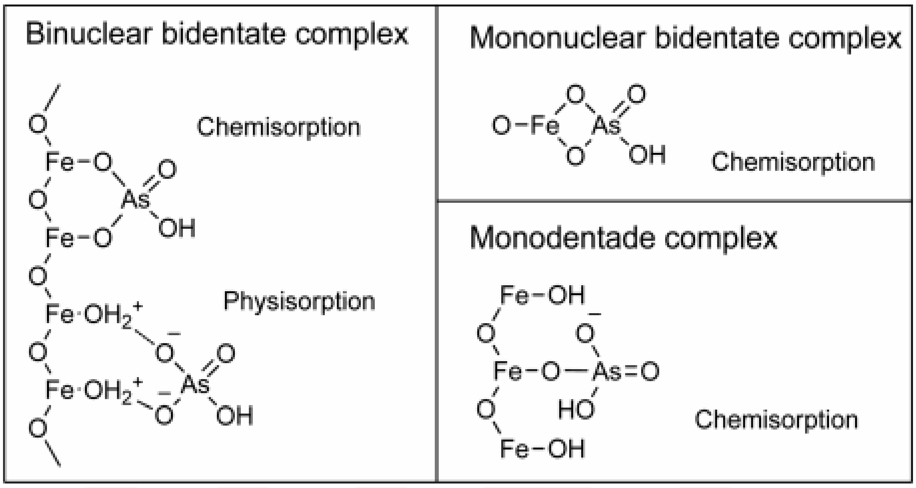

Figure 3.2 Different bonds between arsenate and iron oxide (Mercado-Borrayo et al., 2014)

The regeneration of the adsorption media to recover the used material and to regenerate the adsorbent is quite essential, when adsorptive media reached breakthrough point and so can not reduce the arsenic to less than the allowable limits. Regeneration process can be performed by acid or alkaline washing depending on surface charge of adsorbent media. At high pH values of solution, surface hydroxyl groups become deprotonated and negatively charged. Therefore, negatively charged arsenic species desorpt efficiently. Then, adsorbent media is rinsed with dilute acid allows formation of protonated surface hydroxyl groups and it can be reuse for further treatments (Sengupta, n.d.).

The reactions occur during regeneration of exhausted adsorbent with basic solution and rinsing with dilute acid solution are showed below in Figure 3.3. where “M” represents the metal, e.g. Fe(III).

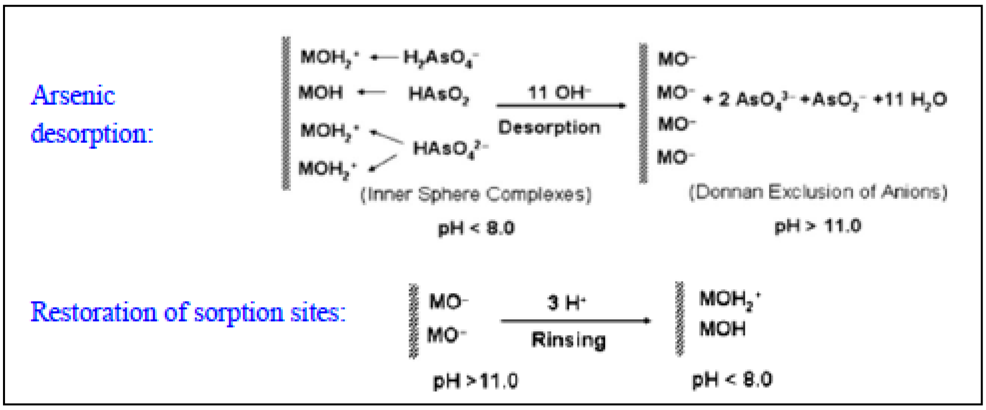

Figure 3.3 Arsenic desorption mechanism (Sengupta, n.d.)

3.6 Design of a Fixed Bed Adsorption Column

When a solution passes through a column, solute was adsorbed by the adsorbent and treated effluent is obtained. Adsorption zone of a column where solute adsorbed actively is called mass transfer zone and it lapses down through the flow direction. Upper side of the mass tansfer zone is accepted as exhausted adsorbent and below this area is accepted as fresh adsorbent.

If the adsorption capacity is enough to eliminate solute from solution, effluent concentration will be provided maximum allowable (desired) concentration at the effluent for a period of time. When the available adsorption sites decreases, then effluent concentration begin to increase. The point where the effluent concentration to influent concentration ratio exceeds the allowable limit called as breakthrough point. When this ratio attains this value, the adsorbent needs to be replaced or regenerated to provide the utilize the column. As long as solution passes through the column, effluent concentration continues to increase and there will no available adsorption site after a while to adsorb the solute. Effluent concentration will nearly same as influent concentration and this point is called as exhaust point. When the column reaches exhaust point, no more adsorption occurs.

breakthrough capacity: the mass of the adsorbate removed by the adsorbent at breakthrough concentration *exhaustion capacity:* the mass of the adsorbate removed by unit weight of the adsorbent at saturation.

degree of column utilization: the mass adsorbed at breakthrough point divided by the mass adsorbed at complete saturation.

To design a fixed bed adsorption column, the breakthrough point and exhaust point must be known to operate the system effectively. For this reason, the breakthrough curve is obtained from column studies and these points are determined. A schematic diagram is given in Figure 3.4.

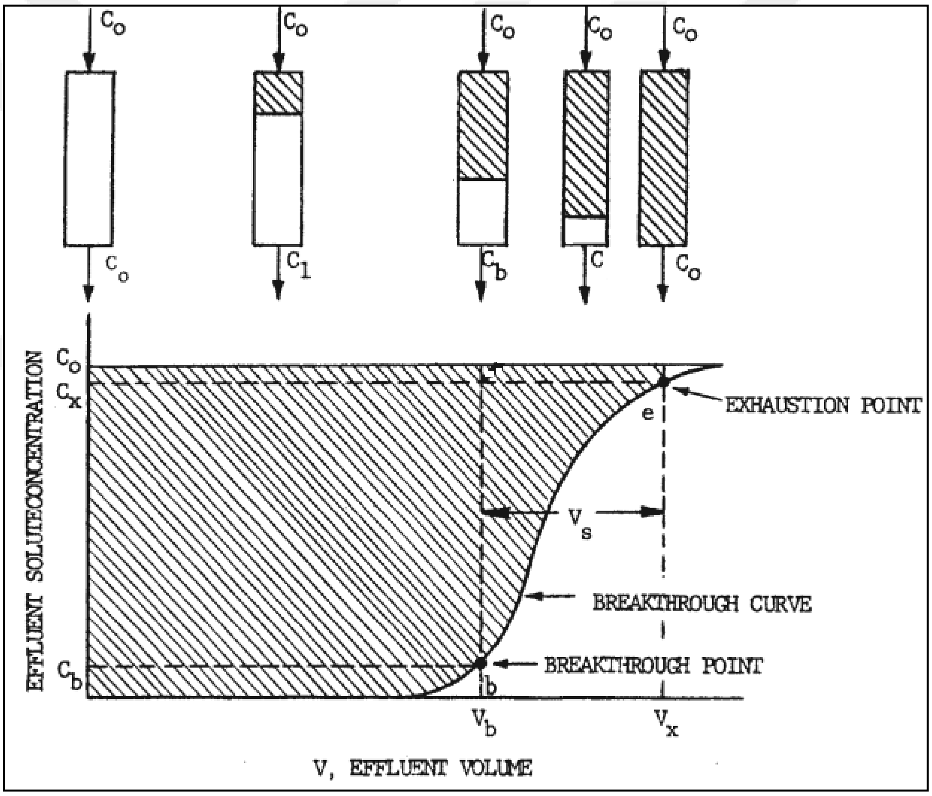

Figure 3.4 Mass transfer zone and idealized breakthrough curve

CHAPTER FOUR
MATERIALS AND METHODS

The principle aim of the thesis is to develop a competent and cost effective adsorbent from natural materials for arsenic removal. In this scope, sand and sepiolite were used as raw materials and modified with iron. Both raw and modified materials were used in batch experiments; and modified materials were used in column experiments in order to investigate the performance of arsenic removal and determine optimum design and operational parameters.

4.1 Reagents

All chemicals used were reagent grade. Deionized water was used to prepare all solutions. Arsenic stock solution was prepared by dissolving H_3AsO_4 (Merc Germany) in deionized water to a concentration 1000 mg/l; and preserved with 0.5 mol/l HNO_3 (Merc, Germany). 0.1 M NaOH and HCl were used to adjust pH.

4.2 Adsorbents

Sepiolite having significant deposits in Turkey, was used as adsorbent in the experiments. Raw sepiolite was provided from Duman Madencilik A.Ş., facilities in the Eskişehir region. Beside, raw sand was provided from IZSU (Water and Sewerage Authority of Izmir) which was utilized in sand filters in the drinking water treatment plants. Raw materials were analyzed by EDX to determine their composition. Components of the raw materials obtained by EDX studies are given in Table 4.1.

Before the experiments, raw materials were sieved in the range of of 212-300µm, 300-425 µm,425-600 µm and 710-1000 µm. Then, they were washed with deionized water and dried at 105°C.

Table 4.1 Components of the raw sand and sepiolite

Component (wt.%)	Raw Sand	Raw Sepiolite
C	17.768	-
O	22.759	21,998
Si	58.936	59.059
Na	0.537	-
Al	-	1.184
Mg	-	16.862
Ca	-	0.897
TOTAL	100.000	100.000

For modification purpose, materials were coated with ferric nitrate solution. In this procedure, 20 g of raw materials were mixed for 2 hours with 50 ml of a 0.5 M ferric nitrate solution at pH 10. The mixture was then dried at 200^{o}C in an oven for 15 hours. The coated materials were washed with deionized water until the water was clear, dried at 200^{o}C and stored in capped bottles.

In order to compare the performance of these materials with adsorbents used in arsenic treatment plants of IZSU, adsorbents I1 and I2 obtained from IZSU and used in the experiments.

4.3 Characterization Techniques

4.3.1 Surface Morphology and Elemental Analysis

In the experiments, surface morphologies and elemental composition of the materials were determined. Samples were coated with Au before SEM observations. The surface morphologies of materials were examined by a scanning electron microscope, SEM (JEOL JSM6060 Japan) at a voltage of 10-15 kV while the elemental analyses were conducted with an EDS attached to the SEM.

4.3.2 Phase Analysis

X-ray diffraction (XRD) analysis was performed to determine the crystal structure and identify the components. X-ray diffraction pattern was taken from X-ray diffractomer (Rigaku D/Max 2200PC diffractometer with Ni-filtered Cu Kα radiation). Randomly orientated samples were collected from 3° to 90° 2θ with a scanning rate of 4°/ min.

4.3.3 Specific Surface Area and Pore Volume Analysis

The Brunauer, Emmet and Teller (BET) method was employed to determine the surface area and pore volume of the materials by Mikromeritics Gemini V. The dry and degassed samples were analysed using a single or multipoint adsorption method for measuring the surface area (m^2/g). Nitrogen gas is used as adsorbent at 77K liquid nitrogen media.

4.4 Arsenic Measurement

Total arsenic, As(T), measurements were performed by an inductively coupled plasma-optical emission spectrometry (HG-ICP-OES) (Optima 2100 DV). Samples were preparad by adding 4.5 ml mixture of potassium iodine - KI (5%) and AA - ascorbic acid (5%) and 1 ml HCl (30%) to 4.5 ml sample (standard solution, reagent blank, and influent/effluent water) and kept for 24 hours before the measurement. In the study, arsenic concentrations were measured at 193.696 nm wavelength.

4.5 Batch Adsorption Studies

Batch adsorption experiments were achieved by mechanical shaker (WiseShake SHO-2D). The impacts of pH, contact time, initial arsenic concentration, adsorbent dose, particle size, and competition of ions were investigated in batch experiments. During the study, batch mode experimental procedure was carried out. Arsenic containing water was put in Erlenmeyer flasks at first, and adsorbents were (i.e. sand, modified sand, sepiolite, modified sepiolite, I1, I2) added to each flasks. After a predetermined contact time, shaking was stopped and the mixture in each flask was settled. After settling, samples were withdrawn from supernatant and prepared for arsenic measurements. Experiments were performed at room temperature (23 ^{o}C±2) shaking the mixtures at 100 rpm, and repeated two times. The photograph of experimental set-up is presented in Figure 4.1.

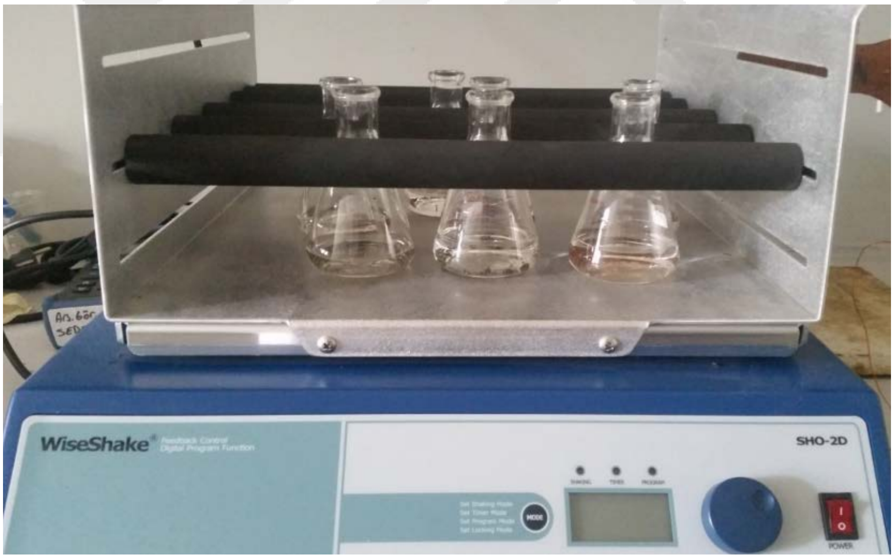

Figure 4.1 Experimental set up

4.5.1 *Effect of pH on Adsorption*

To study the effect of pH, the initial pH of the solution was varied from 4 to 10. The pH of arsenic solutions were adjusted adding 0.1 M NaOH and HCl solutions, and pH of the solutions was controlled by pH meter. Experiments were performed using 50 ml samples of water. Arsenic concentration was prepared as 130 μg/L, and

5 g/L of adsorbents (sand, modified sand, sepiolite, modified sepiolite, I1, I2) was put into each flasks. These solutions were shaken for 2 hours in a mechanical shaker at 100 rpm. After 2 hours, mixtures were settled and samples were taken from supernatant to analyze arsenic concentration at the effluent.

4.5.2 Effect of Contact Time on Adsorption

Experiments were performed at various contact time ranging between 15 minutes and 8 hours. Initial arsenic concentration was 100 µg/L, and adsorbent dosage (sand, modified sand, sepiolite, modified sepiolite, I1, I2) was 5.0 g/L. Experiments were done using 50 ml samples of water. pH of As solutions were adjusted as 7 by adding 0.1 M NaOH and HCl, based on the optimum pH tests. These solutions were shaken at 100 rpm through preset periods (i.e.at the end of 15, 30, 60, 120, 240 and 480 minutes); and after settling, samples were taken from supernatant to analyse arsenic concentration at the effluent.

4.5.3 Effect of Initial Concentration on Adsorption

Adsorption experiments were also performed at various initial arsenic concentrations, from 100 to 10000 µg/L with fixed doses (5g/L) of adsorbents (sand, modified sand, sepiolite, modified sepiolite, I1, I2). Experiments were done using 50 ml samples of water. Based on the previous experiments, pH of arsenic solutions was 7 and contact time was 4 hours. Following to 4 hours reaction period, each flask was settled, and samples were withdrawn from supernatant to analyze arsenic concentration at the effluent.

4.5.4 Effect of Adsorbent Dose on Adsorption

To optimize the adsorbent dose, adsorption studies were carried out with various dosages (1 to 50 g/L) of the adsorbents (sand, modified sand, sepiolite, modified sepiolite, I1, I2). In the experiments, initial arsenic concentration was 110 µg/L.

Experiments were done using 50 ml samples of water. Based on the previous experiments, pH of arsenic solutions was 7 and contact time was 4 hours. Following to 4 hours reaction period, each flask was settled, and samples were withdrawn from supernatant to analyse arsenic concentration at the effluent.

4.5.5 Effect of Particle Size on Adsorption

To investigate the effect of particle size, sand and sepiolite were crushed and sieved in the range of 212-300, 300-425, 425-600,710-1000 micrometers. They were also coated using the procedure as mentioned in part 4.2. In the experiments, initial arsenic concentration was 110 μg/L. For all the size of the materials (sand, modified sand, sepiolite, modified sepiolite), I1 and I2, 5 g/L optimum dose which was found from effect of adsorbent dose experiment was added all the arsenic solutions. pH of arsenic solutions was 7 and contact time was 4 hours. Following to 4 hours reaction period, each flask was settled, and samples were withdrawn from supernatant to analyse arsenic concentration at the effluent.

4.5.6 Arsenic Adsorption Experiments With Groundwater Sample

Arsenic bearing groundwater sample obtained from Balıkesir region was used to exhibit the effect of ions on arsenic adsorption. Major anions measured in the groundwater sample are presented in Table 4.2. Experiments were performed at pH 7 at room temperature (25^{o}C). Experiments were done using 50 ml samples of water. 5 g/L dose of modified sand and modified sepiolite were dosed to flasks. These solutions were shaken for 4 hours in a mechanical shaker at 100 rpm; and after a settling time, samples were taken from supernatant to analyse arsenic concentration at the effluent.

Table 4.2 Concentration of anions in the groundwater (Arsenic concentration is 100 µg/L±5)

Anions (mg/L)	Concentration (mg/L)
Chloride	5.9219
Nitrate	18.1381
Sulphate	10.4277
Bicarbonate	402.6
Phosphate	n.a.

4.6 Column Studies

Borosilicate glass columns filled with adsorbent was used in the fixed bed experiments. The internal diameter and height of a borosilicate glass column was 1.1 and 50 cm, respectively. At the bottom of the column, 1 cm height of glass wool was placed to hold the adsorbents. Modified sand and modified sepiolite, were studied separately in lab-scale column experiments. A peristaltic pump (Thermo Fh100m) was used to set desired flow rate to each column. The columns were operated with distilled water at first until the stable media height is obtained. Then, arsenic solution was fed to the column by a peristaltic pump. The water samples were collected from the outlet at certain time intervals and measured for the remaining arsenic in order to determine the breakthrough and exhaustion volume. The schematic diagram and photograph of the experimental set up are given in Figure 4.2 and 4.3.

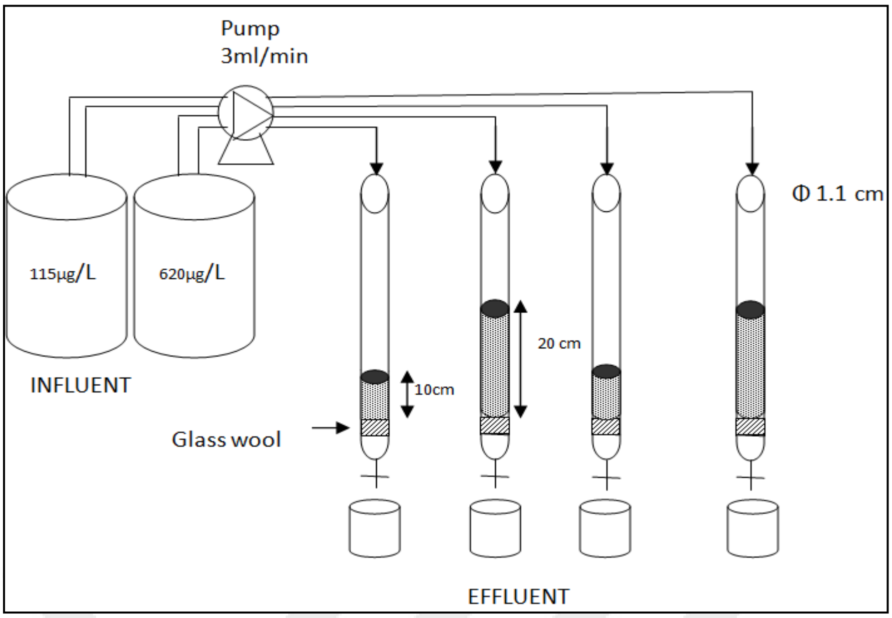

Figure 4.2 Schematic diagram of the experimental set up

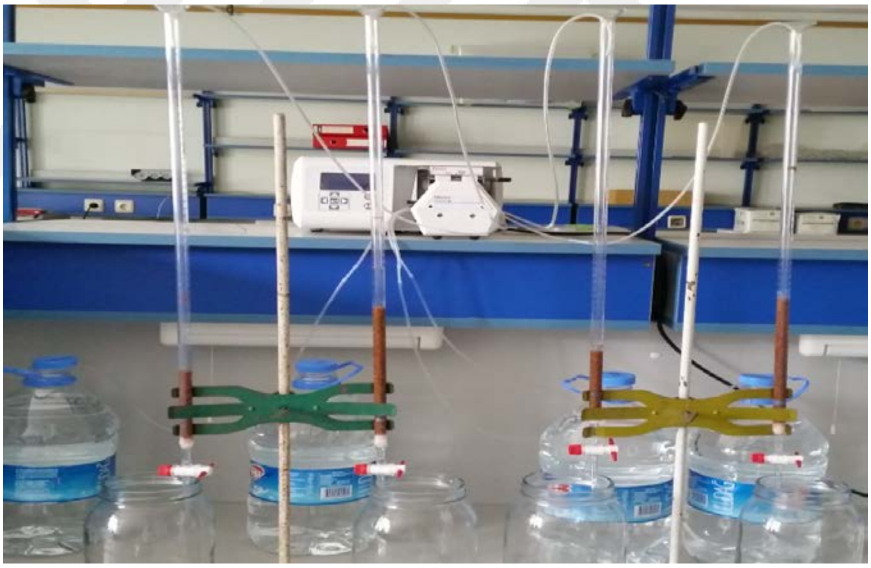
Figure 4.3 Photograph of the experimental set up

4.6.1 Effect of Column Height and Initial Arsenic Concentration on Adsorption

Experiments were performed with two different initial arsenic concentration (i.e. 115 µg/L and 620 µg/L) and bed heights (i.e. 10 and 20 cm) at room temperature (25^{o} C±2). In the first attempt, columns were filled with media (ironoxide modified sand and sepiolite media) at 10 and 20 cm heights. Arsenic containing water (115 μg As/L) was fed to the columns. The solution pH 7, determined in previous batch experiments, was used in the column studies. Columns were run in the down-flow mode and flow rate was set 3 ml/min. Effluent samples were taken from bottom part of the columns in certain time intervals and arsenic measurements were done by ICP-OES to obtain breakthrough and exhaustion volume.

In the second trial, initial arsenic concentration was increased to 620 μg/L to determine the impact of the arsenic concentration on media, and experiments without changing the conditions (i.e.pH, flowrate, temperature, etc) were carried out.

4.6.2 Effect of Flow Rate on Adsorption

In the column experiments, effect of flow rate was investigated, as well. Columns run in the down-flow mode at 3 ml/min and 6 ml/min flow rate for both modified sand and modified sepiolite columns. The length of the media was 20 cm, initial arsenic concentration was around 500 μg/L. The pH was maintained as 7 due to previous findings. Experiment were carried out at room tempereature (25^{o} C±2). Effluent samples were taken from outlet of the columns in certain time intervals and arsenic measurements were done by ICP-OES to obtain breakthrough and exhaustion volume.

4.7 Column Regeneration

Regeneration studies were done by alkaline solution for both iron oxide modified sand and sepiolite media. During the experiments, exhausted media was regenerated by 1% NaOH solution. For regeneration, 1% NaOH solution was fed with same flow rate (3 ml/min) in down flow mode, and samples were taken from outlet in certain time intervals and arsenic measurements were done. Feeding of NaOH solution was terminated when effluent arsenic concentration decreased to the standards (<10 μg/L). Afterward, in order to provide protonated surface, dilute acid solution (HCl) was fed to the column. Following to acid treatment, column was washed with distilled water until the effluent pH was increased to 7.

In order to determine life span of media (in other words total regeneration number), column was operated with same conditions, i.e. 560 μg/L initial arsenic concentration, pH of 7, and 10 cm bed depth. Column was run in the down-flow mode and flow rate was set 3 ml/min. Effluent samples were taken from outlet in certain time intervals and arsenic measurements were done by ICP-OES.

CHAPTER FIVE
RESULTS AND DISCUSSION

5.1 Characterization of the Materials

5.1.1 Surface Morphology and Elemental/Phase Analysis

The materials used in the study (i.e. sand, modified sand, sepiolite and modified sepiolite) are shown in Figure 5.1. The elemental analysis of the materials conducted with an EDX are presented in Table 5.1. As it was expected, the major components of sand were silica (58.9%), oxygen (22.6%) and carbon (17.7%) and no iron was detected. Due to modification with iron, 21% iron was detected at modified sand samples. Beside the iron, other elements, i.e. carbon (16.8%), oxygen (16.7%), silica (40.3%) and sodium (5%) were also measured. Furthermore, sepiolite, a type of clay mineral, was analysed by using EDX. Silica (59%), oxygen (22%) and magnesium (16.9%) were detected at raw sepiolite samples. As a result of the modification process, iron component was 3.4% at modified sepiolite samples. The reason of less iron content of modified sepiolite compared to modified sand is related to property of EDX analysis that gives result only from surface. Since sepiolite is a very porous material, iron could be attached into the pores. Higher treatment performance obtained from the experiments carried out by sepiolite endorsed this result, as well.

Figure 5.1 Photos of materials, a) Sand, b) Modified sand, c) Sepiolite, d) Modified sepiolite

Table 5.1 Elemental analysis of raw sand, modified sand, sepiolite and modified sepiolite

Component (wgt.%)	Raw sand	Modified sand	Sepiolite	Modified sepiolite
C	17.768	16.869	-	-
O	22.759	16.789	21,998	22.568
Si	58.936	40.308	59.059	60.708
Na	0.537	5.031	-	-
Al	-	-	1.184	2.323
Mg	-	-	16.862	10.628
Ca	-	-	0.897	0.333
Fe	-	21.002	-	3.440
Total	100.000	100.000	100.000	100.000

Phase analysis of the materials were determined by XRD analysis and given in Figure 5.2 (a-b) and Figure 5.3 (a-b). Regarding to XRD analysis, the main phase of sand is quartz, however for sepiolite, as it was expected, mullite and magnesium silicate are found beside quartz. Iron oxide and ferrosilite was only detected for modified sand and sepiolite, respectively.

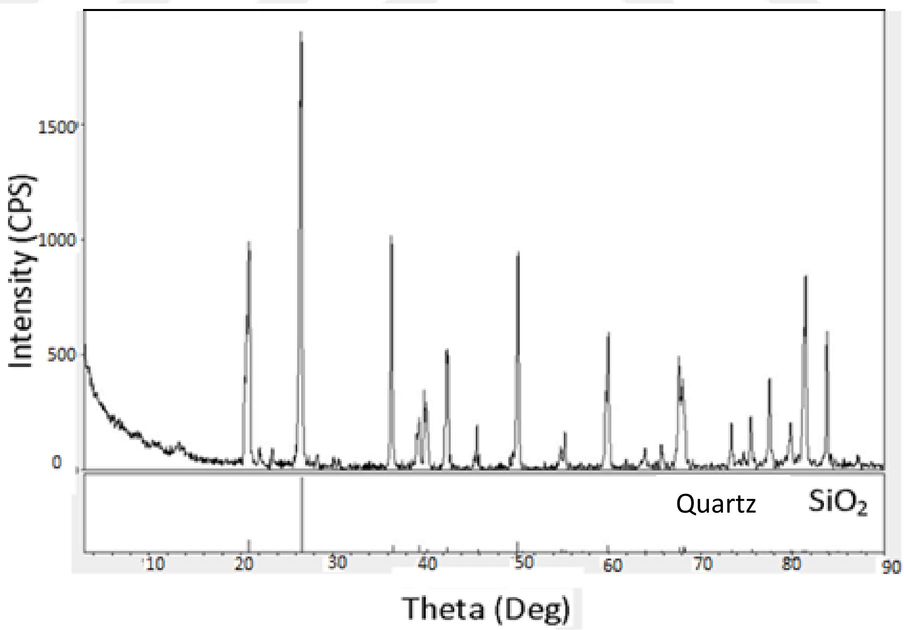

Figure 5.2 XRD analysis of sand materials, a) sand, b) modified sand

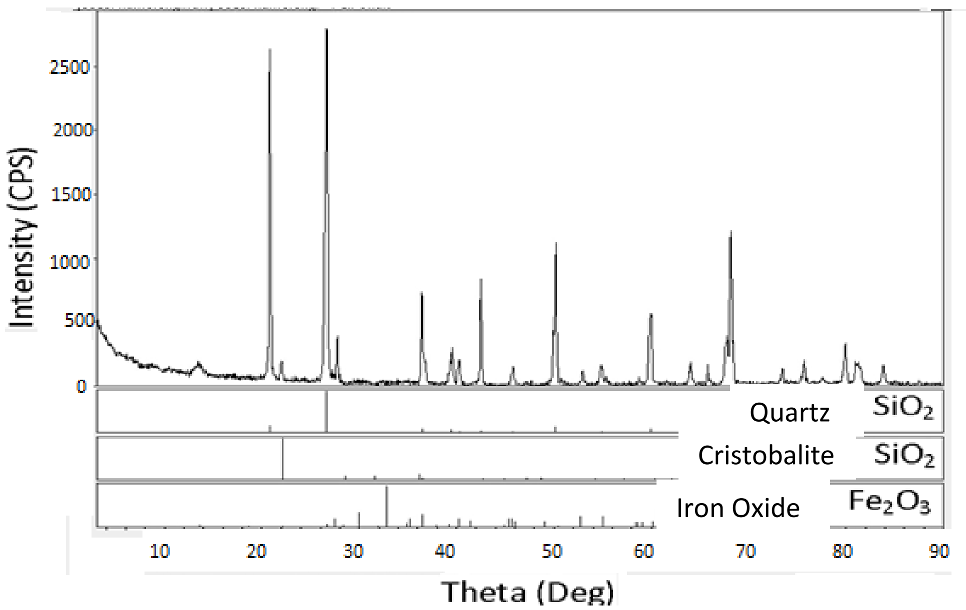

(b)

Figure 5.2 XRD analysis of sand materials, a) sand, b) modified sand (cont.)

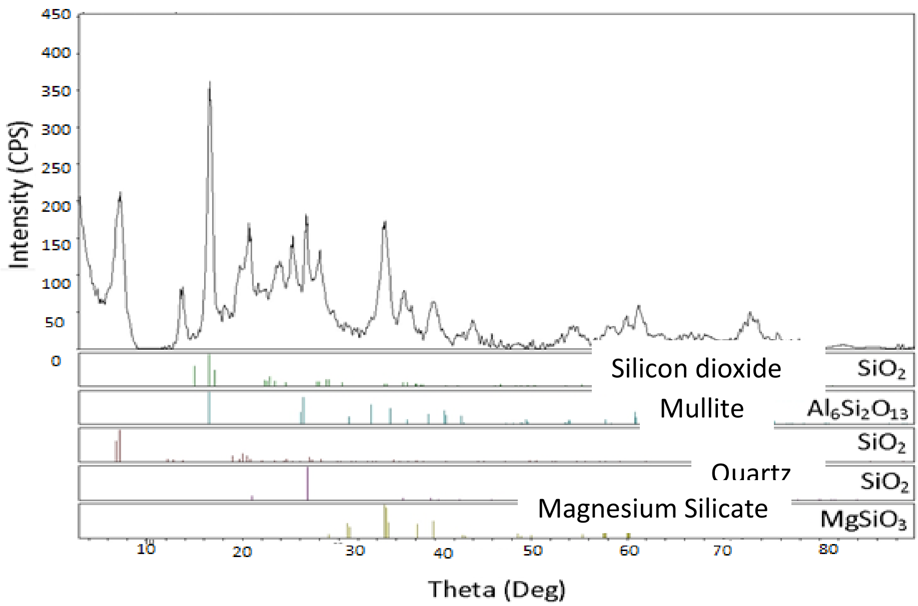

Figure 5.3 XRD analysis of sepiolite materials, a) sepiolite, b) modified sepiolite

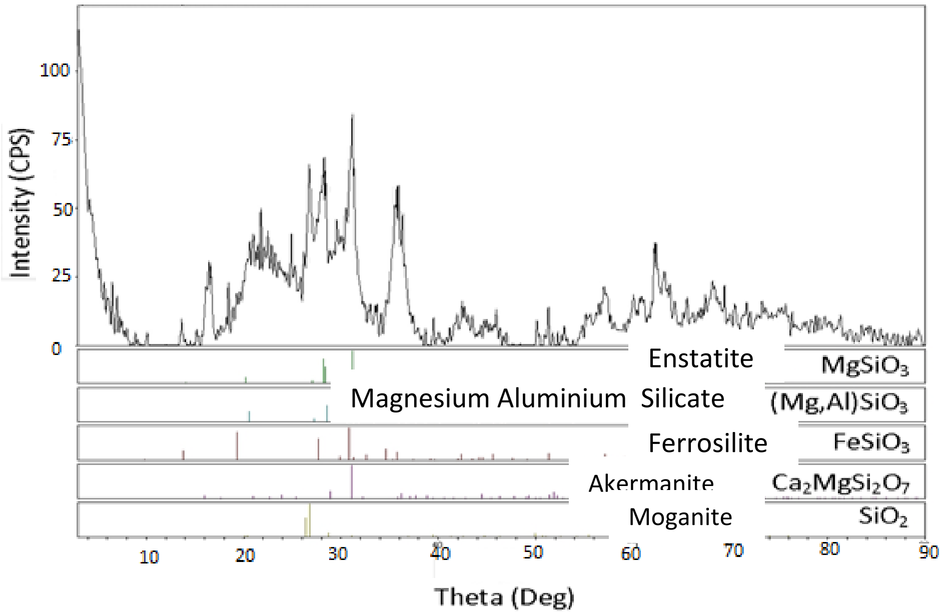

(b)

Figure 5.3 XRD analysis of sepiolite materials, a) sepiolite, b) modified sepiolite (cont.)

SEM images in Figure 5.4 and 5.5 were taken both at 75x and 1000x magnifications to observe the surface morphology of sand, modified sand, sepiolite and modified sepiolite, respectively. As seen in Figure 5.4 raw sand has a quite smooth surface due to non porous structure, whereas modified sand has a rough surface. In addition, sand surface occupied by the iron oxide coating which were formed during modification process (see Figure 5.4 -d).

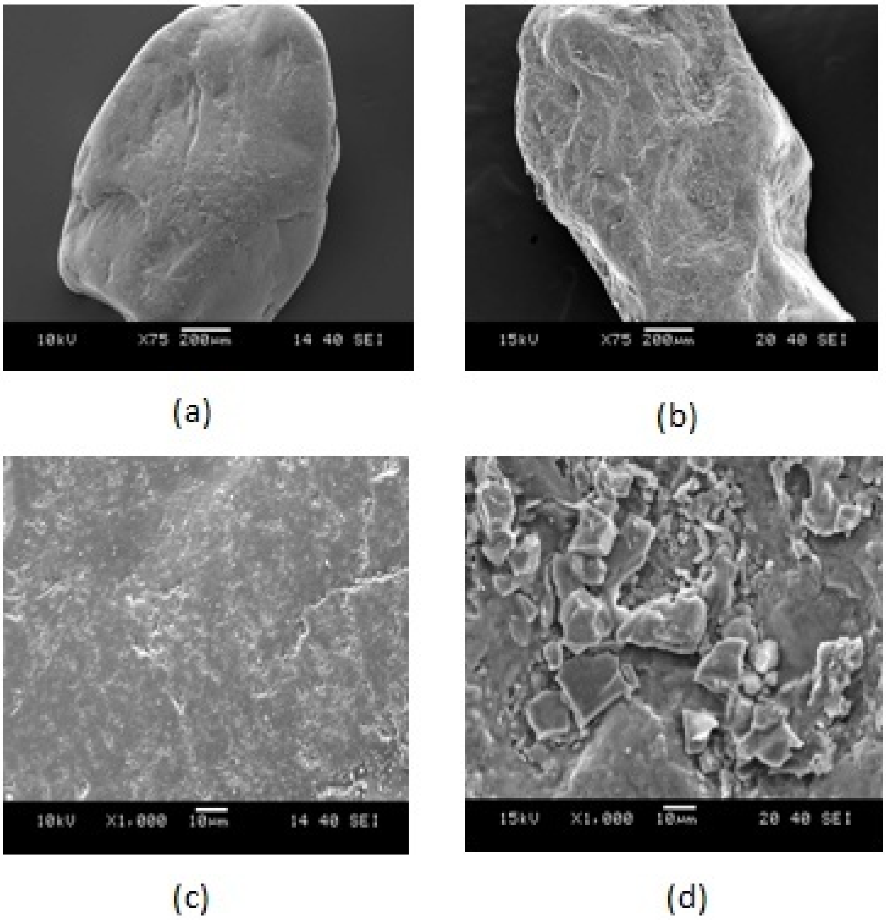

Figure 5.4 SEM images of sand materials, a) 75x magnification of sand, b) 75x magnification of modified sand, c)1000x magnification of sand and d) 1000x magnification of modified sand

As can be seen in Figure 5.5, both sepiolite and modified sepiolite has a quite porous structure. Micropores or roughness can be found on the sepiolite surface. Contrast to modified sand samples, iron oxide coating attached to the surface of sepiolite particles due to modification process cannot be seen clearly because of surface properties (see Figure 5.5 (1000x magnification).

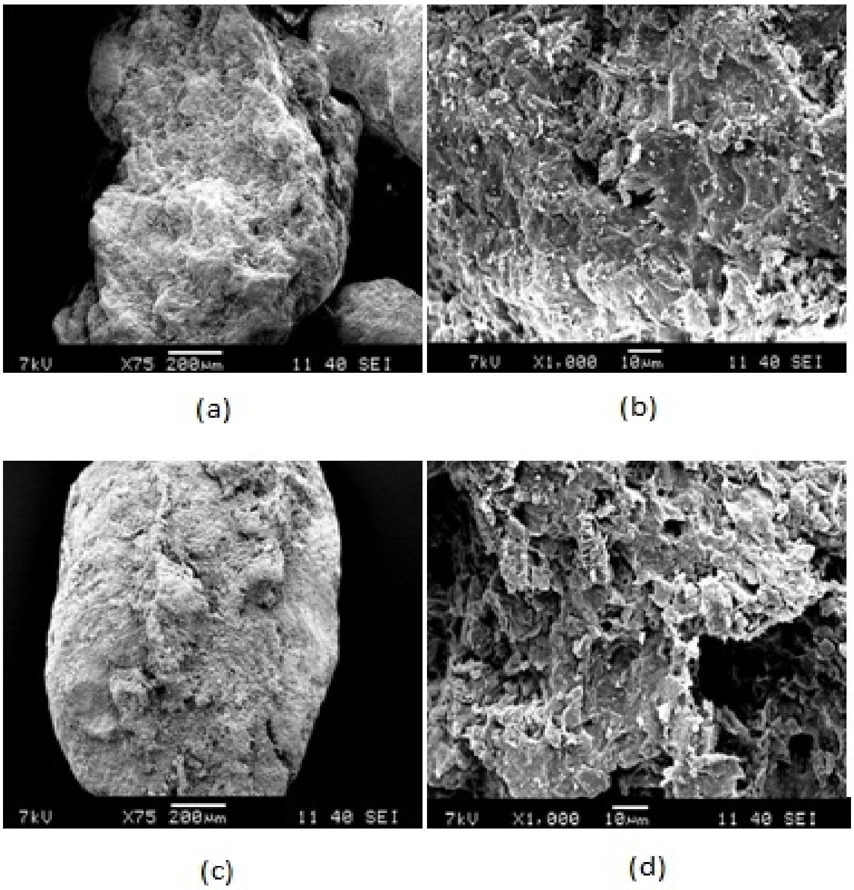

Figure 5.5 SEM images of sepiolite materials, a) 75x magnification of sepiolite, b) 75x magnification of modified sepiolite, c)1000x magnification of sepiolite and d) 1000x magnification of modified sepiolite

5.1.2 Surface Area and Pore Volume Analysis

Surface area, pore volume and average pore size of the materials were determined by BET analysis. Since size of the particles is important to determine the adsorption capacity, particles having different diameters between 300-1000 µm were used in the experiments. Results of the BET analyses are presented in Table 5.2. BET surface area of raw sand ranged 710-1000 µm was measured as 0.9 m^2/g. Modification with iron was resulted an increase in the surface area. BET surface area was increased to 1.1581 m^2/g yielding 30% expansion. Total pore volume was increased from 0.0011 cm^3/g to 0.0015 cm^3/g, when material modified with iron. Average pore size was 48.54Å for raw sand material, and raised to 52.55 Å. Results showed that iron oxide coating process increased the pore size as well as surface area of sand material. In addition, decreasing the particle size resulted by an increase in surface area, as well.

BET surface area of the modified sand particles having size 710-1000 μm, 425-710 μm and 300-425 μm were determined as 1.1581 m^2/g, 1.68 m^2/g, and 3.21 m^2/g, respectively. No micropore area was detected for all of the sand samples due to its nonporous surface. Total pore volumes of sand samples were quite small and no micropore volume was detected.

Table 5.2 Surface area and pore volume of adsorbents used in the experiments

Material	**Surface Area (m^2/g)**		**Pore Volume (cm^3/g)**		**Avg. Pore Size (Å)**
	BET	Micropore Area	Total	Micropore Volume	
Sand (710-1000 μm)	0.9039	-	0.0011	-	48.54
Modified Sand (710-1000 μm)	1.1581	-	0.0015	-	52.55
Modified Sand (425-710 μm)	1.68	-	0.0035	-	83.74
Modified Sand (300-425 μm)	3.21	-	0.0059	-	73.75
Sepiolite (710-1000 μm)	197.28	46.33	0.41	0.0195	82.35
Modified Sepiolite (710-1000 μm)	183.24	33.92	0.39	0.0139	85.72
Modified Sepiolite (425-710 μm)	177.01	34.38	0.37	0.0142	84.14
Modified Sepiolite (300-425 μm)	188.80	35.11	0.38	0.0144	81.48

As can be seen in Table 5.2, BET surface area of sepiolite was quite high comparing to sand samples. Raw sepiolite, ranged in 710-1000 μm, had 197.3 m^2/g BET surface area whereas 0.9039 m^2/g surface area was provided for raw sand material. BET surface area of modified sepiolite ranged in 710-1000 µm was 183.24 m^2/g, thus relatively small decrease was observed when sepiolite was modified with iron. Unlike the sand, decreasing the particle size of sepiolite did not resulted by an increase in surface area. BET surface area of the modified sepiolite particles having size 710-1000 µm, 425-710 µm and 300-425 µm were determined as 183.24 m^2/g, 177.01 m^2/g, and 188.80 m^2/g, respectively. Raw sepiolite particles have micropores in its structure and its micropore area was 46.33 m^2/g for 710-1000 µm. Micropore areas were 33.92 m^2/g, 34.38 m^2/g, and 35.11 m^2/g for modified sepiolite samples having diameter between 710-1000 µm, 425-710 µm and 300-425 µm, respectively. In general, modification with iron resulted with decrease in the micropore area. Decrease in micropore area could be explained with the occupying the pores with iron in modified material. And, total pore volume was 0.41 cm^3/g for raw sepiolite having diameter 710-1000 µm, and changed between 0.39 and 0.38 cm^3/g for modified sepiolite in different sizes. Regarding to pore volumes, it could be stated that significant variations did not measure for modified sepiolite. Additionally, insignificant variations in average pore size were measured for sepiolite.

As conclusion, sepiolite has much larger area than sand due to porous structure, and has micropores. However, in contrast to sand samples, ironoxide coating caused a slight decrease in micropore area and pore volumes as well as surface area for sepiolite particles.

5.2 Batch Experiments

5.2.1 Effect of pH on Adsorption

The effect of the pH (4-10) on adsorption of As (T) is illustrated in Figure 5.6-5.9. Materials experienced in this study were sand, modified sand, sepiolite and modified sepiolite. Besides that, two different packing materials that have been used in the arsenic filters in İzmir were tested to compare the performance of materials utilized in this study. The maximum As (T) removal efficiency (i.e. 76%) was obtained at pH 7 for modified sand material. The removal rate was reduced to 68% for pH 4 and to

52% for pH 10. The efficiency of the raw sand material was negligible within the pH range investigated. The increase in As (T) uptake for modified sand material is explained with increasing of positive surface charges. Surface modification by iron was resulted with positive surface charge on the material and arsenic could be adsorbed on this available active sites at optimum pH condition. However, the negative surface sites on the raw sand material hindered As (T) adsorption, therefore As (T) uptake did not carry out by raw sand material. In general, adsorption occurred more effectively at neutral pH, and alkaline and acidic conditions were not favourable for As (T) uptake.

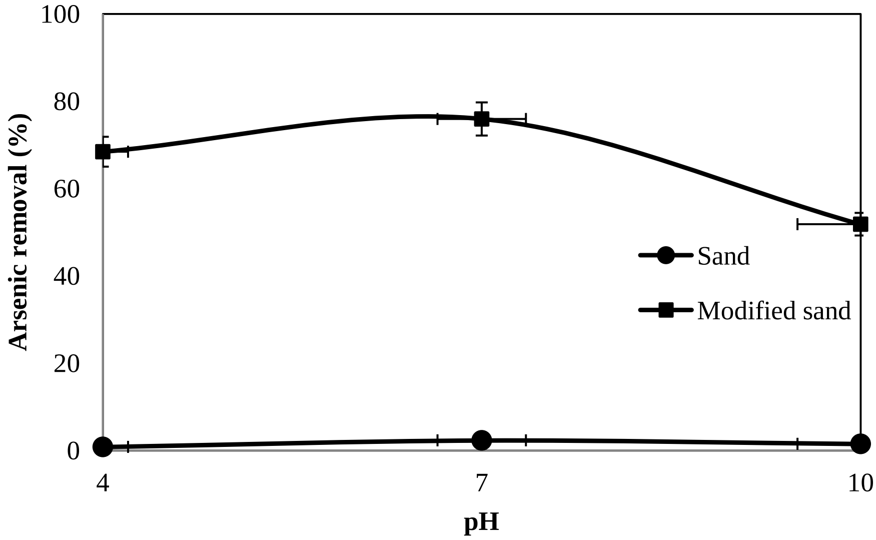

Figure 5.6 Effect of pH on arsenic removal for sand and modified sand

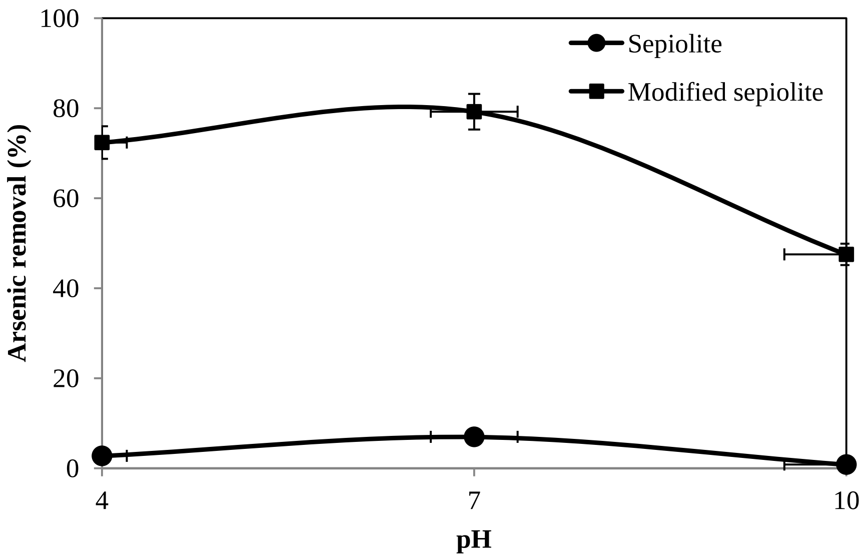

Figure 5.7 Effect of pH on arsenic removal for sepiolite and modified sepiolite

Figure 5.7 shows effect of pH on arsenic removal for sepiolite and modified sepiolite. Similar to sand experiments, sepiolite was effective under neutral and acidic conditions. The performance of raw sepiolite was poor under acidic, alkaline and neutral condition, however, modification with iron increased arsenic uptake. The lowest performance (i.e. 47.5%) was obtained for alkaline conditions, at pH 10. However for pH 7, approximately 80% removal efficiency was obtained. Decreasing pH from 7 to 4, was resulted with reduced removal rates. The pH of the arsenic contained water in the experiments was 7. Therefore $H_2AsO_4^{-}$ and $HAsO_4^{2-}$ were predicted to be the main arsenic species in the water and could be adsorbed onto the positive surfaces of modified materials via ion exchange/ion attraction (Maji et al., 2011).

As it was explained in previous paragraph, adsorbents I1 and I2 obtained from IZSU were used to compare their performances. Figure 5.8 and 5.9 show the effect of pH on arsenic removal for I1 and I2. Removal efficiency was obtained as 97% for I1 and did not change with the solution pH. The performance of I2 was slightly lower than I1. The lowest efficiency (83.5%) was obtained under alkaline condition (i.e. pH 10) whereas it reached to 92% under neutral conditions.

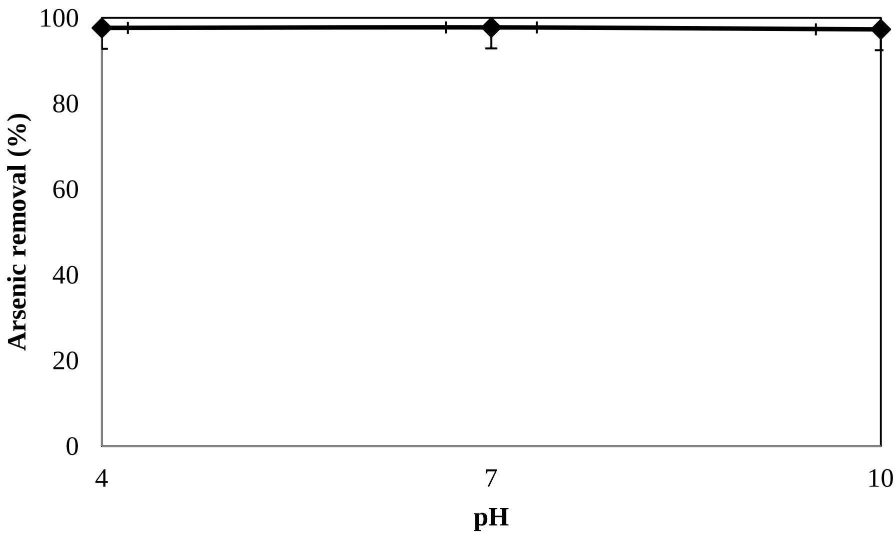

Figure 5.8 Effect of pH on arsenic removal for I1

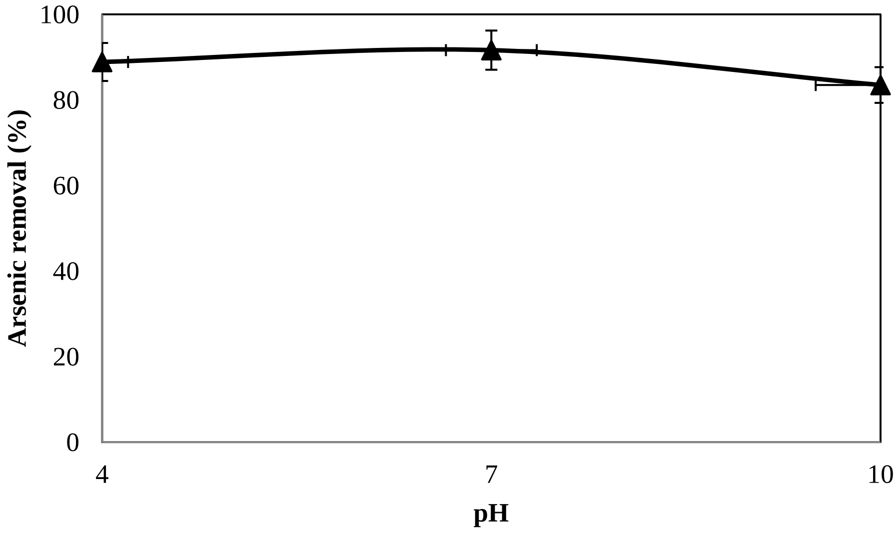

Figure 5.9 Effect of pH on arsenic removal for I2

5.2.2 Effect of Contact Time on Adsorption

Effect of the contact time on adsorption of As (T) is illustrated in Figure 5.10-5.13. Materials experienced in this study were sand, modified sand, sepiolite and modified sepiolite. Besides that, two different packing materials that have been used in the arsenic filters in İzmir were tested to compare the performance of materials utilized in this study. The pH of the solution was 7, and the contact time varied from 15 minutes to 8 hours. Initial arsenic concentrations were about 100 µg/L and adsorbent dose of 5 g/L for all materials.

Contact time had negligible effect with 2-2.3% removal rate for sand as shown in Figure 5.10. However, for modified sand, approximately 50% of arsenic was removed within 30 minutes, and at the end of 2 hours removal rate increased to about 78%. After that, arsenic uptake slightly increased and reached to approximately 90% at the end of the 8 hours. Since the increases in removal rates were not significant after 4 fours, optimum contact time was taken as 4 hours.

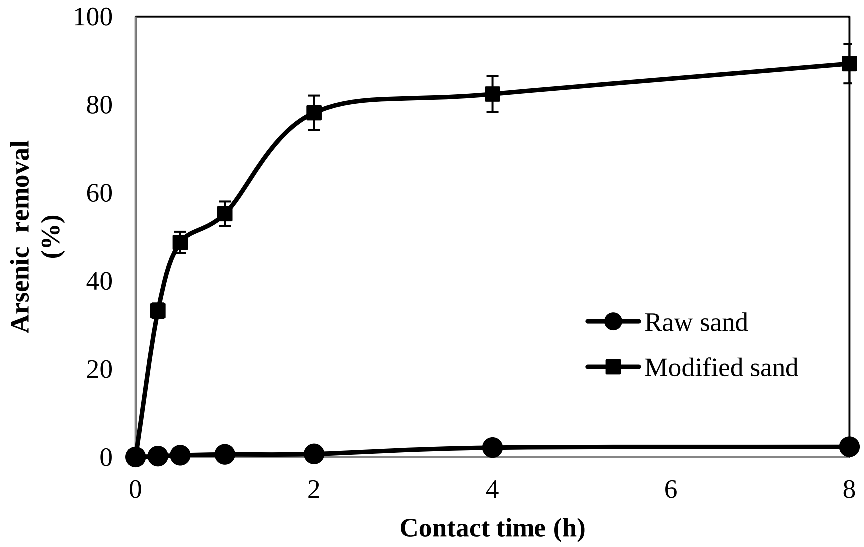

Figure 5.10 Effect of contact time on sand and modified sand

Figure 5.11 shows effect of contact time on arsenic removal for sepiolite and modified sepiolite. It can be clearly seen from Figure 5.11 that raw sepiolite had not any adsorption capacity for a period of eight hours. However, for modified sepiolite, approximately 60% arsenic uptake was achieved within 30 minutes. Removal rates continued to rise for 2 hours and reached to 82% at the end of the 2 hours. After that, removal rates relatively descended and at the end of the 4 hours, 89% of initial arsenic concentration was removed. Since the efficiency between 4 and 8 hours did not show significant variation, optimal contact time was accepted as 4 hours for modified sepiolite, too.

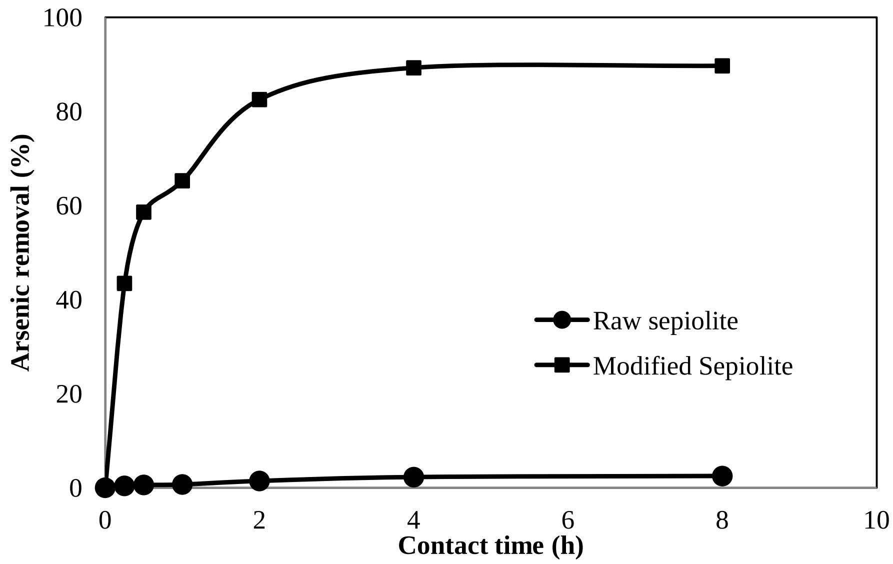

Figure 5.11 Effect of contact time on sepiolite and modified sepiolite

Effect of contact time on arsenic removal for the materials I1 and I2 are shown in Figure 5.12 and 5.13. Superior removal rates were obtained for I1, within the first fifteen minutes arsenic removal rate reached to 93.8%. And, almost all of the arsenic removed at the end of the four hours contact time. On the other hand, performance of the I2 was comparable with modified sand and modified sepiolite (see in Figure 5.13). Approximately 70% of initial arsenic concentration was removed within first 30 minutes. Arsenic uptake reached to 96% at the end of the 2 hours.

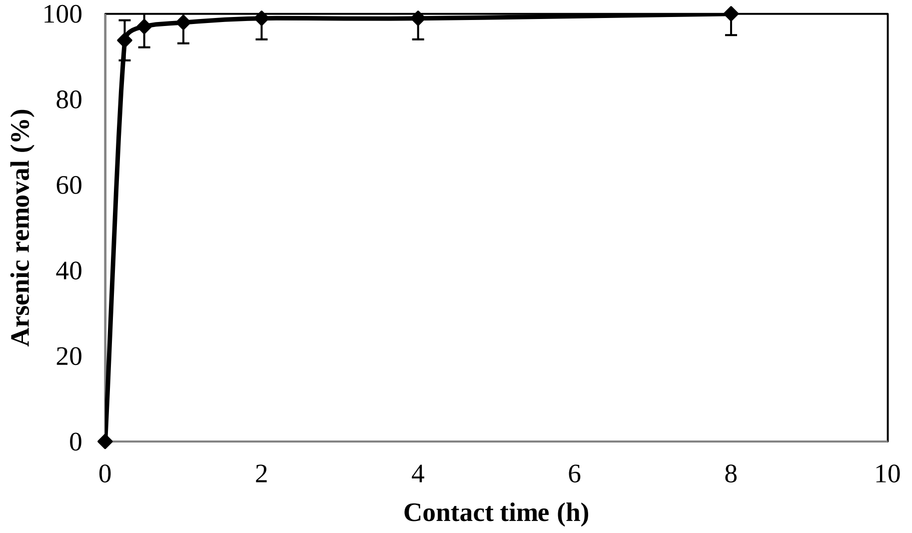

Figure 5.12 Effect of contact time on I1

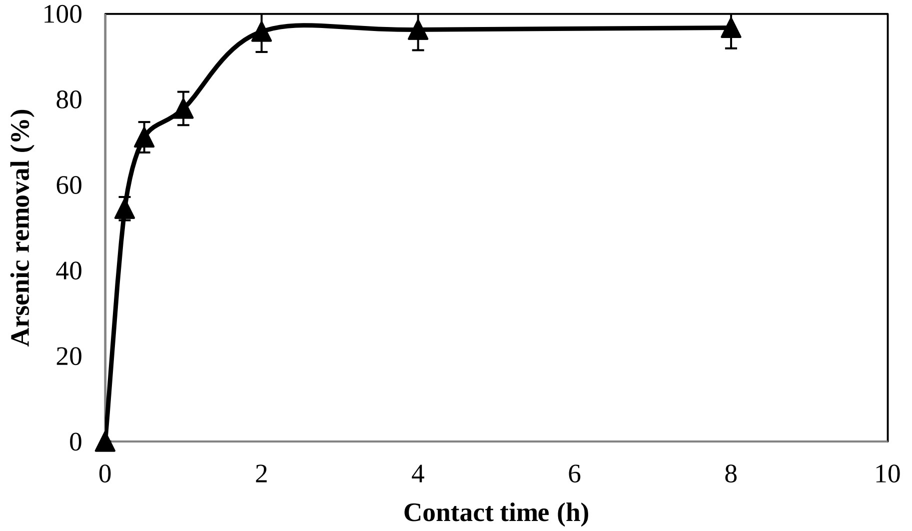

Figure 5.13 Effect of contact time on I2

5.2.3 Effect of Initial Arsenic Concentration on Adsorption

In order to investigate effect of initial arsenic concentration on adsorption, solutions including various arsenic concentrations were prepared. Contact time was taken four hours as optimum time, and 5 g/L of adsorbent was used in the study. Experiments were performed at a wide range of arsenic concentration between 110 μg/L and 9961 μg/L.

Figure 5.14 shows the effect of initial arsenic concentration on sand and modified sand. Adsorption capacity was very poor even at lower initial arsenic concentrations for raw sand (see Figure 5.14). For modified sand, as can be seen in Figure 5.14, arsenic removal rates reduced gradually when initial arsenic concentration increased. In the experiments, the maximum arsenic adsorption was obtained as 91.2% for initial arsenic concentration of 110 µg/L. When initial arsenic concentration increased two folds (i.e. 273 µg/L) and ten folds (i.e. 1613 µg/L), 70% and 44% of arsenic could be removed. Limited surface area and nonporous surface of sand resulted with decrease in removal efficiency for increasing concentrations. The lowest efficiency was obtained for initial arsenic concentration of 3200 µg/L, only 27% of As (T) was removed.

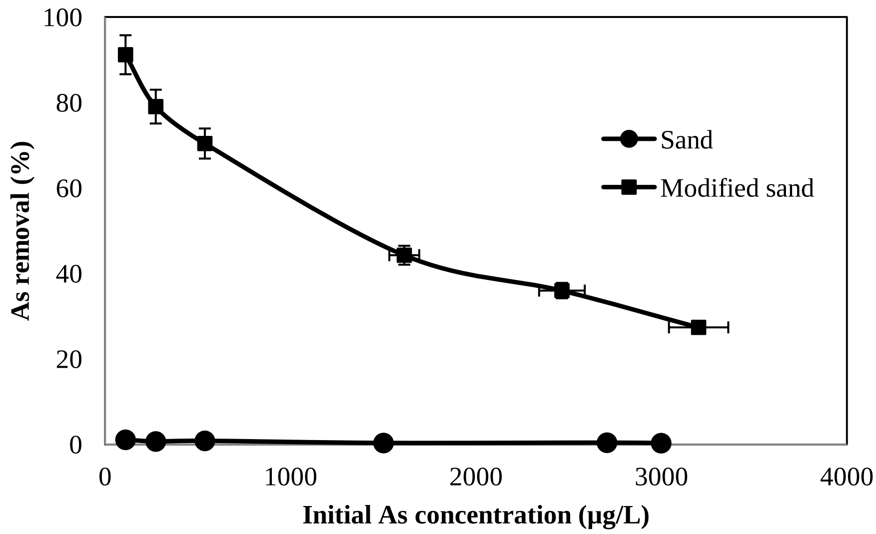

Figure 5.14 Effect of initial arsenic concentration on sand and modified sand.

Figure 5.15 shows the effect of initial arsenic concentration on sepiolite and modified sepiolite. Similar to previous results, the performance of the raw sepiolite was not sufficient, and even at low initial concentrations (110 µg/L), only 3.5% of initial concentration could be removed. For modified sepiolite, initial concentrations of As (T) from 110 to 538 µg/L, did not cause significant variations on removal rates (i.e. 92-94% removal). Afterwards, a sharp decrease was observed when initial arsenic concentration reached to 1613 μg/L, and 80% removal efficiency were achieved. And, for higher concentrations (i.e. above 1613 μg/L) removal efficiency did not significantly change. The lowest efficiency was 72.8% for initial concentrations of 9961 μg/L. From Figure 5.15, it can be clearly stated that modified sepiolite has a great adsorption capacity. Adsorption occurred not only on surface also in pores of sepiolite. Due to porous surface and higher surface area of sepiolite, arsenic removal efficiency was not affected so much from initial concentration like sand experiments. Although decreasing arsenic removals in increasing concentrations, modified sepiolite had a considerable performance even such a high concentration like 1613 μg/L without pre-treatment.

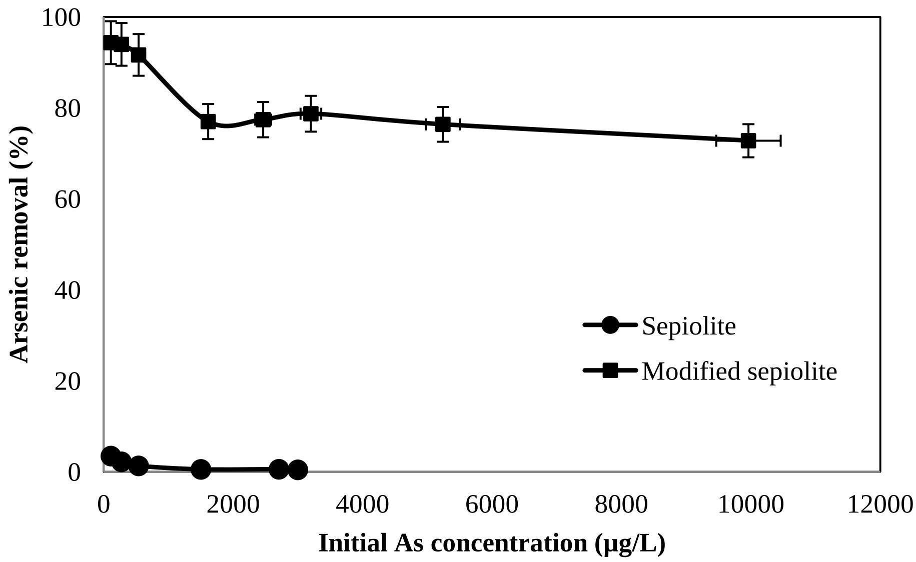

Figure 5.15 Effect of initial arsenic concentration on sepiolite and modified sepiolite

Effect of initial arsenic concentration on I1 and I2 are illustrated in Figure 5.16 and Figure 5.17. As it was indicated before, adsorptive performance of I1 was excellent. Approximately 99% removal efficiency was obtained for all initial concentrations, and higher concentrations did not affect the arsenic removal rate for I1. The performance of I2 was comparable with modified sepiolite especially for moderate initial As (T) concentrations (from 110 to 538 μg/L). However, after that point (i.e. above 538 μg/L), arsenic uptake of I2 did not significantly change. For the highest initial arsenic concentration (i.e. 9961 μg/L), 91% of removal was obtained.

Thus, the results indicated that I1 and I2 have high adsorption capacities even at high arsenic concentrations.

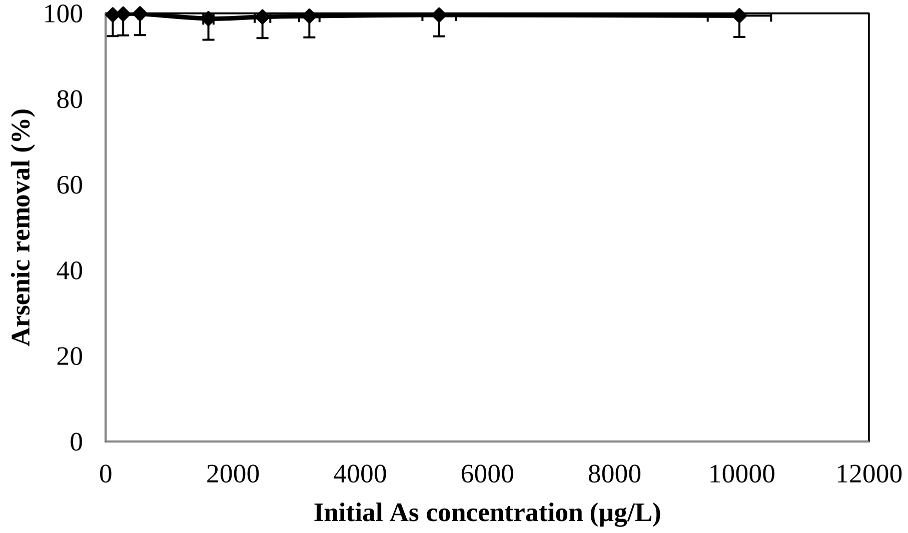

Figure 5.16 Effect of initial arsenic concentration on I1

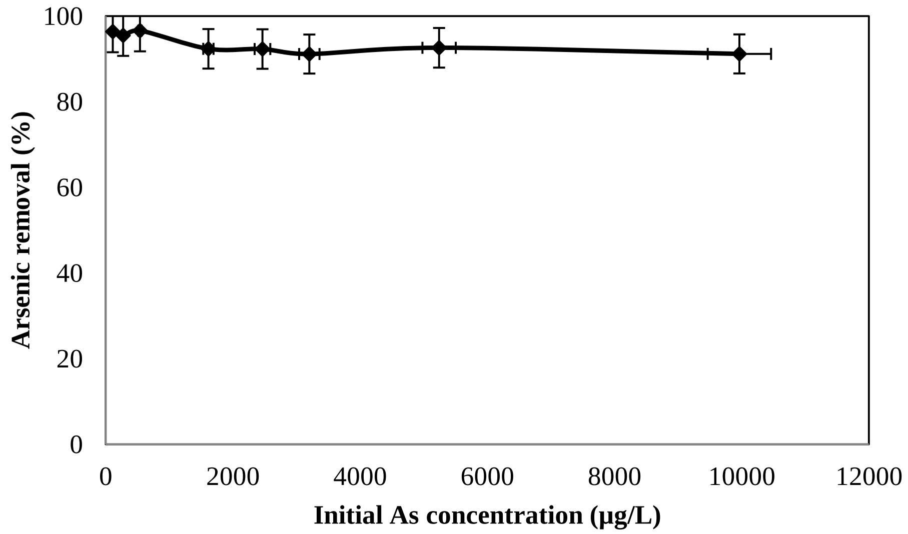

Figure 5.17 Effect of initial arsenic concentration on I2

5.2.4 Effect of Adsorbent Dose on Adsorption

In order to determine the optimum adsorbent dose, experiments were done with varied adsorbent dosages. In the experiments initial As (T) concentration was about 110 µg/L, contact time 4 hours, and pH was 7. Raw materials did not perform effectively, and results were fitted well with previous experiments. As can be seen in Figures 5.18 and 5.19, for both modified sand and sepiolite, adsorbent doses less than 5 g/L resulted with lower removal rates (<50%). However, arsenic removal was considerably increased for 5g/L and reached to 91% efficiency. After that, removal rates did not significantly change and reached to 96-97% for 50 g/L adsorbent dose. Higher removal efficiency for increasing adsorbent doses can be explained with providing additional available adsorption sites. The experiments performed with adsorbent dosages greater than 5g/L, did not result with increased removal efficiency due to low initial concentration. The results showed that 5 g/L adsorbent dose is sufficient to obtain desired arsenic levels for 110µg/L initial arsenic solution.

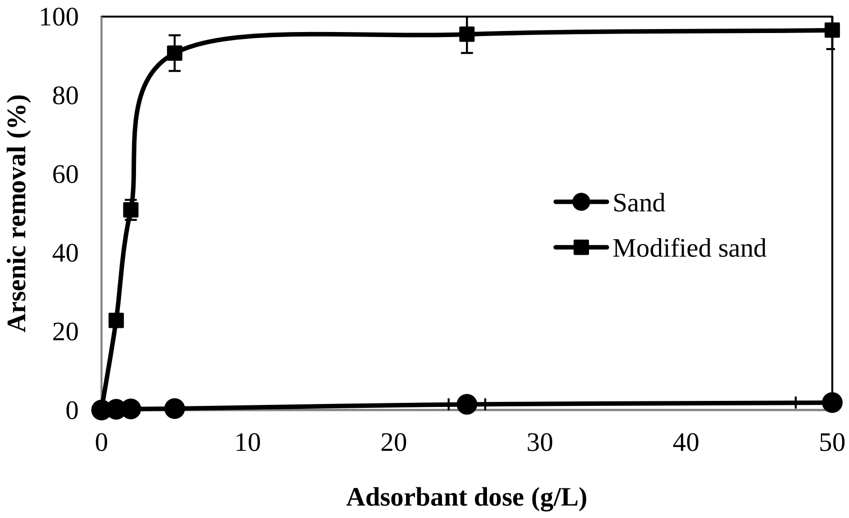

Figure 5.18 Effect of adsorbent dose on sand and modified sand

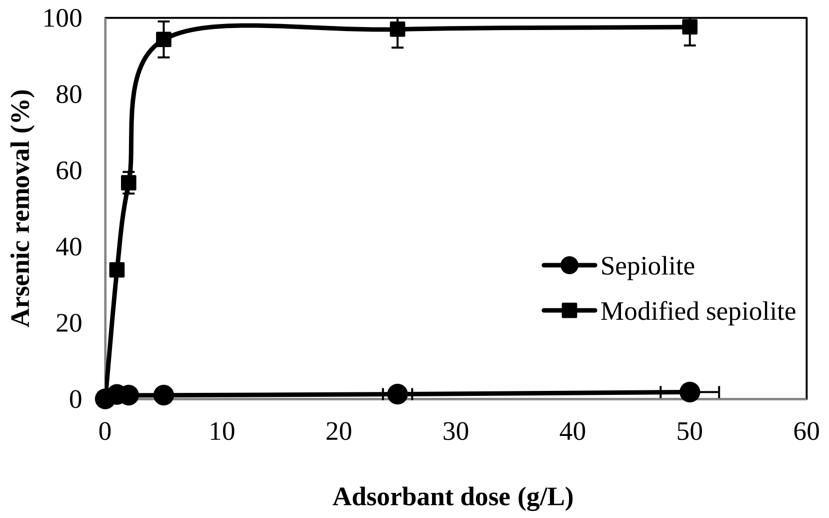

Figure 5.19 Effect of initial adsorbent dose on sepiolite and modified sepiolite

Figure 5.20 and Figure 5.21 show the effect of adsorbent dose for I1 and I2. As can be seen in Figure 5.20, 1 g/L of adsorbent was sufficient to obtain 94% removal efficiency for I1. For 2 g/L adsorbent, efficiency were increased to 97% and did not significantly change after 2 g/L. These results indicate that I1 has a large surface area and pore volume. It has high adsorption capacity even though less dosage was used. However, I2 showed similar trend with modified sand and modified sepiolite as shown in Figure 5.21. For 1 g/L and 2 g/L adsorbent doses, removal rates were 58.6% and 76.0%, respectively. Up to 5 g/L arsenic removal efficiency rapidly increased and reached 95.5%. Arsenic removal rates did not considerably increase at 25 g/L and 50 g/L and obtained 97.8% and 98.1%, respectively.

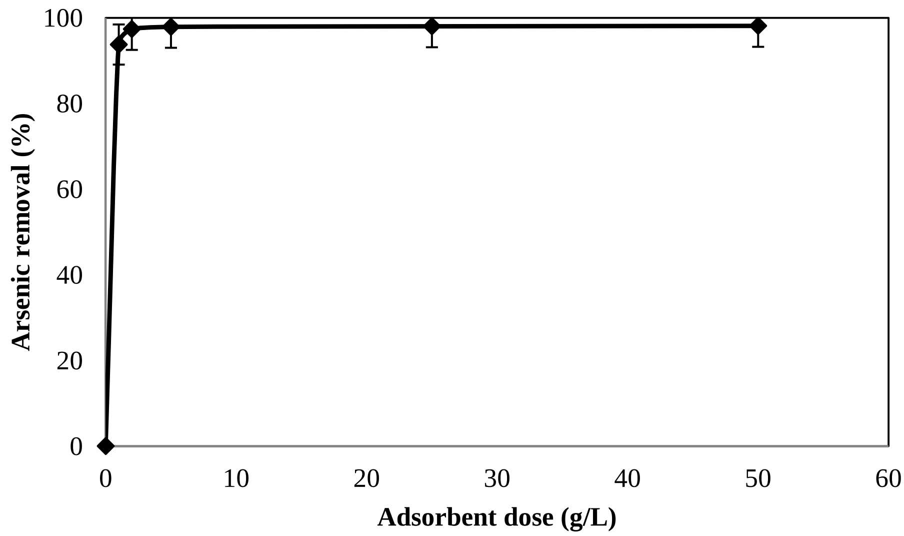

Figure 5.20 Effect of initial adsorbent dose on I1

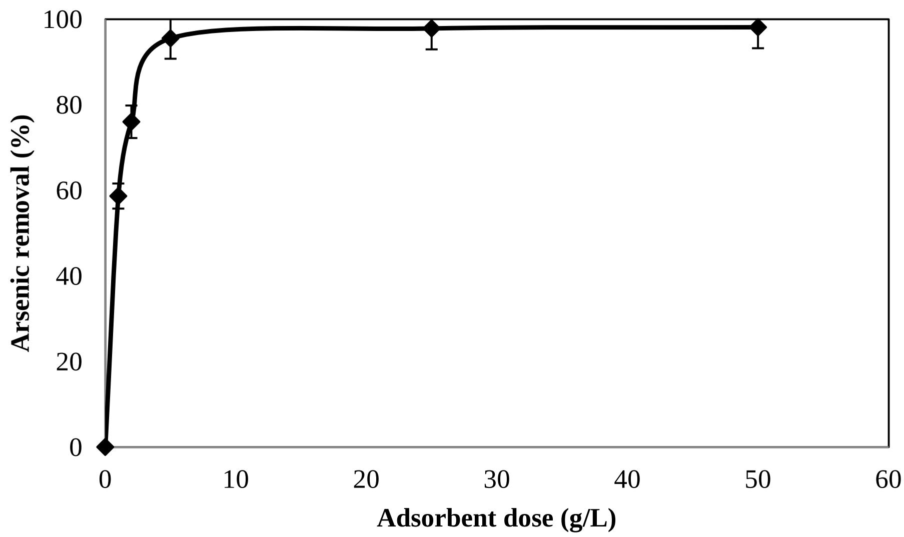

Figure 5.21 Effect of initial adsorbent dose on I2

5.2.5 Effect of Particle Size on Adsorption

Since the particle size has an effect on adsorption capacity by affecting the surface area and pore volume, effect of particle size on arsenic removal were experienced. In the experiments, initial As (T) concentration was about 110 μg/L, contact time 4 hours, and pH was 7. Adsorbent dose was 5 g/L for both raw and modified materials.

Particle sizes were ranged in 212-1000 μm. The effect of particle size on adsorption was represented in Figures 5.22 and 5.23. As it was expected, no particle size impact was obtained for raw materials. For the modified sand having diameter 212-600 μm, removal efficiencies were about 95-96%. However, for the modified sand particles having diameter 710-1000 μm, removal efficiency slightly reduced to 90.7%. According to the BET analyses results (see Table 5.2), smaller particles resulted with greater surface area. Since the micropores of sand particles were negligible, adsorption limited solely on surface. Therefore, decreasing the particle size was resulted with increased removal efficiently. However, in the experiments, particles having diameter 710-1000 μm was used because it is competent to reduce arsenic concentrations to obtain desired level. In addition, clogging problem that might be faced with smaller particles was considered.

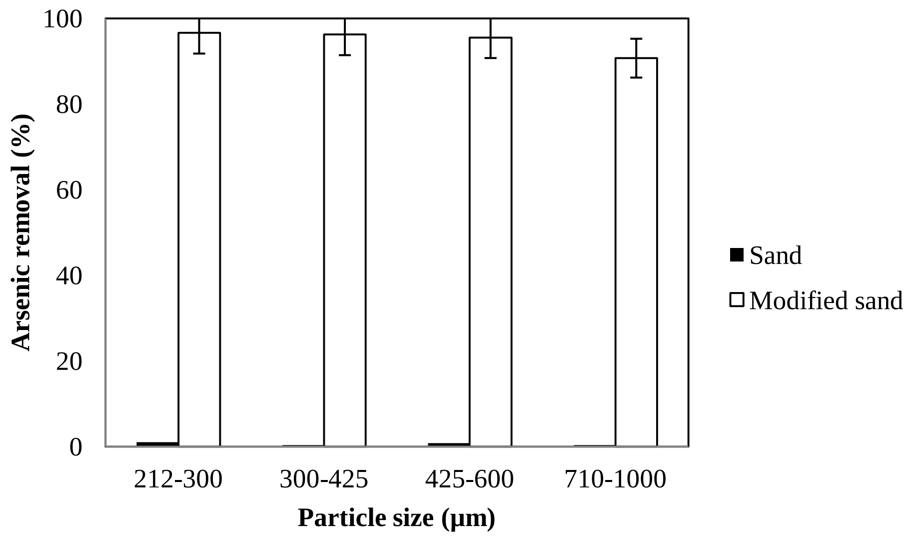

Figure 5.22 Effect of particle size on adsorption by sand and modified sand

In contrast to modified sand, modified sepiolite showed lower performances in the smaller size ranges as seen in Figure 5.23. For the particle sizes from 212 to 600 μm, removal rates did not significantly change, and removal efficiencies were between 85-87%. However, for the particles having diameter 710-1000 μm, removal efficiency increased to 94.0%. This situation could be explained with destruction of pores by grinding of the particles to smaller sizes. In addition, as it stated in previous sections, decreasing the particle size of sepiolite did not result by an increase in surface area. Therefore, for sepiolite, particles having relatively greater diameters were more efficient, thus 710-1000 µm size range of modified sepiolite was used in the experiments.

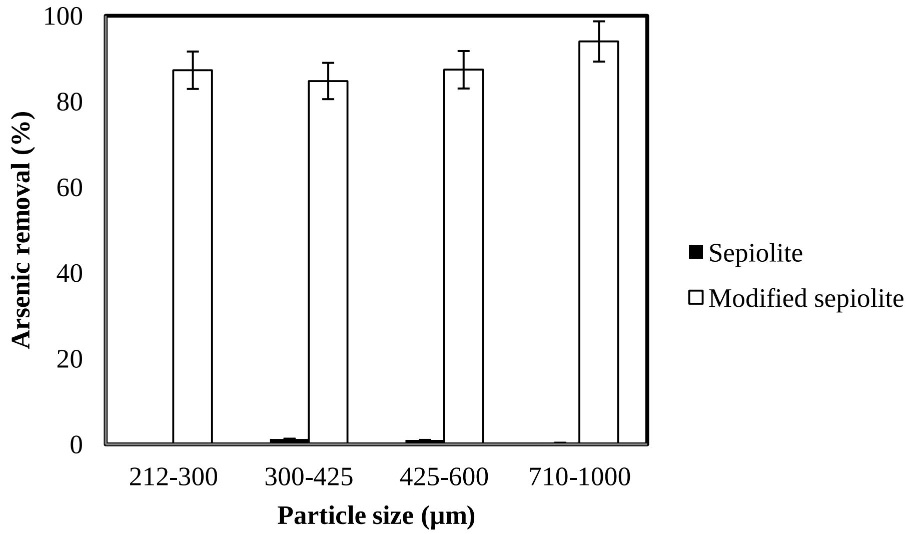

Figure 5.23 Effect of particle size on adsorption by sepiolite and modified sepiolite

5.2.6 Effect of Ions Existing in Groundwater Sample on Arsenic Adsorption

Real groundwater sample was used to determine the effect of other ions on arsenic adsorption. 5 g/L dose of modified sand and modified sepiolite were used in the experiments at pH 7 at room temperature (25^{o}C). The remaining concentrations of anions were measured after the adsorption process was completed and results are shown in Table 5.3. As seen in Table 5.3., the concentration of all anions reduced after adsorption for each modified materials. Especially bicarbonate concentration, as major anion, decreased dramatically after the adsorption. However, removal efficiencies of other anions were quite low. Gao et al., 2011, studied existing anions on arsenic adsorption and observed an increase of 56 µg/L of arsenic concentration with initial bicarbonate content up to 1500 mg/L. They reported that desorption of arsenic by bicarbonate is significant, even at relatively low concentration levels. Stachowicz et al. (2007), observed that the presence of (bi)carbonate increased the arsenate as well as arsenite concentration in solution, particularly evident in the pH range relevant for Bangladesh groundwater. They obtained from the experiments, the As(III) concentration increased about 10 times at the lowest pH value due to the presence of 0.01 M bicarbonate.

Table 5.3 Concentration of anions in groundwater before and after adsorption

Anions (mg/L)	Groundwater (bearing 100 µg/L As)	After modified sand treatment	After modified sepiolite treatment
Chloride	5.92	5.71	5.0603
Nitrate	18.13	16.74	12.10
Sulphate	10.42	9.5807	6.18
Bicarbonate	402.6	85.4	244
Phosphate	n.a.	n.a.	n.a.

Arsenic removals for both modified sand and sepiolite are illustrated in Figure 5.24. Approximately 42% of arsenic treated from groundwater samples with modified sand however when the synthetic water was used, the efficiency increased to 91%. For sepiolite, adsorption experiments with real groundwater samples were completed with 77.4% of arsenic removal efficiency whereas 94% of arsenic from synthetic water was effectively treated. The results gathered from experiments with real ground water samples were shown that anions have a significant impact on the treatment performance for both modified materials. Results indicated that existence of competing anions was resulted by decreasing in arsenic removal efficiency approximately 50% for modified sand. Due to high adsorption capacity of modified sepiolite, the reduction of percent removal was only 17±5%, comparing to synthetic water.

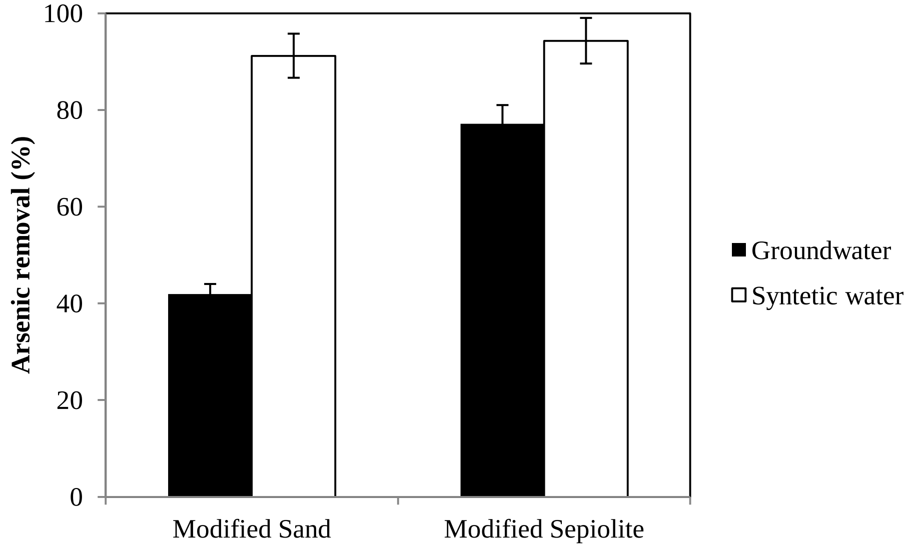

Figure 5.24 Effect of anions on arsenic removal removal

5.3 Kinetic Studies

The rate at which arsenic compounds are removed from solution by adsorbent material is significant issue for adsorption practices. From the kinetic analysis, the solute uptake rate can be calculated by using various contact time required for the adsorption process. Therefore, kinetic studies were performed for 5 g/L adsorbent dose of modified sand, modified sepiolite, I1 and I2. The kinetic tests were conducted for a period of 8 hours at speed of 100 rpm. Experiments were carried out for initial arsenic concentrations of 100.8, 494 and 1503 µg/L. Samples were taken with different time intervals (i.e. 15, 30, 60, 120, 240 and 480 minutes) and arsenic measurements were done. Adsorption capacity was calculated as mentioned in Chapter 4.4.

The kinetic data for As (T) sorption from modified sand is shown in Figure 5.25. In this figure, q_e, which defines the amount of As (T) adsorbed per gram of the modified sand at equilibrium, is depicted with respect to time. As seen in the Figure 5.25, for about 101 µg/L initial arsenic concentration, the amount of arsenic adsorbed by modified sand was 0.017 mg/g within 4 hours yielding 82.4% removal efficiency. Adsorption capacity slightly increased at the end of the 8 hours of contact time and reached 0.018 mg/g. Adsorption capacities reached to 0.0692 and 0.1372 mg/g for initial arsenic concentrations of 494 and 1503 µg/L. The conducted results revealed that the adsorption capacity of modified sand increased with increasing initial arsenic concentrations due to the availability of sufficient adsorption sites.

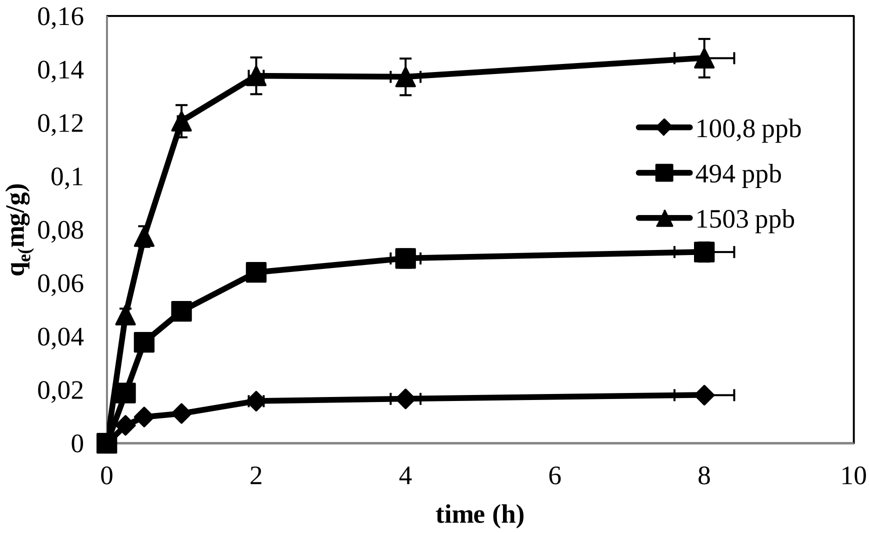

Figure 5.25 Adsorption kinetics of arsenic for modified sand

The kinetic data were fitted using different models, e.g. first order reaction model, pseudo-first order reaction model, second order reaction model and pseudo-second-order reaction model. Figure 5.26, Figure 5.27, Figure 5.28 and Figure 5.29 show linear model of first order, linear model of pseudo first order, linear model of second order and linear model of pseudo second order reaction kinetics for modified sand. Beside the Figures 5.26-5.29, the equations for all reaction kinetic models with their R^2 values are presented in Table 5.4.

As it was explained in Chapter 3, first-order rate equation is based on the solution concentration and defined in Eq.3.8. Kinetic parameters can be determined from the plot of $\ln C_t$ versus time at a given initial concentrations. The co-efficient of determination value (R^2) was determined as 0.8226, 0.6811, and 0.5178 for initial arsenic concentrations of 101, 494, 1503 µg/L (see Table 5.4). The pseudo-first order kinetic model is based on the solid capacity (see Chapter 3.3.2) and defined in the Eq. 3.10. Linear model of pseudo-first order reaction kinetics is graphed in Figure 5.26.

The co-efficient of determination value (R^2) was determined as 0.9060, 0.971, and 0.7721 for initial arsenic concentrations of 101, 494, 1503 µg/L (see Table 5.4). The second order rate equation given in Eq.3.12 in linearised form is widely used for the adsorption process. Kinetic data is illustrated in Figure 5.28 plotting the 1/Ct value versus time. As can be seen in Table 5.4, the co-efficient of determination values (R^2) were 0.9705, 0.7869, and 0.5646 for the initial arsenic concentrations of 101, 494, 1503 µg/L, respectively.

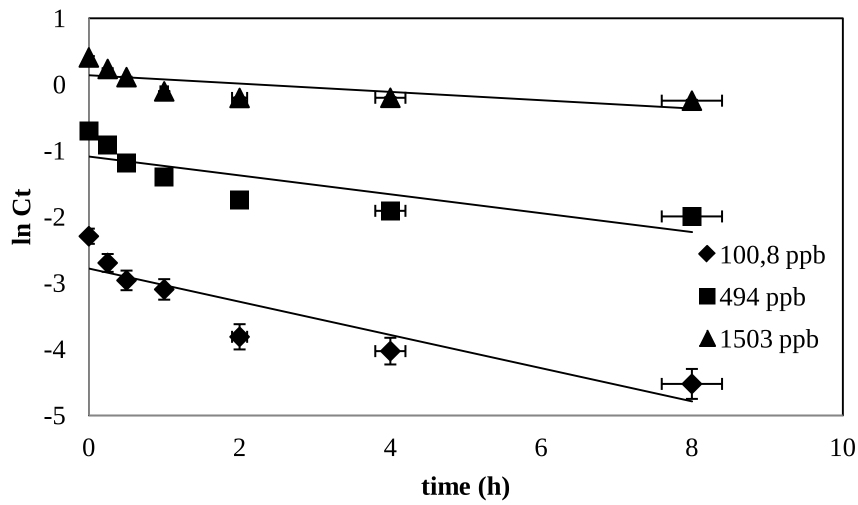

Figure 5.26 Linear model of first order reaction kinetics for modified sand

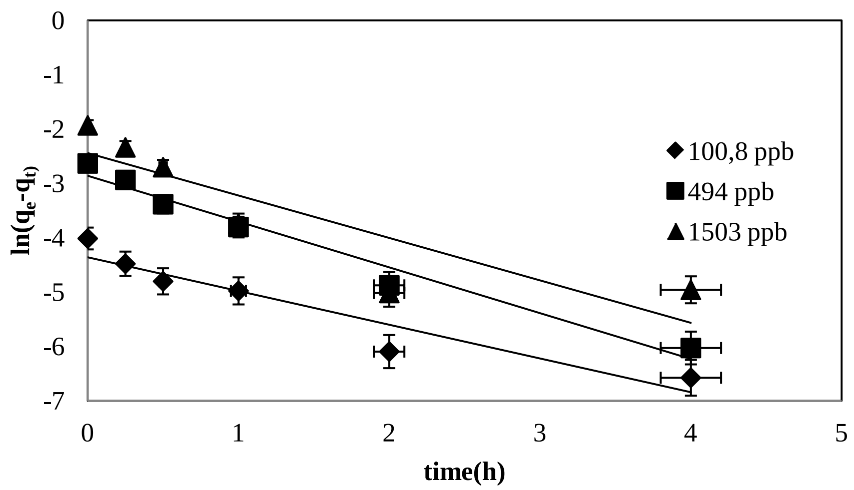

Figure 5.27 Linear model of pseudo first order reaction kinetics for modified sand

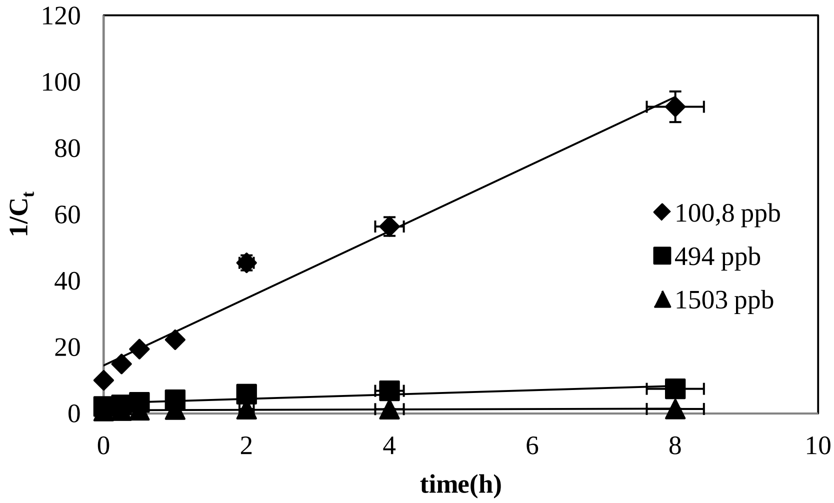

Figure 5.28 Linear model of second order reaction kinetics for modified sand

And, the last model fitted to data was pseudo-second order reaction model. The expression of the reaction was based on the adsorption capacity and presented in Eq.3.15 in linearized form. From the plotting the $\ln(t/q_t)$ versus (t), Figure 5.29 is obtained. The highest co-efficient of determination values (> 0.9981) were calculated for the pseudo-second order reaction equation. Based on the co-efficient of determination values, the adsorption process followed the pseudo-second order reaction better than the other three kinetic models. As it was explained in Chapter 3.3, adsorption rate can be determined from the slop of lines. The experiments showed that adsorption rate decreased with increased initial concentration using due to limited adsorption site.

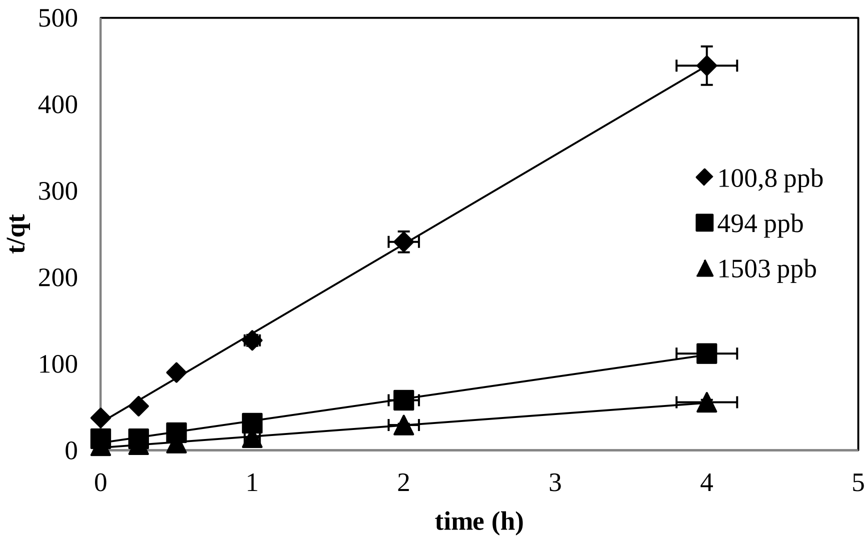

Figure 5.29 Linear model of pseudo second order reaction kinetics for modified sand

Table 5.4 Kinetic equations for modified sand

Kinetic of reaction	**Initial concentration**	**Equation of reaction**	R^2
First order	100.8	$\ln C_t = -0.2509t - 2.7819$	0.8226
	494	$\ln C_t = -0.143t - 1.087$	0.6811
	1503	$\ln C_t = -0.0634t + 0.1416$	0.5178
Pseudo-first-order	100.8	$\ln(q_e - q_t) = 0.6215t - 4,3584$	0.9060
	494	$\ln(q_e - q_t) = = -0.8434t - 2.8581$	0.971
	1503	$\ln(q_e - q_t) = = -0.7803t - 2.4442$	0.7721
Second-order	100.8	$1/C_t = 10.127t + 14,407$	0.9705
	494	$1/C_t = 0.6479t + 3,072$	0.7869
	1503	$1/C_t = 0.0632t + 0.8856$	0.5646
Pseudo-second-order	100.8	$t/q_t = 52.271t + 27.869$	**0.9986**
	494	$t/q_t = 12.916t + 7.3532$	**0.9981**
	1503	$t/q_t = 6.5871t + 2.5634$	**0.9981**

The kinetic data for As (T) sorption from modified sepiolite is shown in Figure 5.30. In this figure, q_e, which defines the amount of As (T) adsorbed per gram of the modified sepiolite at equilibrium, is depicted with respect to time. As seen in the Figure 5.30, for about 101 µg/L initial arsenic concentration, the amount of arsenic adsorbed by modified sand was 0.018 mg/g within 4 hours yielding 89.3% removal efficiency. Adsorption capacity did not change after 4 hours contact time. Adsorption capacities reached to 0.0906 and 0.418 mg/g for initial arsenic concentrations of 494 and 1503 µg/L, respectively. The results revealed that the adsorption capacity of modified sepiolite increased with increasing initial arsenic concentrations due to the availability of sufficient adsorption sites.

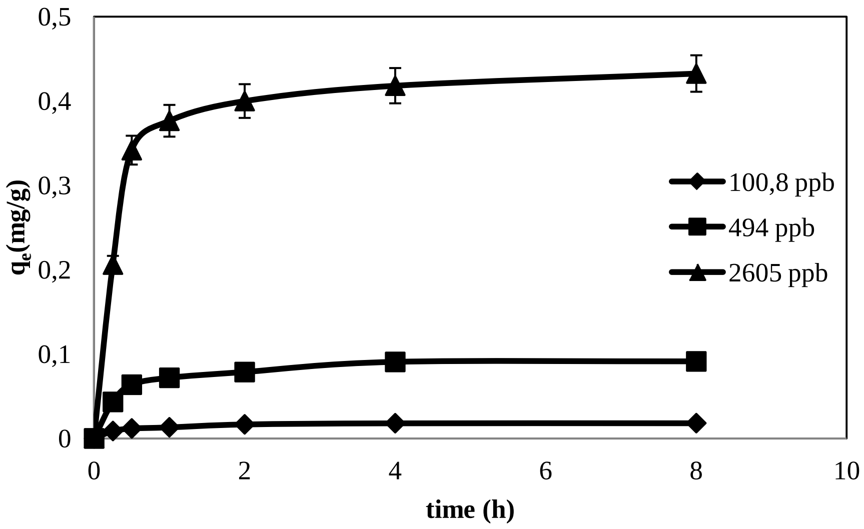

Figure 5.30 Adsorption kinetics of arsenic for modified sepiolite

Different models, e.g. first order reaction model, pseudo-first order reaction model, second order reaction model and pseudo-second-order reaction model, were also applied to the kinetic data. Linear forms of first order reaction model, pseudo-first order reaction model, second order reaction model and pseudo-second-order reaction models are presented in Figure 5.31, Figure 5.32, Figure 5.33 and Figure 5.34. Beside the figures, the equations for all reaction kinetic models with their R^2 values are presented in Table 5.5.

For first-order rate equation, kinetic parameters can be determined from the plotting ln C_t values versus time at a given initial concentrations. The co-efficient of determination value (R^2) was determined as 0.707, 0.7475, and 0.5479 for initial arsenic concentrations of 101, 494, 1503 µg/L (see Table 5.5). Linear model of pseudo-first order reaction kinetics is graphed in Figure 5.32. The co-efficient of determination value (R^2) was determined as 0.9898, 0.9619, and 0.8254 for initial arsenic concentrations of 101, 494, 1503 µg/L (see Table 5.5). Kinetic data of second order rate equation is illustrated in Figure 5.33 plotting the 1/Ct value versus time. As can be seen in Table 5.5, the co-efficient of determination values (R^2) were 0.8339, 0.8749, and 0.7477 for the initial arsenic concentrations of 101, 494, 1503 µg/L, respectively.

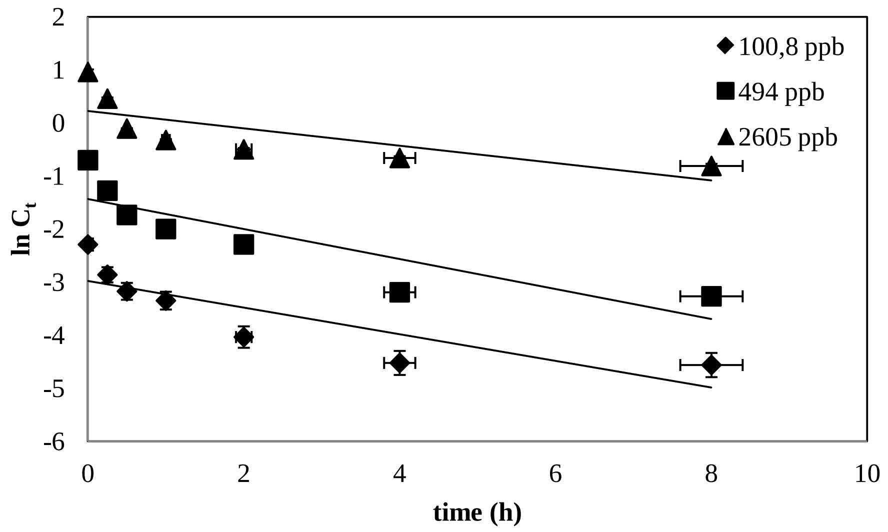

Figure 5.31 Linear model of first order reaction kinetics for modified sepiolite

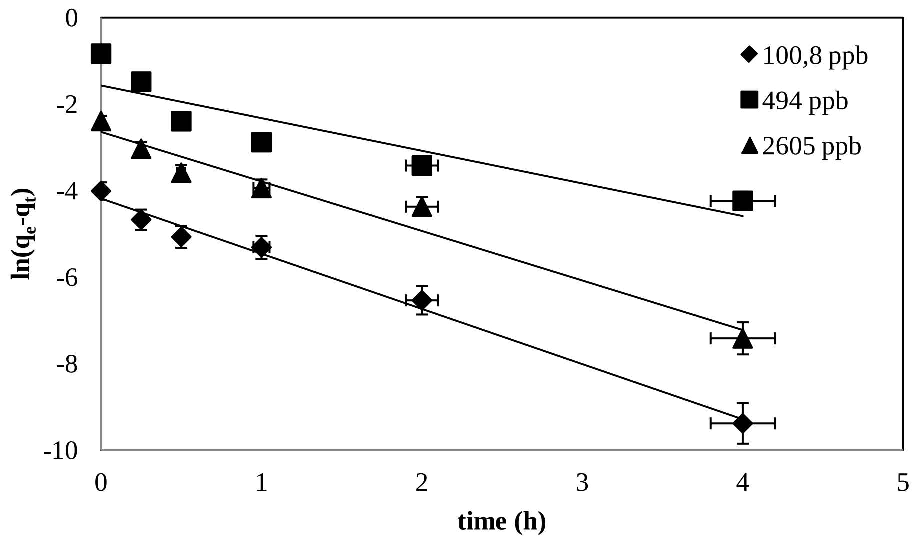

Figure 5.32 Linear model of pseudo first order reaction kinetics for modified sepiolite

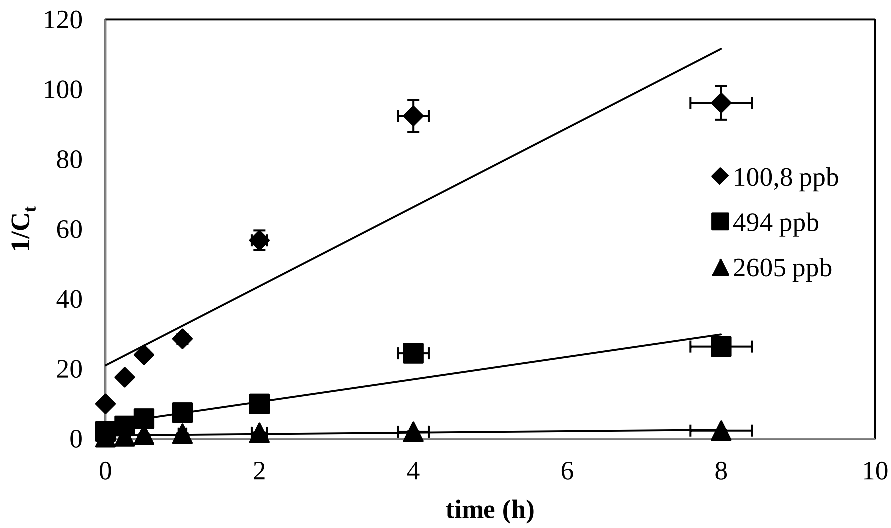

Figure 5.33 Linear model of second order reaction kinetics for modified sepiolite

And, the last model fitted to data was pseudo-second order reaction model. From the plotting the $\ln(t/q_t)$ versus (t), Figure 5.34 is obtained. The highest co-efficient of determination values (> 0.9993) were calculated for the pseudo-second order reaction equation. Based on the co-efficient of determination values, the adsorption process followed the pseudo-second order reaction better than the other three kinetic models. As it was explained in Chapter 3.3, adsorption rate can be determined from the slop of lines. The experiments showed that adsorption rate decreased with increased initial concentration due to limited adsorption site.

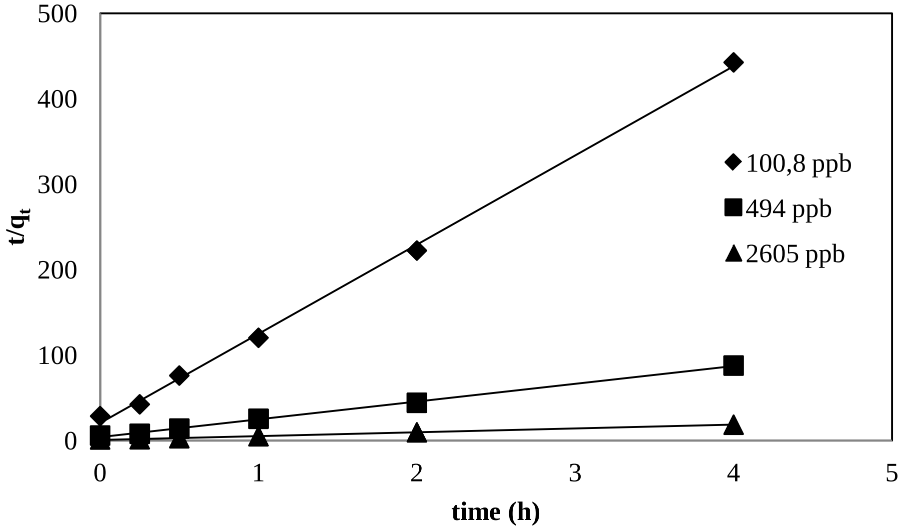

Figure 5.34 Linear model of pseudo second order reaction kinetics for modified sepiolite

Table 5.5 Kinetic equations for modified sepiolite

Kinetic of reaction	**Initial concentration (µg/L)**	**Equation of reaction**	**R^2**
First order	100.8	$\ln C_t$=-0.251t-2.9802	0.707
	494	$\ln C_t$ = -0.2833t - 1.4314	0.7475
	2605	$\ln C_t$ = -0.1641t + 0.2264	0.5479
Pseudo-first-order	100.8	$\ln(q_e-q_t)$= -1.2768t-4.184	0.9898
	494	$\ln(q_e-q_t)$ = -0.2833t - 1.4314	0.9619
	2605	$\ln(q_e-q_t)$ = -0.7556t - 1.569	0.8254
Second-order	100.8	$1/C_t$=11.324t+20.961	0.8339
	494	$1/C_t$ = -0.2833t - 1.4314	0.8749
	2605	$1/C_t$ = 0.2035t + 0.88	0.7477
Pseudo-second-order	100.8	t/q_t=52.942t+16.357	**0.9993**
	494	t/q_t = 10.535t + 3.1607	**0.9993**
	2605	t/q_t = 2.2554t+ 0.4808	**0.9997**

Evaluation of the results proved that the adsorption process followed the pseudo second order reaction model better than the other three kinetic models for both modified sand and sepiolite (see Table 5.4 and 5.5). For modified sand, the pseudo second order adsorption rate constants (k_{p2}) was calculated as 98.08 g/mgmin, 22.68 g/mgmin, and 16.92 g/mgmin for initial arsenic concentrations of 100, 494, and 1503µg/L, respectively. And, for modified sepiolite, the pseudo second order adsorption rate constant (k_{p2}) was calculated as 171.25 g/mgmin, 35.12 g/mgmin, and 10.58 g/mgmin for initial arsenic concentrations of 100, 494, and 1503 µg/L respectively. The summary of the data, i.e. adsorption rate constants, is presented in Table 5.6 for both materials.

Table 5.6 The pseudo-second-order adsorption rate constants for modified sand and sepiolite

Material	**Initial concentration (µg/L)**	**R^2**	**k_{p2} (g/mgmin)**
Modified sand	100.8	0.9986	98.08
	494	0.9981	22.68
	2605	0.9981	16.92
Modified sepiolite	100.8	0.9993	171.25
	494	0.9993	35.12
	2605	0.9997	10.58

As it stated above, for both modified sand and modified sepiolite materials, the kinetic data could be best described by the pseudo-second-order kinetic equation which was based on the assumption that the rate limiting step may be chemical sorption or chemisorptions involving valency forces through sharing or exchange of electron between adsorbent and adsorbate (Yao et al., 2014; Ho and McKay, 2000). In chemisorption, the metal ions bind to the adsorbent surface by forming a chemical (usually covalent) bond and tend to find sites that maximize their coordination number with the surface (Atkins, 1995). Similar results for arsenic removal were obtained by Attinti et al. (2015) and Mostafa et al. (2011).

The kinetic data of adsorbent I1 is illustrated in Figure 5.35. In this figure, the amount of As (T) adsorbed per gram of the I1 at equilibrium (i.e. q_e) is depicted with respect to time. The performance of I1 was excellent. Rapid uptake of As (T) was achieved within the first 15 minutes to reach the equilibrium conditions. Adsorption capacity reached to 0.021 mg/g in fifteen minutes, and yielded 92.1% removal efficiency. Then, q_e did not significantly change through 8 hours and 99.9% removal efficiency was obtained.

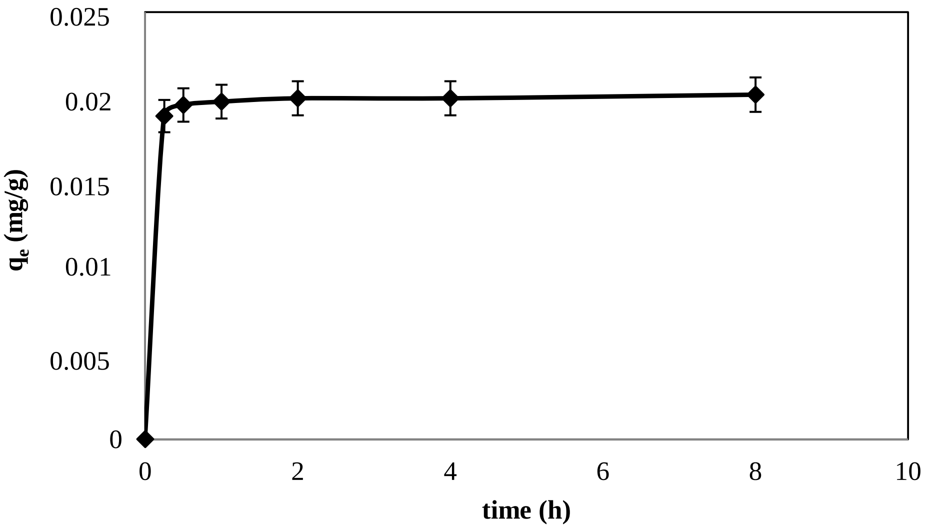

Figure 5.35 Adsorption kinetics of arsenic for I1

Figure 5.36, Figure 5.37, Figure 5.38 and Figure 5.39 show linear model of first order, pseudo first order, second order and pseudo second order reaction kinetics for I1, respectively. Beside the Figures 5.36-5.39, the equations for all reaction kinetic models with their R^2 values are presented in Table 5.7.

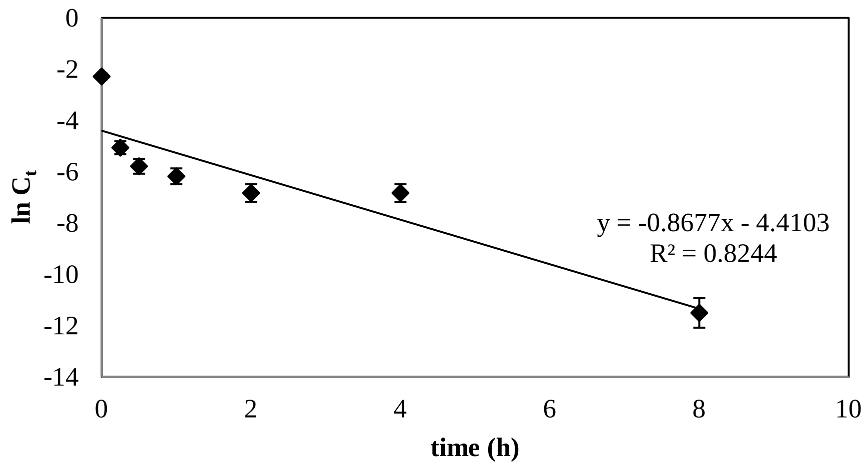

Figure 5.36 Linear model of first order reaction kinetics for I1

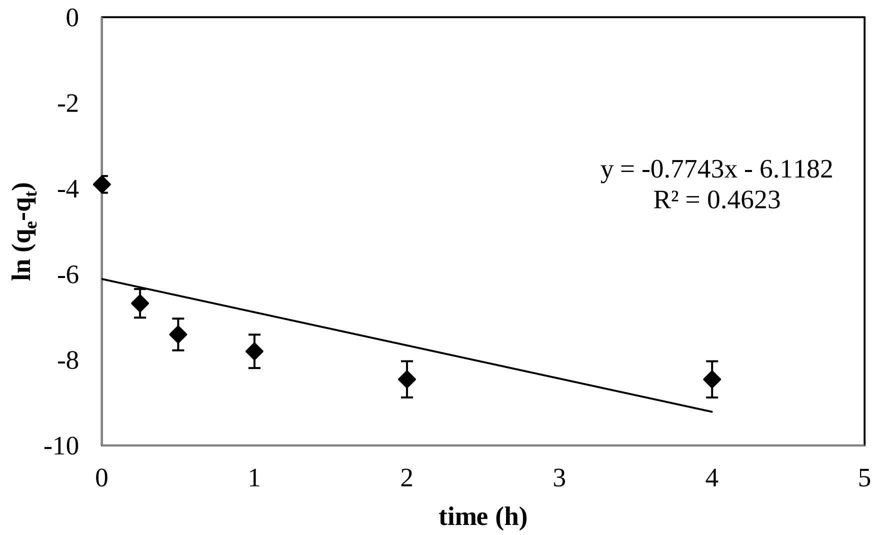

Figure 5.37 Linear model of pseudo first order reaction kinetics for I1

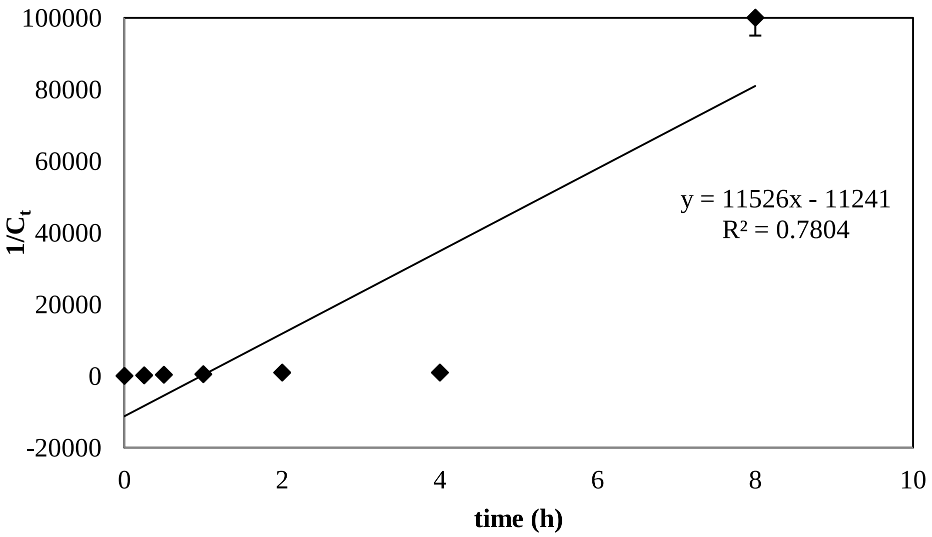

Figure 5.38 Linear model of second order reaction kinetics for I1

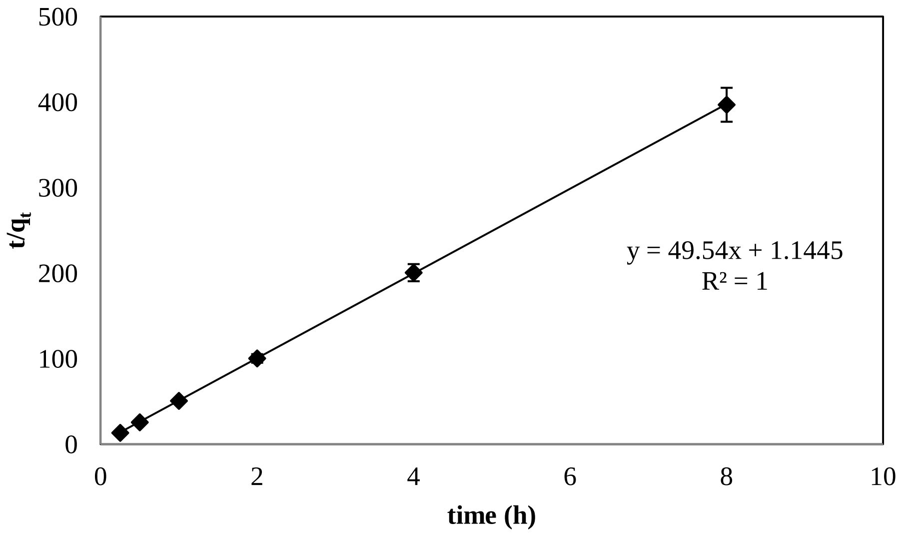

Figure 5.39 Linear model of pseudo second order reaction kinetics for I1

High coefficient of determination (i.e. 1.0) was obtained for I1. Similar to modified sand and sepiolite, based on co-efficient of determination values, the adsorption process followed the pseudo second order reaction model better than the other three kinetic models (see Table 5.8). The adsorption rate (k_{p2}) was calculated as 2145 g/mgmin for I1 which was considerably higher from the materials tested in this study. The k_{p2} value was also quite higher than the literature values. For instance;

Mostafa et al. were reported the rate constant of pseudo second order adsorption for iron oxide coated perlite in between 26 to 73 g/mgmin.

Table 5.7 Equation of kinetic models for I1

Material	Kinetic of reaction	Equation of reaction	R^2
I1	First-order	$\ln C_t$=-0.8677t-4.4103	0.8244
	Pseudo-first-order	$\ln(q_e-q_t)$=-0.7743t-6.1182	0.4623
	Second-order	$1/C_t$=11526t-11.241	0.7804
	Pseudo-second-order	t/q_t=49.54t+1.1445	1.000

Finally, adsorption kinetics of I2 is presented in Figure 5.40. Arsenic uptake was reached to 0.019 mg/g within two hours, and 95.8% of arsenic was removed. At the end of eight hours, adsorption capacity was 0.023 mg/g. Reaction kinetics were also determined for I2, and linear models of first order, pseudo first order, second order and pseudo second order reaction kinetics are shown in Figures 5.41 to 5.44. Beside the figures, the equations for all reaction kinetic models with their R^2 values are presented in Table 5.8. The experimental data was fitted to the pseudo second order equations for I2, too. The co-efficient of determination value (R^2) was quite high and obtained as 0.9994. The pseudo order rate constant (k_{p2}) was calculated as 266 g/mgmin for I2.

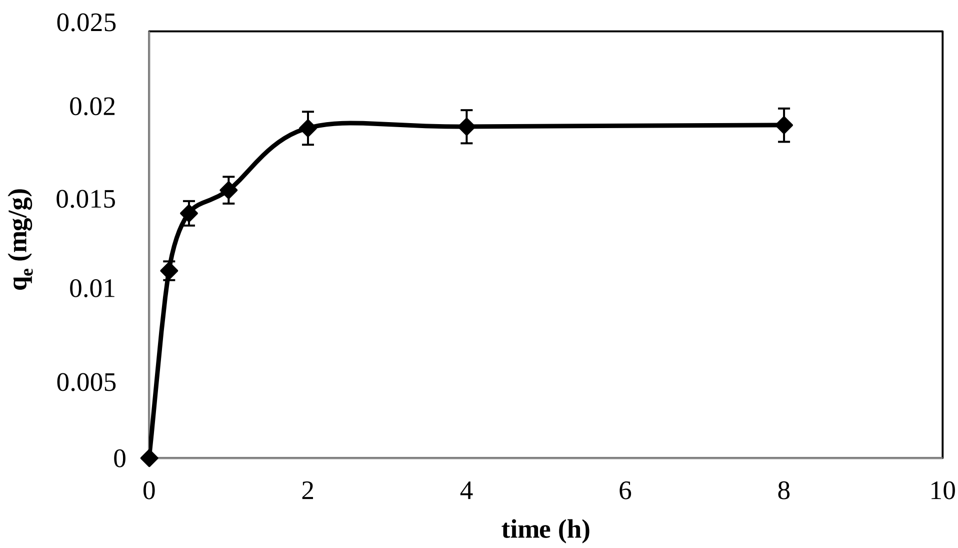

Figure 5.40 Adsorption kinetics of arsenic for I2

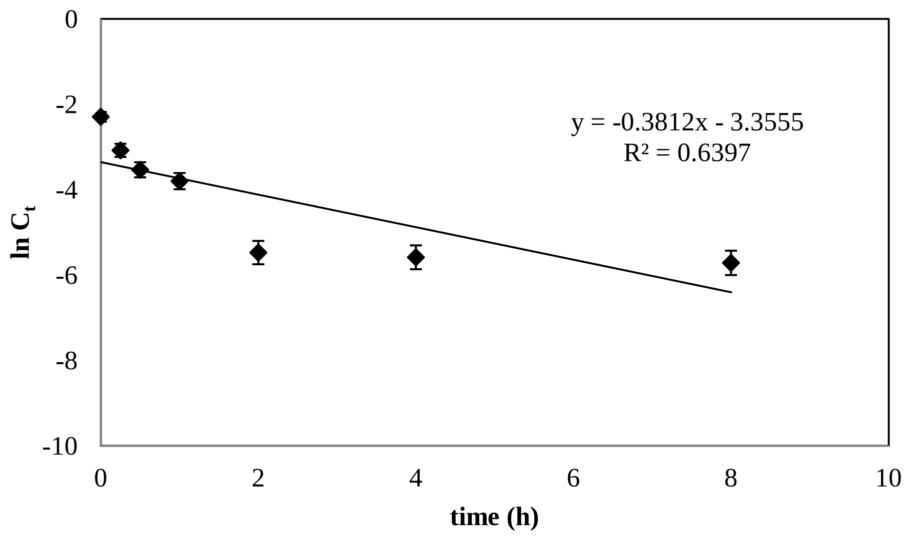

Figure 5.41 Linear model of first order reaction kinetics for I2

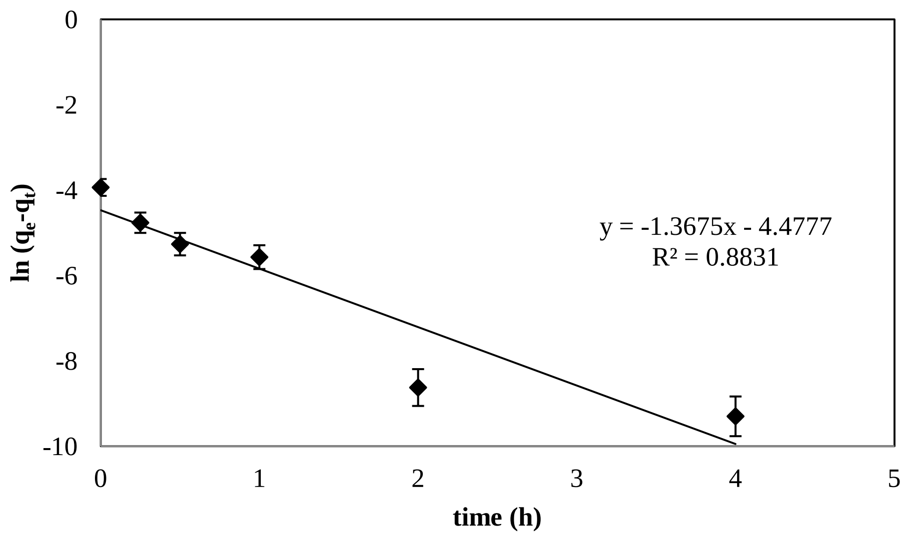

Figure 5.42 Linear model of pseudo first order reaction kinetics for I2

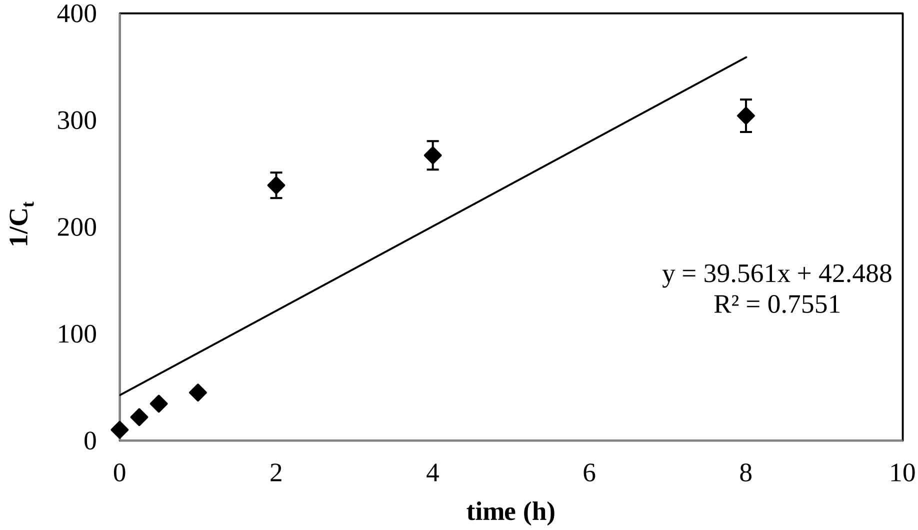

Figure 5.43 Linear model of second order reaction kinetics for I2

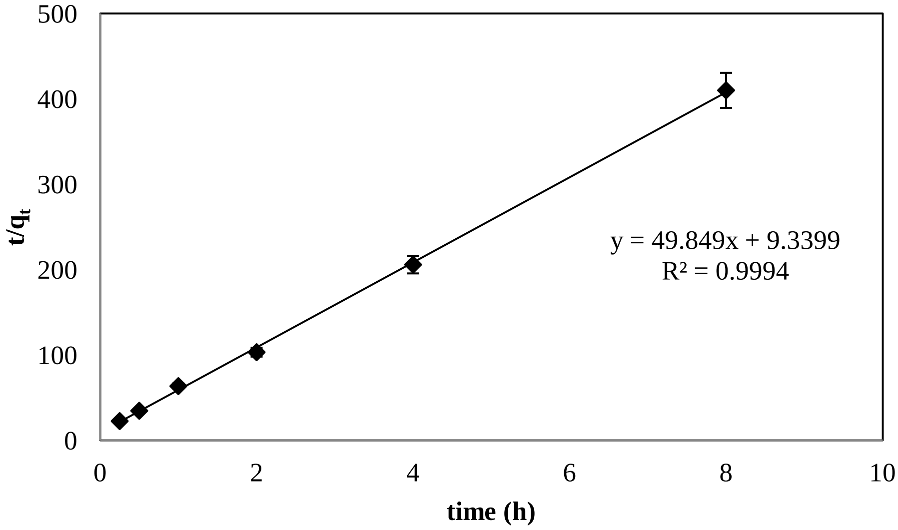

Figure 5.44 Linear model of pseudo second order reaction kinetics for I2

Table 5.8 Equation of kinetic models for I2

Material	Kinetic of reaction	Equation of reaction	R^2
I2	First-order	$\ln C_t$=-0.3812t-3.3555	0.6397
	Pseudo-first-order	$\ln(q_e-q_t)$=-1.3675t-4.4777	0.8831
	Second-order	$1/C_t$=39561t+42.488	0.7551
	Pseudo-second-order	t/q_t=49.849t+9.3399	0.9994

The result of the kinetic studies showed that adsorption of arsenic by modified sand, modified sepiolite, I1 and I2 followed the pseudo-second-order kinetic model. From the kinetic study, it is indicated that As (T) is predominantly chemisorbed on the surface of the materials which is similar to the research results of Wu et al, 2001, Mostafa et al, 2011. In chemisorption, the metal ions bind to the adsorbent surface by forming a chemical (usually covalent) bond and tend to find sites that maximize their coordination number with the surface (Atkins, 1995).

5.4 Isotherm Studies

The adsorption isotherm is fundamentally important to evaluate the adsorption capacity. Therefore, isotherm studies were performed for modified sand, modified sepiolit, I1 and I2 to investigate the adsorption characteristics as well as adsorption capacities. In this study, varying adsorbent dosages ranged in 5-20 g/L were used with fixed initial arsenic concentration. Experiments were conducted for a period of 4 hours at speed of 100 rpm. Samples were taken after four hours and analysed for arsenic. The amount of adsorbate, adsorbed per unit mass of adsorbent (i.e. adsorption capacity) at particular temperature, was determined as mentioned in Chapter 3.2.

Both Langmuir and Freundlich isotherms were studied to determine the isotherm constants. Figure 5.45 and 5.46 show Langmuir and Freundlich isotherms for modified sand. In addition, isotherm constants are presented in Table 5.9. The experimental data are plotted with $1/q_e$ against $1/C_e$ values; and Langmuir constants q_{max} and b are calculated from the slope and intercept of the linear equation (Eq.3.5). The linearized form of Freundlich isotherm is depicted by plotting the $\ln C_e$ values vs. $\ln q_e$. The equilibrium constants for the Freundlich equation are determined from the slope and the intercept of the straight line.

The results showed that Freundlich model was fitted better than Langmuir model with relatively higher R^2 values for modified sand. High R^2 values ($R^2 > 0.988$) were attained by fitting experimental data into the Freundlich isotherm model (see Table

5.8). The maximum adsorption capacity determined by Freundlich model was 0.142 mg/g, 0.102 mg/g, and 0.063 mg/g for 5 g/L, 10 g/L, and 20 g/L doses of modified sand, respectively. Besides that, Freundlich constant “1/n” which represents the adsorbent intensity indicating the deviation of the adsorption isotherm from linearity was calculated from the slope of this straight line. If n= 1, the adsorption is linear i.e. the adsorption sites are homogeneous and there is no interaction between the adsorbed species. If $1/n < 1$, the adsorption is favourable; the adsorption capacity increases and new adsorption sites appear. If $1/n > 1$, the adsorption is unfavourable; the adsorption bonds become weak and the adsorption capacity decreases (Isa et al. 2007). In this study, the 1/n values were calculated as 0.409, 0.439, and 0.461 for 5 g/L, 10 g/L, and 20 g/L doses of modified sand, respectively. The values of 1/*n* for modified sand being less than 1 indicate favourable adsorption.

Moreover, isotherms with n > 1 reflect a high affinity between adsorbate and adsorbent and are indicative of chemisorption (Boparai et al, 2011). In this study, the n values was around 2, therefore high n values attributed to greater affinity of between the iron oxide coated sand particles and arsenic compounds. Similar results were also presented at various studies in the literature by Gang et al. (2010), Thirunavukkarasu et al. (2003) and Jimenez-Cedillo et al.(2009).

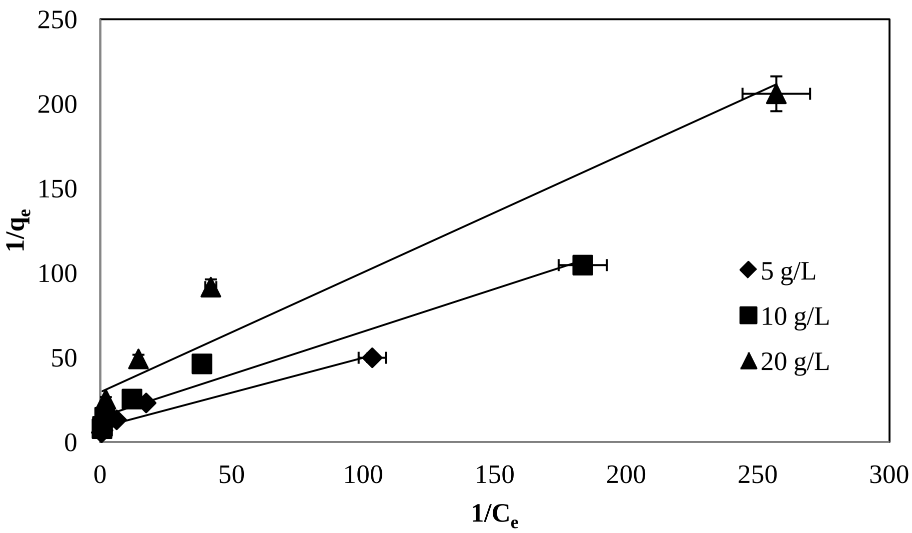

Figure 5.45 Langmuir isotherm for modified sand

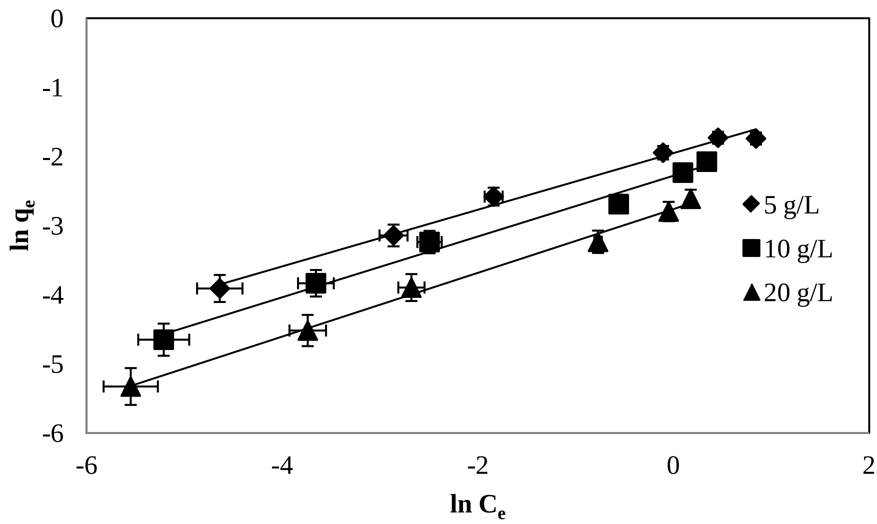

Figure 5.46 Freundlich isotherm for modified sand

Table 5.9 Langmuir and Freundlich isotherm constant at 25 ˚C for modified sand

Adsorbent	**Adsorbent dose (g/L)**	**Langmuir**			**Freundlich**		
		qmax (mg/g)	**b (L/mg)**	**R^2**	**1/n**	**k_f (mg/g)**	**R^2**
Modified Sand	5	0.117	20.720	0.9435	0.409	0.142	**0.9895**
	10	0.068	29.11	0.9624	0.439	0.102	**0.9882**
	20	0.034	41.52	0.9393	0.461	0.063	**0.9946**

Data from isotherm studies for modified sepiolite are illustrated in Figures 5.47 and 5.48. Table 5.10 shows isotherm constants and the co-efficient of determination values (R^2). Co-efficient of determination values proved that the Langmuir model was more appropriate to explain the results than the Freundlich model. The values of R^2 were 0.9958, 0.9857, and 0.9912 for 5, 10, and 20 g/L dosages of modified sepiolite. Langmuir isotherm assumes monolayer adsorption (chemisorption) onto a homogeneous surface with limited number of identical sites (Jeon et al., 2009). Once a site is filled, no further sorption can take place at that site. This indicates that the surface reaches a saturation point where the maximum adsorption of the surface will be achieved. The maximum adsorption capacity was found as 0.501 mg/g for 5 g/L dose of modified sepiolite whereas it was 0.117 mg/g for modified sand. Higher adsorption capacity of modified sepiolite was attributed to more active sites due to porous surface structure providing higher surface area.

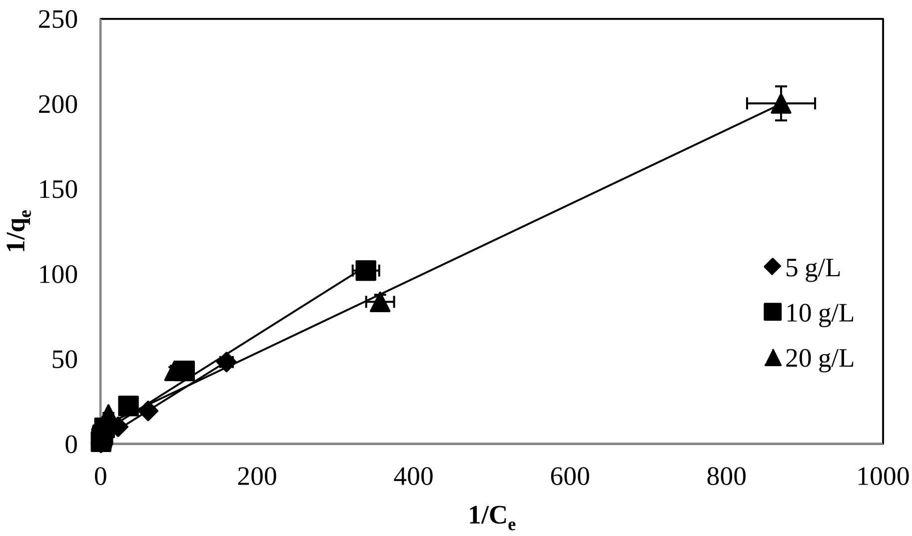

Figure 5.47 Langmuir isotherm of modified sepiolite

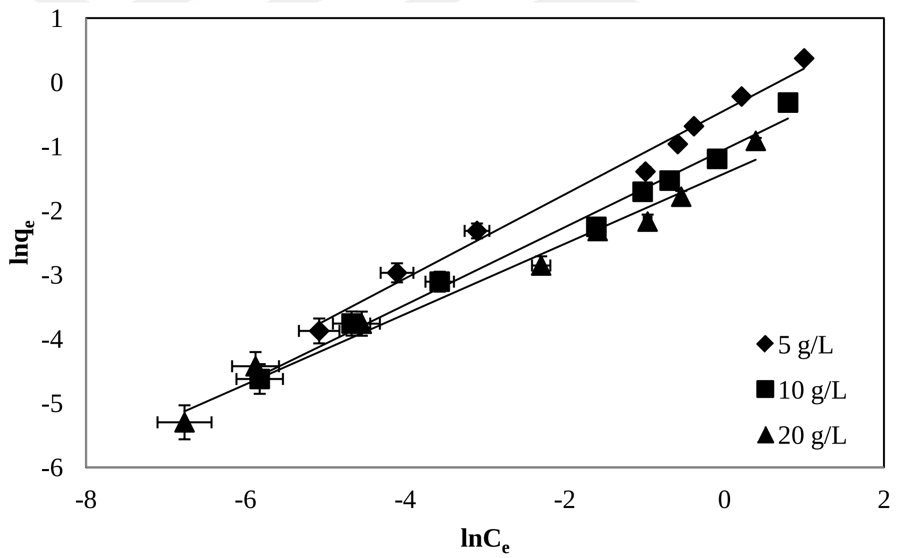

Figure 5.48 Freundlich isotherm of modified sepiolite

Table 5.10 Langmuir and Freundlich isotherm constant at 25 ˚C for modified sepiolite

Adsorbent	Adsorbent dose (g/L)	Langmuir			Freundlich		
		q_{max} (mg/g)	b (L/mg)	R^2	1/n	k_f (mg/g)	R^2
Modified Sepiolite	5	0.501	6.909	**0.9958**	0.654	0.644	0.9860
	10	0.164	21.03	**0.9857**	0.606	0.351	0.9890
	20	0.102	44.85	**0.9912**	0.549	0.242	0.9819

The results showed that modified sepiolite has higher adsorption capacity than most of the iron modified natural materials in the literature such as ironoxide coated rock 0.36 mg/g (Maji et al., 2011), iron-oxide coated perlite 0.39 mg/g (Mostafa et al., 2011), iron coated zeolite 0.68mg/g (Jeon et al., 2009) and ironoxide coated sand 0.02857mg/g (Gupta et al., 2005).

Data obtained from commercial adsorbents (i.e. I1 and I2) are illustrated in Figures from 5.49 to 5.52 by plotting $1/q_e$ against $1/C_e$ to obtain the Langmuir constants, and plotting ln q_e against ln C_e to obtain the Freundlich constants. And, isotherm results are summarized in Table 5.11 for each adsorbent. Table 5.10 shows that the coefficients b and k_f are higher for I1 than I2, which means that more arsenic adsorption can be expected with I1. Freundlich's equation states that higher the value of n the stronger the bond between the adsorbate and the adsorbent. Higher "n" value for I1 along with higher adsorption coefficients obtained from Langmuir and Freundlich equation suggests strongly that I1 has a better affinity for arsenic adsorption.

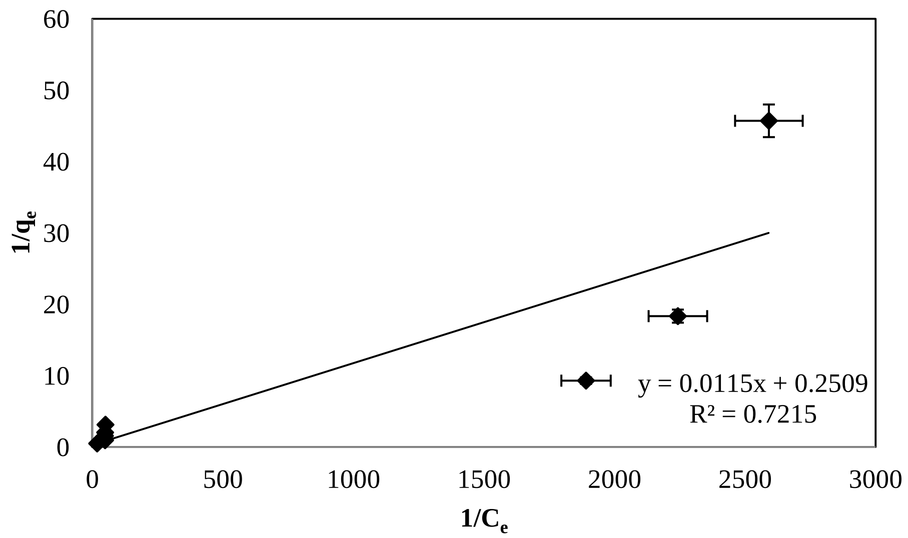

Figure 5.49 Langmuir isotherm for I1

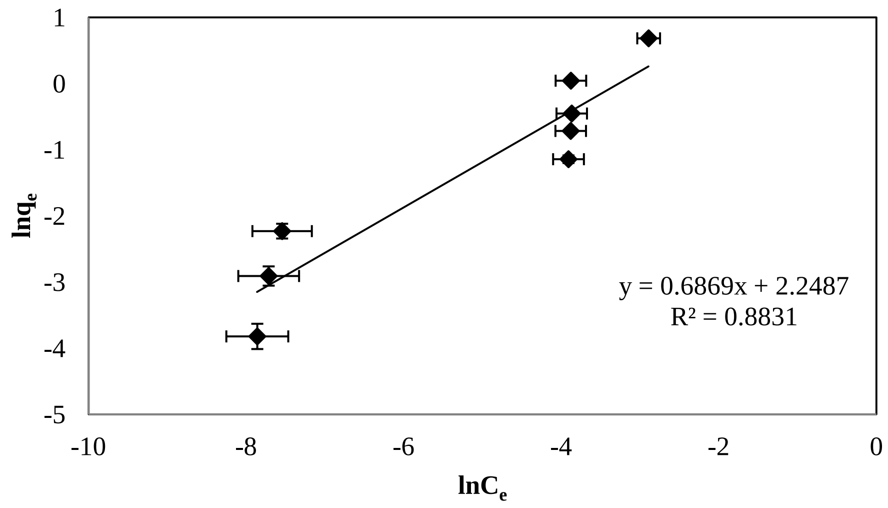

Figure 5.50 Freundlich isotherm for I1

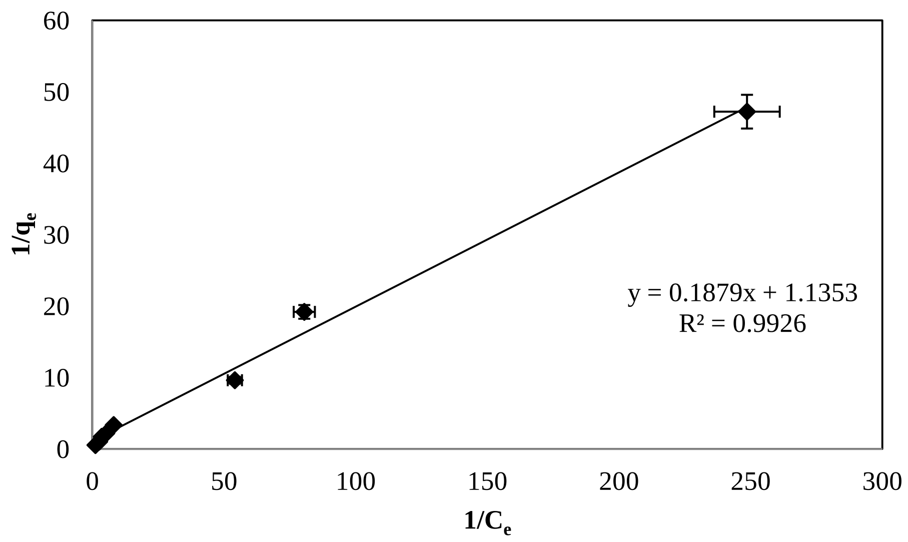

Figure 5.51 Langmuir isotherm for I2

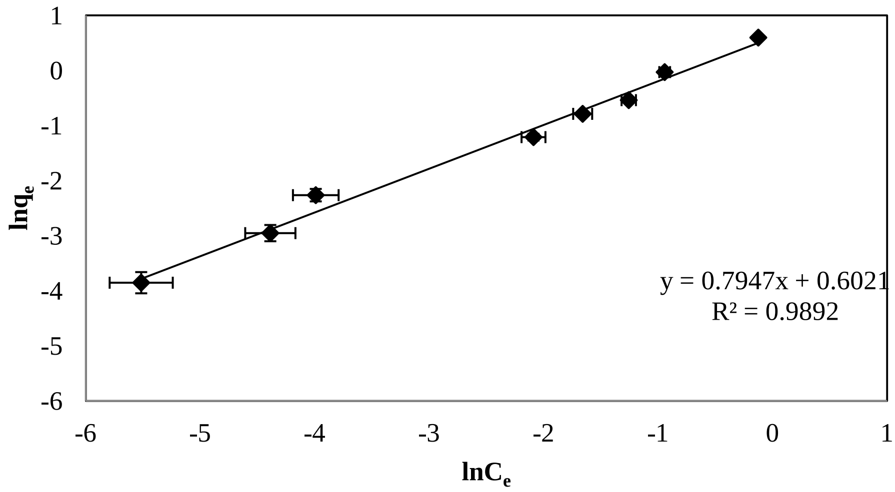

Figure 5.52 Freundlich isotherm for I2

Table 5.11. Langmuir and Freundlich isotherm constants at 25 ˚C for I1 and I2.

Adsorbent	Adsorbent dose (g/L)	Langmuir			Freundlich		
		q_{max} (mg/g)	b (L/mg)	R^2	1/n	k_f (mg/g)	R^2
I1	5	3.985	21.82	0.7215	0.686	9.475	0.8831
I2	5	0.881	6.042	0.9926	0.794	1.826	0.9892

5.5 Column Studies

5.5.1 Effect of Initial Arsenic Concentration on Adsorption in Column Studies

The sorption performance of modified sand was investigated at two different initial As (T) concentrations, i.e. 115 μg/L and 620 μg/L. The effect of the initial arsenic concentrations at a flow rate of 3 ml/min and 10 cm bed depth are presented in Figures 5.53-5.54 for modified sand. Breakthrough curves are obtained plotting the ratio of C/C_e (initial As (T) concentration / effluent As (T) concentration) versus time and are also presented in Figures 5.55 and 5.56. The S-shaped breakthrough curve was obtained as shown in Figures 5.55 and 5.56. The results revealed that lower initial arsenic concentrations resulted with higher volume of treated water. The breakthrough point occurred at 13L and 1L volumes of treated water for 115 µg/L and 620 µg/L inlet As concentrations, respectively. The early breakthrough observed at a higher arsenic concentration is due to faster exhaustion of adsorption sites.

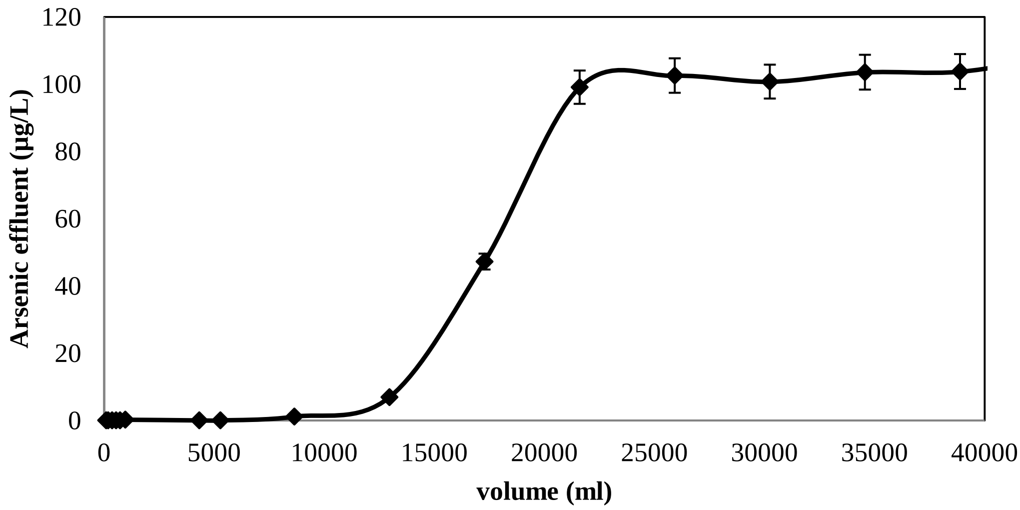

Figure 5.53 Variation of arsenic effluent concentration by treated volume for modified sand (As_{in}=115µg/L)

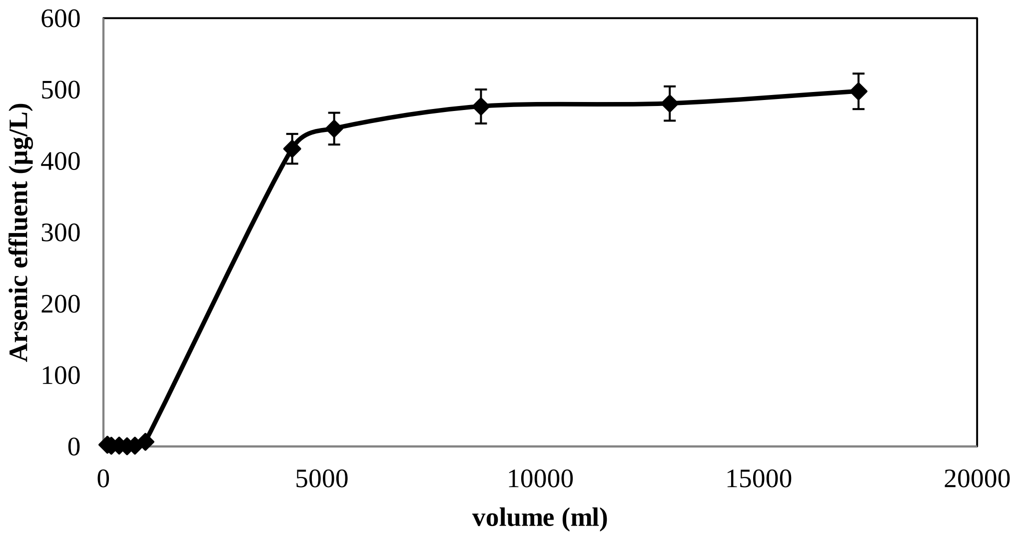

Figure 5.54 Variation of arsenic effluent concentration by treated volume for modified sand (As_{in}=620µg/L)

The cumulative volumes of effluent (mL) at the exhausted point were determined as 21.6L and 4.3L for 115 µg/L L and 620 µg/L of As(T) inlet concentrations, respectively. Higher inlet arsenic concentration was resulted with rapid saturation. Adsorption zones were almost completely exhausted at that point and no available site was provided to adsorb arsenic ions. After the exhausted point, effluent arsenic concentrations did not change significantly.

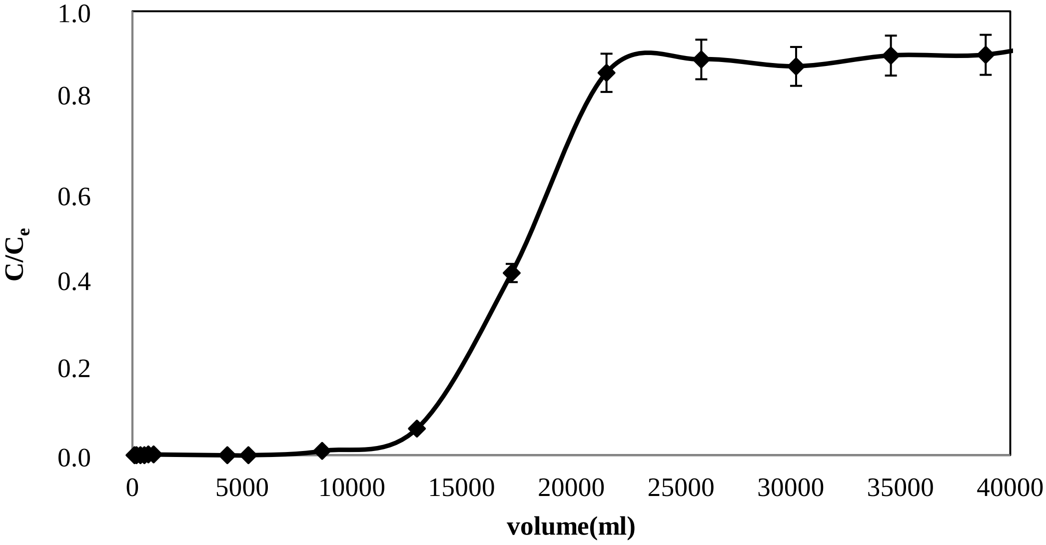

Figure 5.55 The breakthrough curve of modified sand for 115 μg/L initial arsenic concentration

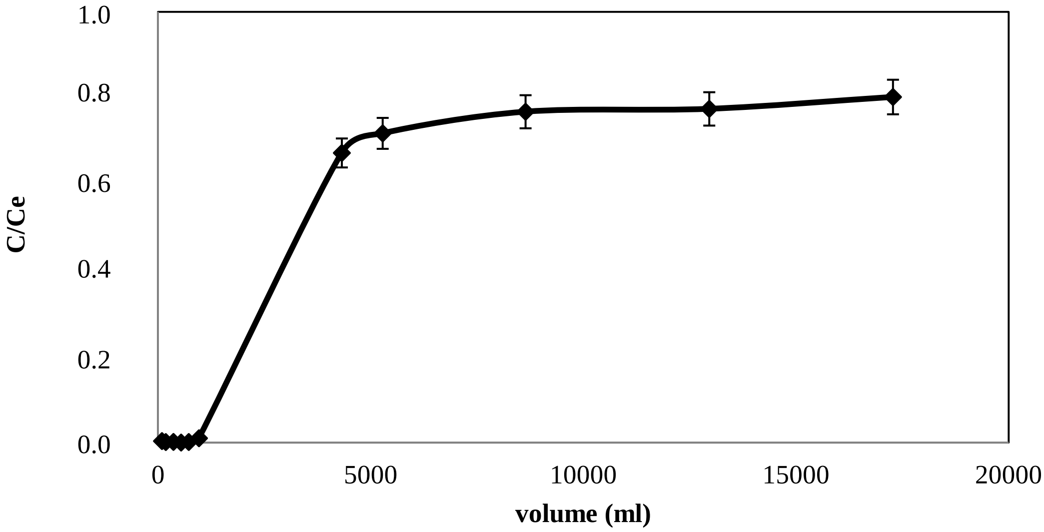

Figure 5.56 The breakthrough curve of modified sand for 620 μg/L initial arsenic concentration

The effect of initial arsenic concentration on breakthrough behavior was also investigated for modified sepiolite. The columns were operated with two different initial arsenic concentrations, i.e. 104 μg/L and 514 μg/L. The bed height and flow rate were kept constant as 10 cm and 3 mL/min, respectively. The cumulative quantity of effluent (mL) is plotted against effluent arsenic concentration (μg/L) and presented in Figures 5.57 and 5.58. Breakthrough curves plotting the ratio C/C_e versus time are also presented in Figures 5.59 and 5.60 for modified sepiolite. The S-shaped breakthrough curve was obtained for modified sepiolite, as well. Experimental results stated that arsenic adsorption was strongly affected from the influent arsenic concentration variations. For higher concentrations, breakthrough formed early as compared to lower concentration of arsenic in the feed. This early breakthrough observed at a higher solute concentration is due to faster exhaustion of adsorption sites. For the initial arsenic concentration of 104 μg/L, the breakthrough point occurred at 26L for modified sepiolite which was approximately two times higher than modified sand. Then, effluent arsenic concentration rapidly increased and column exhausted at about 40 L. It can be explained that the adsorption zone was almost completely exhaust (C/C_e=0.98). After the exhaustion point, effluent concentration was nearly same with the influent concentration.

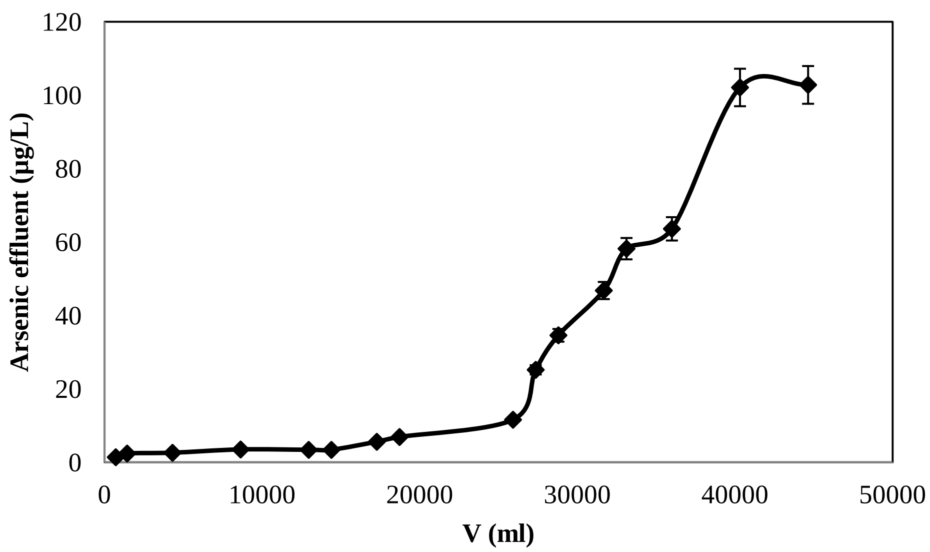

Figure 5.57 Variation of arsenic effluent concentration by treated volume for modified sepiolite (As_{in}=104μg/L)

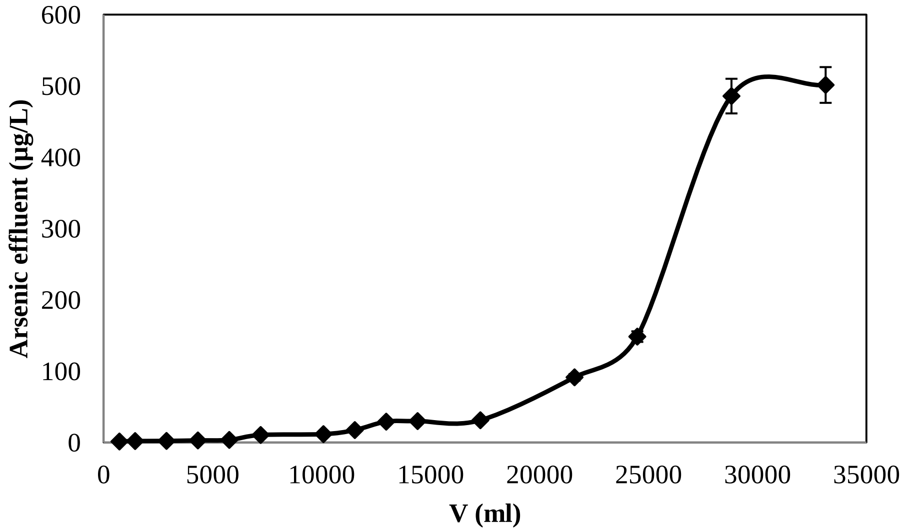

Figure 5.58 Variation of arsenic effluent concentration by treated volume for modified sepiolite (As_{in}=514µg/L)

For the initial arsenic concentration of 514 µg/L, the breakthrough point occurred at 7.2L of treated water for modified sepiolite (see Figure 5.60). Then, effluent arsenic concentration rapidly increased and reached to 485 µg/L for the bed volumes of 30 L. As seen in Figure 5.59, the breakthrough point (C/C_e) was 0.02, assuming ~10 µgAs/L in the effluent and 7.2 L of treated water was obtained. The exhaustion point occurred at 30 L for 0.95 C/C_e value. The results showed that 10 cm height modified sepiolite column has sufficient treatment capacity for such a high initial arsenic concentration (~500 µg/L).

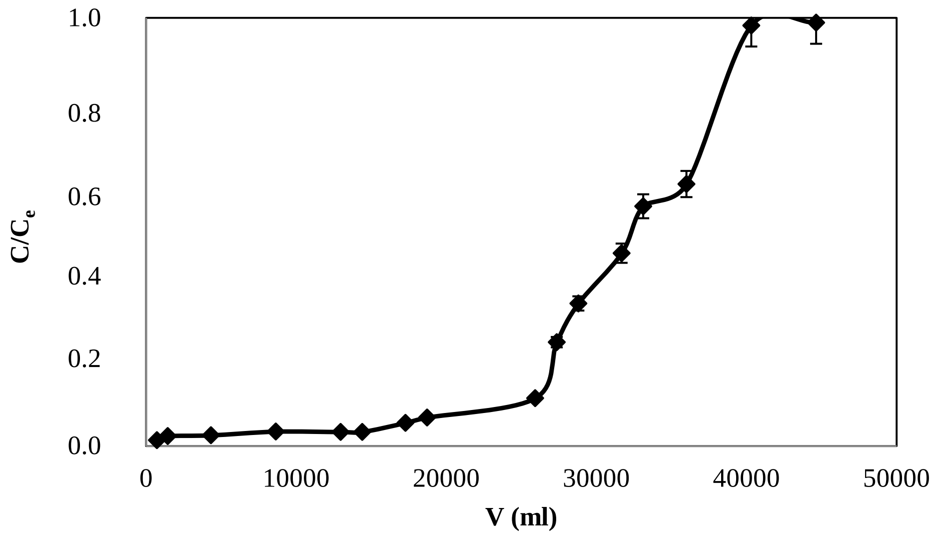

Figure 5.59 The breakthrough curve of modified sepiolite for 104 μg/L initial arsenic concentration

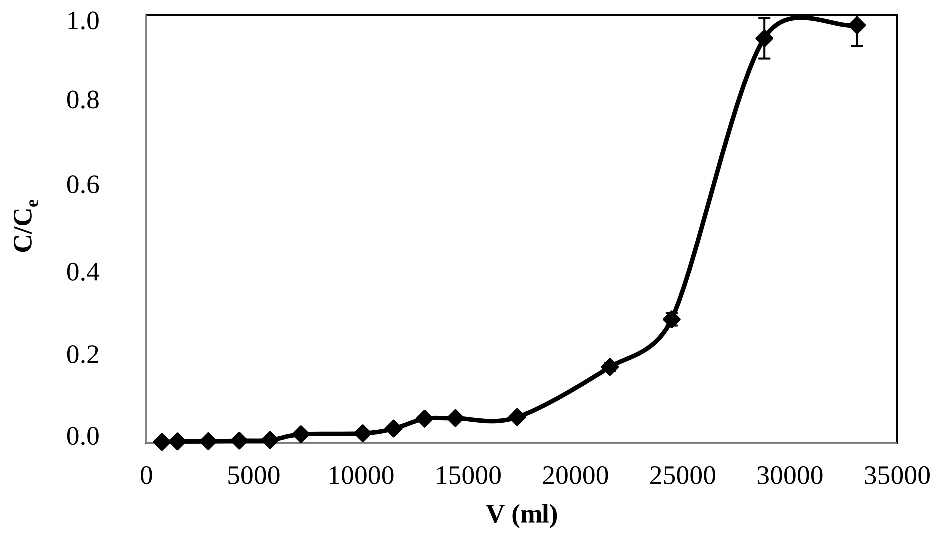

Figure 5.60 The breakthrough curve of modified sepiolite for 514 μg/L initial arsenic concentration

5.5.2 Effect of Bed Depth on Adsorption in Column Studies

The accumulation of arsenic in a fixed-bed column is dependent on the quantity of adsorbent filled in the column. In order to study the effect of bed height, each material was filled into the columns at two different bed heights, i.e. 10 and 20 cm. Arsenic solution of fixed concentration (app. 100 μg/L) was passed through the fixed-bed columns in down-flow mode at a constant flow rate of 3 mL/min. The effluent arsenic concentrations were depicted against volumes for each depth in Figures 5.61 and 5.62. In addition, breakthrough curves obtained for arsenic adsorption onto modified sand at different depts. (i.e. 10 cm and 20 cm) are shown in Figures 5.63 and 5.64.

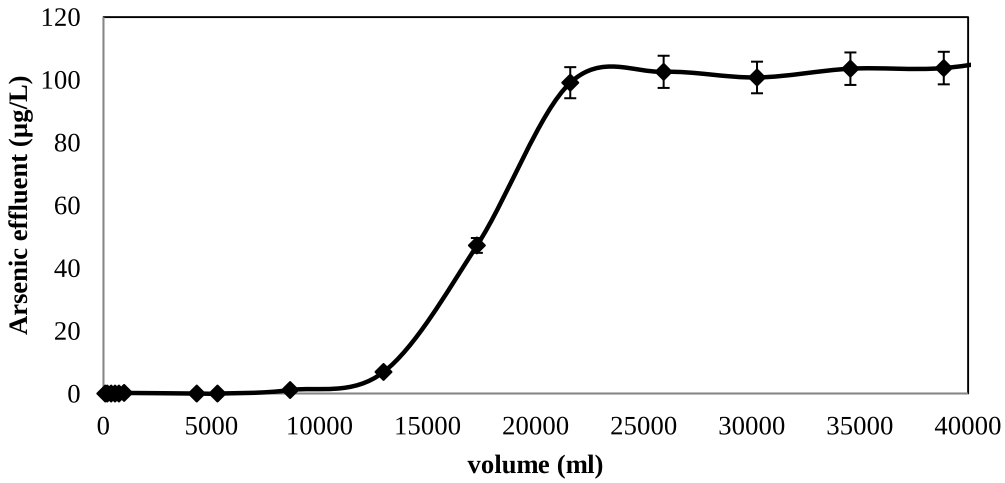

Figure 5.61 Variation of arsenic effluent concentration by treated volume for 10 cm bed depth of modified sand

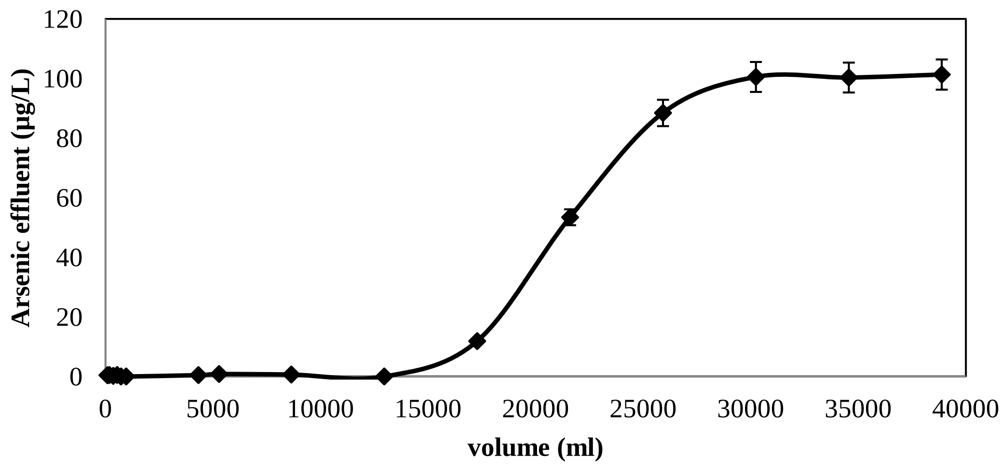

Figure 5.62 Variation of arsenic effluent concentration by treated volume for 20 cm bed depth of modified sand

As depicted by Figure 5.63 and 5.64, the breakthrough volumes varied with bed height. The breakthrough (C/C_e=0.1) was obtained as 13L for 10cm bed depth whereas it was increased to 17 L for 20cm depth of bed . The breakthrough volume reduced with a decreasing bed depth from 20 to 10 cm, as binding sites were restricted at low bed depths. At low bed depth, as the arsenic ions did not have enough time to diffuse into the surface of the modified sand and a reduction in breakthrough occurred. Conversely, with an increase in bed depth, the residence time of arsenic solution inside the column was increased, allowing the arsenic ions to diffuse deeper into the modified sand.

For 10 cm bed depth, the ratio of influent to effluent arsenic concentration (C/C_e) rapidly increased after breakthrough point and reached to exhaustion at 25 L of effluent volumes. However, about 35 L of feed water passed through the column until exhaustion point for 20 cm bed depth. Therefore, the results revealed that increasing bed depth caused more active adsorption site providing additional treated volume until exhaustion point.

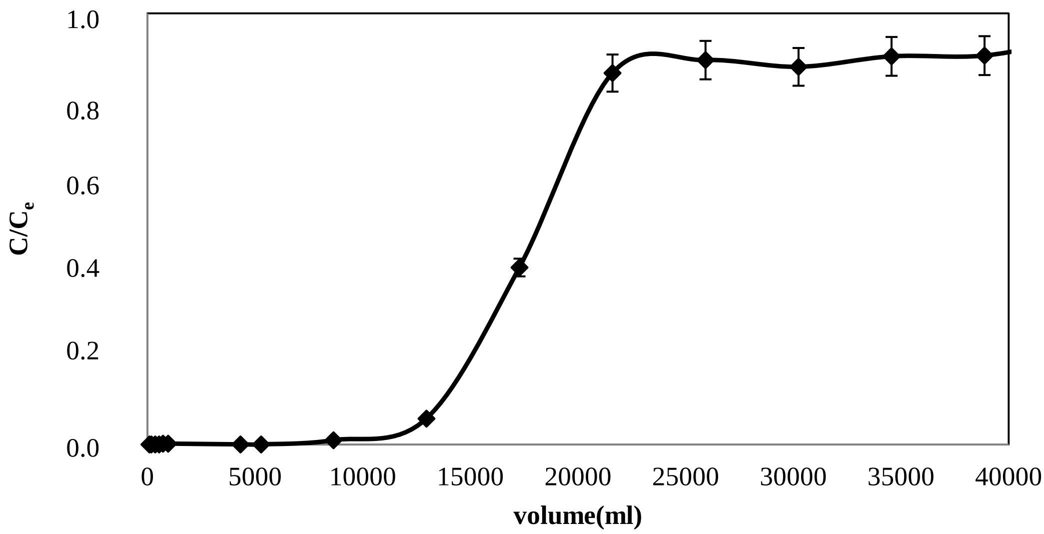

Figure 5.63 The breakthrough curve of 10 cm bed depth of modified sand

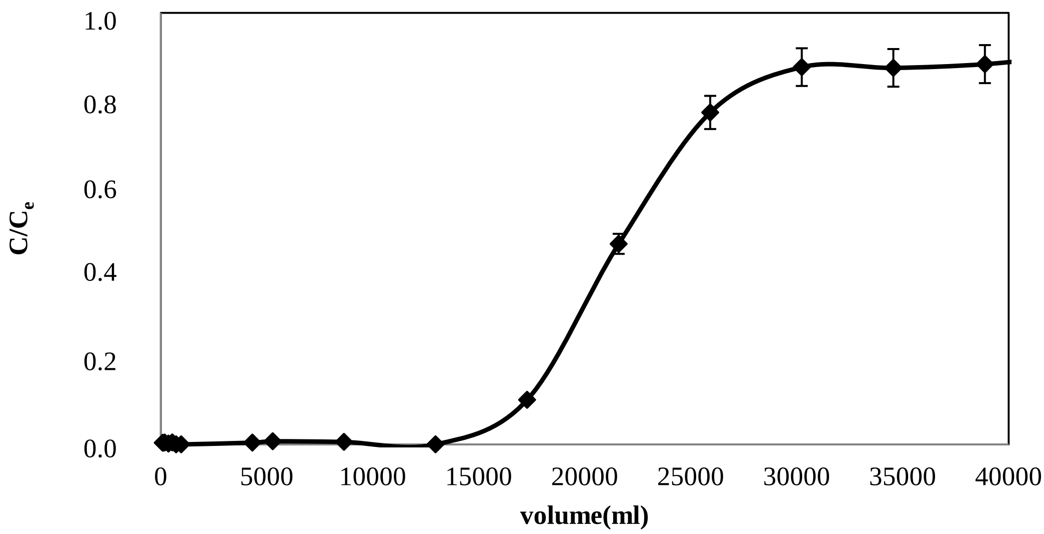

Figure 5.64 The breakthrough curve of 20 cm bed depth modified sand

For modified sepiolite, the effluent arsenic concentrations are also plotted against effluent volumes, at different bed depths, i.e. 10 cm and 20 cm, and presented in Figures 5.65 and 5.66. In addition, the breakthrough curves obtained for arsenic adsorption onto modified sepiolite at different depths are shown in Figures 5.67 and 5.68.

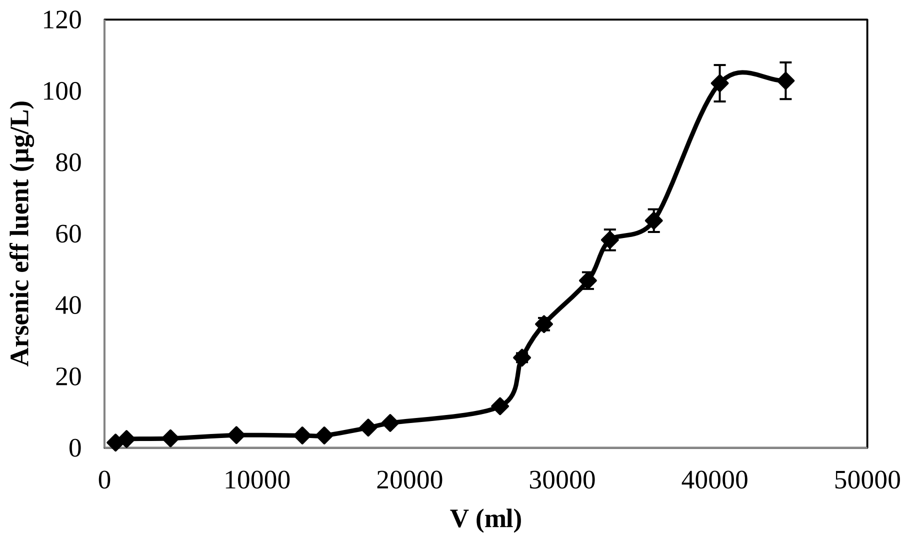

Figure 5.65 Variation of arsenic effluent concentration by treated volume for 10 cm bed depth of modified sepiolite

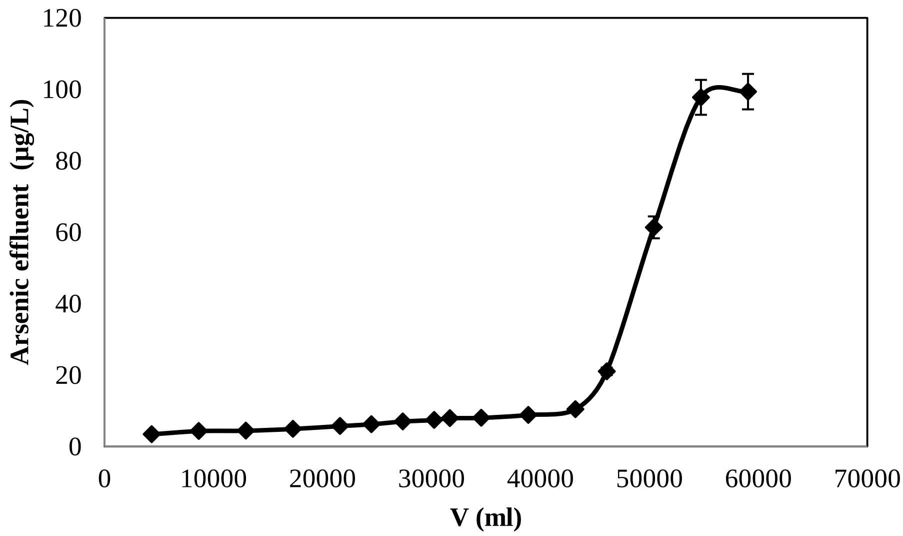

Figure 5.66 Variation of arsenic effluent concentration by treated volume for 20 cm bed depth of modified sepiolite

As can be seen in Figure 5.65, approximately 26 L of feed water could be treated to below 10 µg/L effluent arsenic concentration. Thus, breakthrough point (C/C_e =0.10) occurred at 26L of effluent volume and after the breakthrough point, C/C_e value increased rapidly up to 40.3 L. It can be explained that the adsorption zone was almost completely exhaust (C/C_e=0.98).

The breakthrough volume increased with a increasing bed depth from 10 to 20 cm. C/C_e=0.10 was taken as breakthrough point which indicates 10 µg/L arsenic concentration in the effluent. The column reached to breakthrough point at 43L of effluent volume. Column started to exhaust rapidly after 43L and effluent arsenic concentration increased to 98 µg/L at 55 L volume. The C/C_e value was 0.94 at the exhaustion point (i.e. 55 L effluent volume); and after that no further arsenic adsorption was observed.

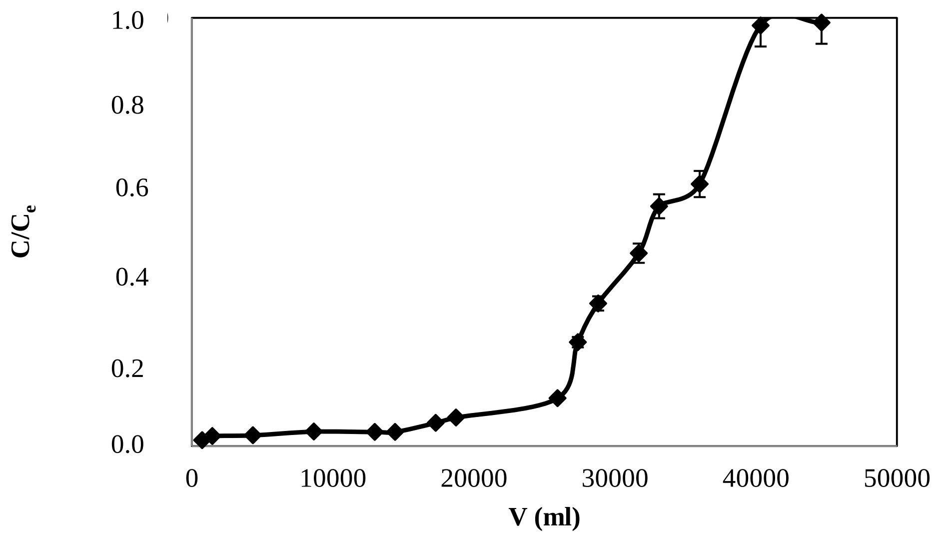

Figure 5.67 The breakthrough curve of 10 cm bed depth modified sepiolite

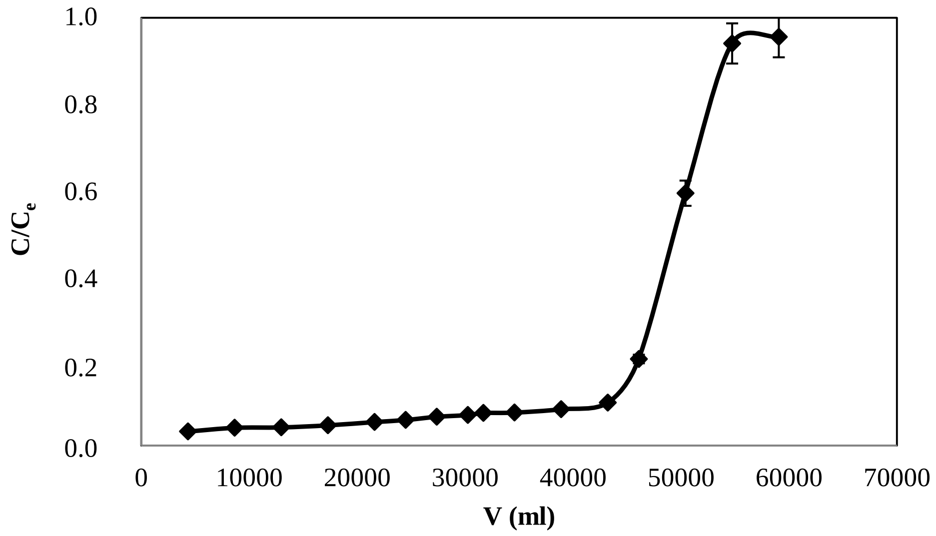

Figure 5.68 The breakthrough curve of 20 cm bed depth modified sepiolite

5.5.3 Effect of Flow Rate on Adsorption in Column Studies

The adsorption columns were operated with two different flow rates (i.e. 3 and 6 mL/min) to investigate the effect flow rate on adsorption efficiency. Columns were filled with adsorbents at 20 cm bed height, and run in the down-flow mode

Approximately 500 µg/L arsenic solutions were prepared and pH adjusted as 7. The variations of effluent arsenic concentration against treated volume for different flow rate are shown in Figures 5.69 and 5.70. In addition, the breakthrough curve for a column was determined by plotting the ratio of the Ce/C_o against time, as shown in Figures 5.71 and 5.72. The column performed well at the 3 mL/min flow rate. The effluent arsenic concentration was below the limits, and 5 L of feed water could be treated with an adequate efficiency. Breakthrough point occurred at C/C_e=0,016 for about 10µg/L effluent arsenic concentration (see Figure 5.71). Then, effluent arsenic concentration increased until no further arsenic adsorption was achieved (i.e. exhausted point). Therefore, breakthrough curve reached exhaustion point at the ratio of C/C_e=0.86 for 13 L water volume and after this, adsorbent capacity was almost completely used as seen in Figure 5.71.

Earlier breakthrough and exhaustion times were achieved, when the flow rate was increased from 3 to 6 mL/min. Effluent arsenic concentration for modified sand at 6 ml/min flow rate is given in Figure 5.70. The effluent arsenic concentration was below the limits, and 2 L of feed water could be treated with an adequate efficiency. Breakthrough point occurred at the ratio of C/C_e=0.02. Then, effluent arsenic concentration increased until no further arsenic adsorption was achieved (i.e. exhausted point). The effluent arsenic concentration rapidly increased and reached to 490 µg/L for 15,5 L effluent volume. For exhausted point, C/C_e value was 0.94, and 15.5 L of feed water could be treated until exhaustion.

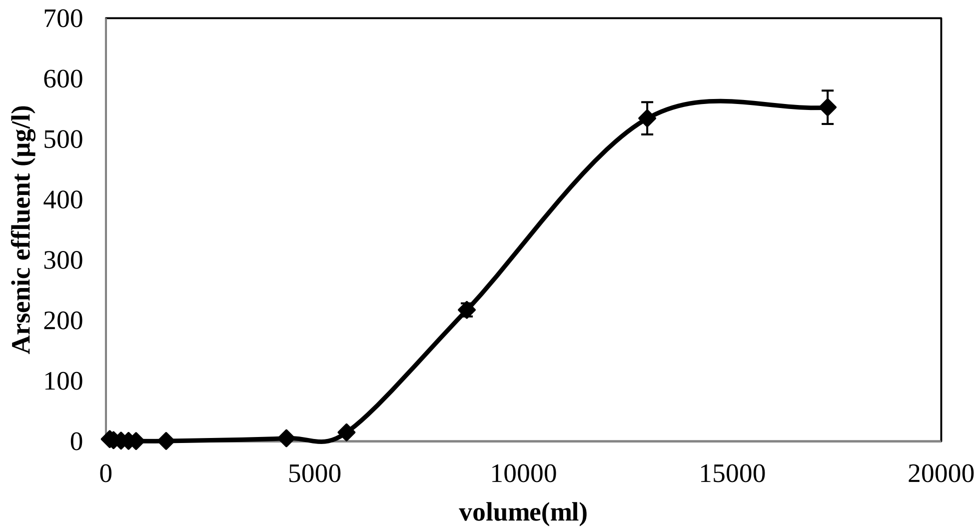

Figure 5.69 Variation of arsenic effluent concentration by treated volume for modified sand column at 3ml/min flow rate

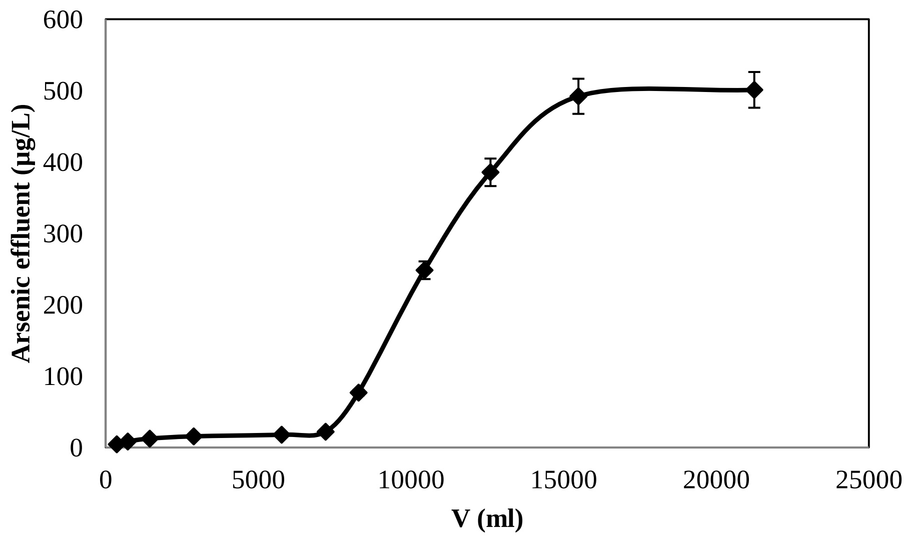

Figure 5.70 Variation of arsenic effluent concentration by treated volume for modified sand at 6ml/min flow rate

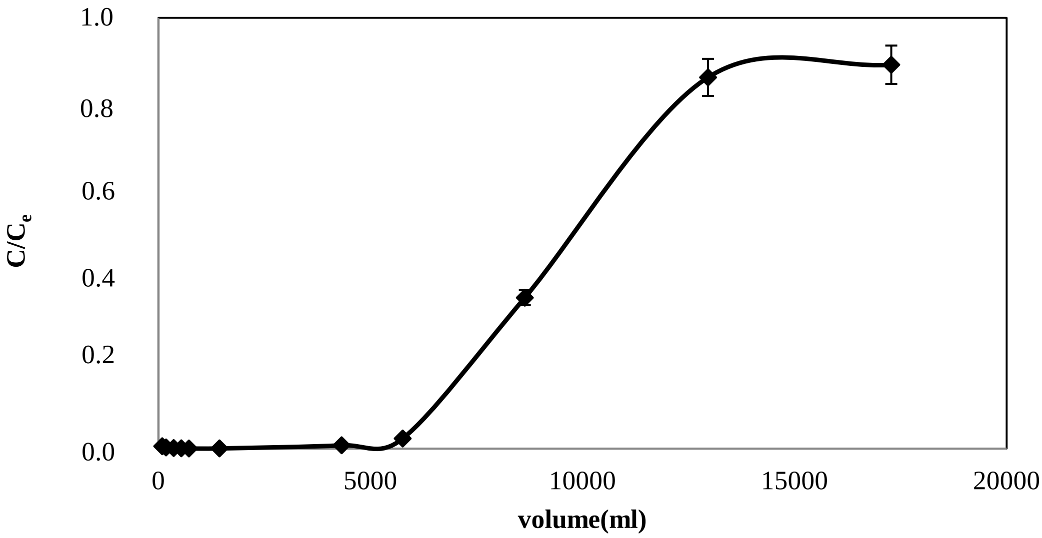

Figure 5.71 The breakthrough curve for 3 ml/min flow rate of modified sand

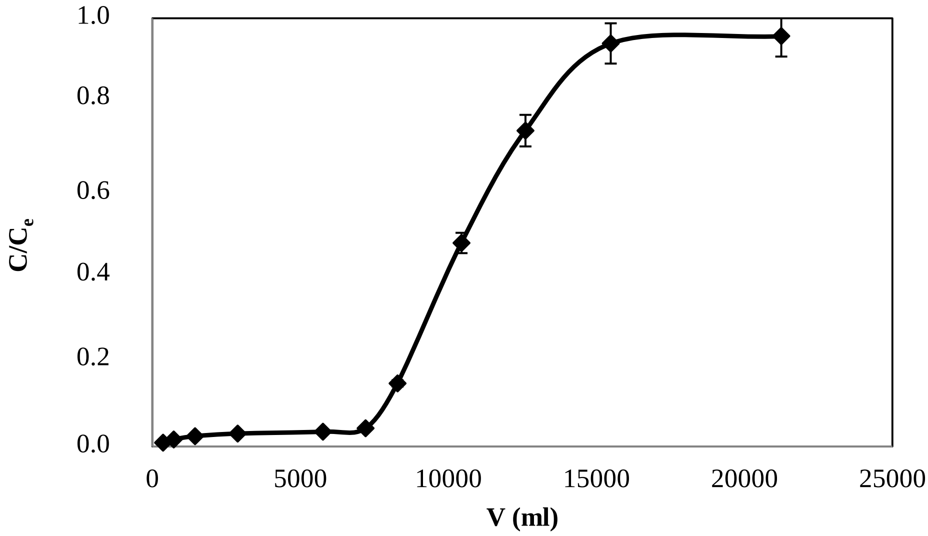

Figure 5.72 The breakthrough curve of modified sand at 6 ml/min flow rate

The results showed that, the breakthrough volume was reduced from 5L to 2L with an increase in flow rate from 3 to 6 mL/min. An increase in the flow rate resulted with the reduction in the effluent treated volume up to breakthrough volume and therefore decreased the utilization time of the column. This was due to a decrease in the residence time, which restricted the contact of arsenic solution to the modified sand. At higher flow rates, the arsenic ions did not have enough time to diffuse into the pores of the modified sand and they exited the column before equilibrium occurred.

Figure 5.73 and 5.74 shows the effluent arsenic concentration for modified sepiolite at 3 ml/ min and 6 ml/min flow rates, respectively. The breakthrough curves for columns were determined by plotting the ratio of the C/C_e against time, as shown in Figures 5.74 and 5.75. For modified sepiolite, breakthrough and exhaustion points were certainly higher than modified sand at the same flow rates. At 3 ml/min flow rate, the modified sepiolite was capable to treat 23 liters of feed water whereas only 5 liters of water could be treated at the same conditions by modified sand. At 3 ml/min flow rate, breakthrough point (C/C_e=0.02) occurred at 23 L volume of feed water. Then, effluent As (T) concentration increased until no more arsenic adsorption was achieved (i.e. exhausted point). Approximately 46 L of feed water treated through the column until the exhaustion point(C/C_e=0.96).

Similar to previous experiments with modified sand, breakthrough and exhaustion volumes were reduced when the flow rate was increased from 3 to 6 mL/min. The effluent As (T) concentrations were depicted against volumes of treated water in Figure 5.74 for 6 ml/min flow rate. The results revealed that 6 L of feed water could be treated with efficiently (i.e. Ce < 10 µg/L) at 6 ml/min flow rate. The increase in effluent concentrations relatively low until the 24 L of feed water was treated. However, after that point, effluent As (T) concentrations were sharply increased and reached to about 500 µg/L for 35 L of treated water. Thus, column saturated with 35 L water volume and reached exhaustion point at C/C_e= 0.95. Compared to 3 ml/min flow rate, 75% less water could be treated when the flow rate was increased to 6 ml/min.

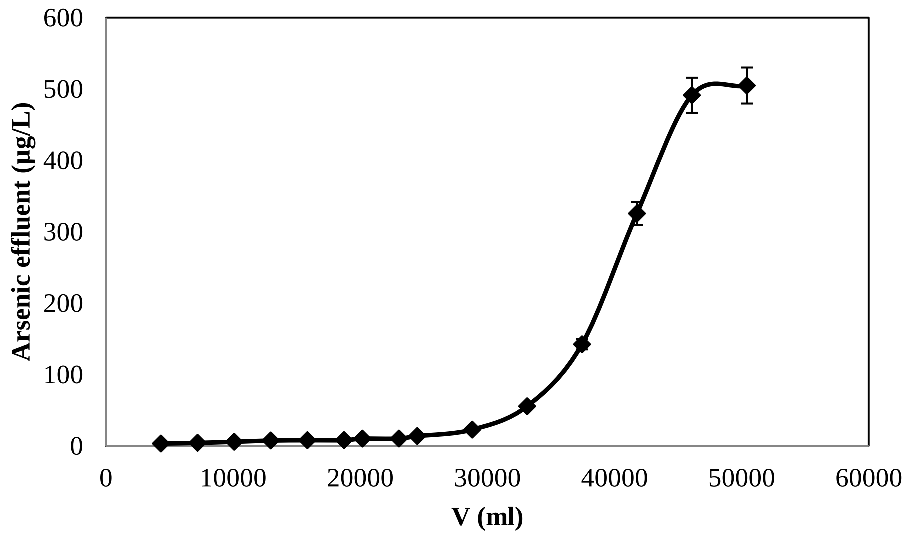

Figure 5.73 Variation of arsenic effluent concentration by treated volume for modified sepiolite at 3 ml/min flow rate

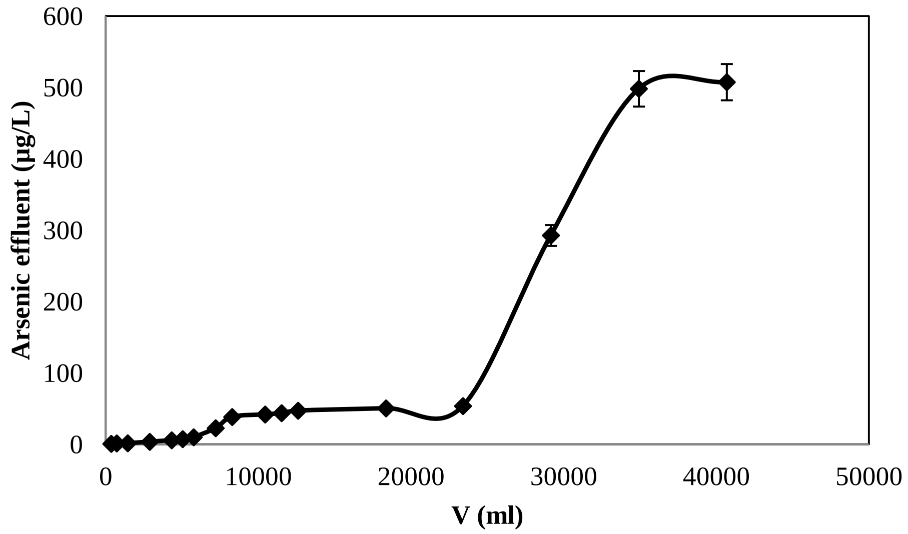

Figure 5.74 Variation of arsenic effluent concentration by treated volume for modified sepiolite at 6 ml/min flow rate (As_{in}= 523 µg/L)

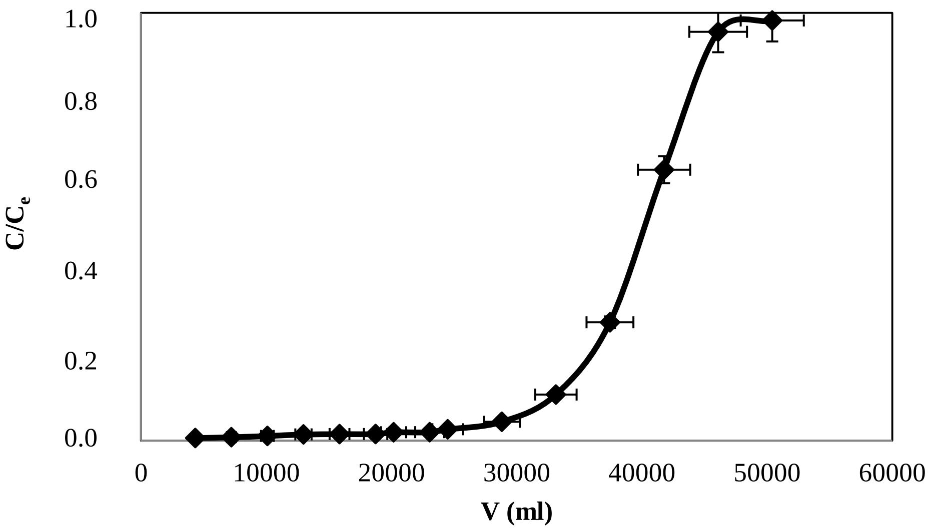

Figure 5.75 The breakthrough curve of modified sepiolite at 3ml/min flow rate

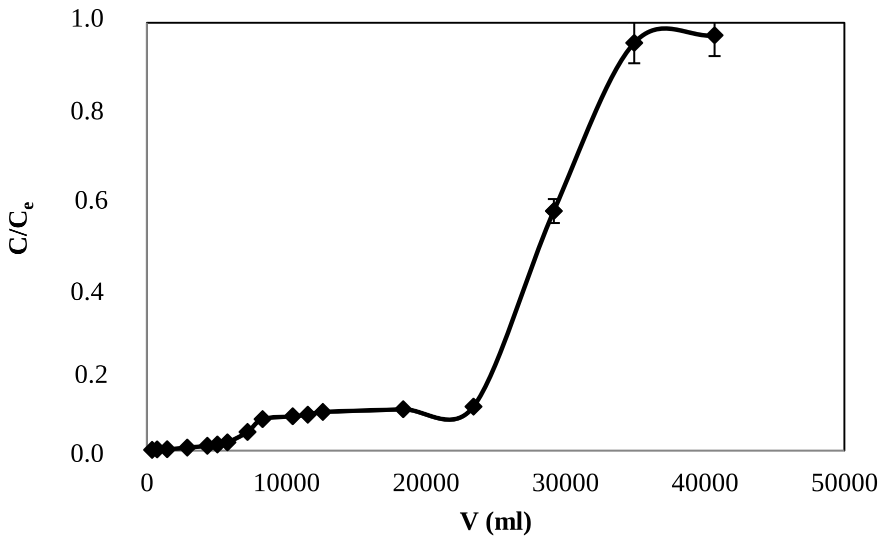

Figure 5.76 The breakthrough curve of modified sepiolite at 6ml/min flow rate (As_{in}= 523 µg/L)

Breakthrough volumes of modified sepiolite were obtained as 23 L and 6 L, whereas, by same parameter for modified sand was 5 L and 2 L at flow rates of 3 and 6 ml/min, respectively. Thus, higher reduction (as per cent) was achieved when flow rate increased from 3 to 6 ml/min for modified sepiolite. This situation proved that adsorption occurs into the pores not only surface of sepiolite, whereas adsorption is only surface of nonporous sand. Water passed through sepiolite column before reaching to the pores at 6 ml/min flow rate. Thus, the available sites could not be used effectively and resulted less water treatment until the breakthrough point versus sand column. For this reason, modified sepiolite is more sensitive than modified sand column in case of increase of flow rate.

5.6 Kinetic Models

The prediction of the breakthrough curves and estimation of the characteristic parameters are useful for column design. However, breakthrough behavior of fixed-bed adsorbents may change under various operational conditions. Hence, a number of pilot-scale experiments are required to evaluate the column performance under different operating conditions to obtain the design parameters. This may not be always feasible due to limited time and economic considerations. Mathematical models can be used as an alternative tool for design and analysis of full-scale systems by reducing the number of pilot-scale studies (Maliyekkal & Philip, 2011). In this study, Thomas Model and Bohart & Adams Model are evaluated to predict arsenic adsorption by modified sand and modified sepiolite. In all model fittings, linear regression analyses were used to predict the breakthrough behavior.

5.6.1 Thomas Model

The Thomas model is one of the most widely used models in assessing column performance. The model calculates the adsorption capacity and rate constant for an adsorption column (Thomas, 1944). The expression by Thomas for an adsorption column is given as follows:

$$\frac{C_t}{C_0} = \frac{1}{1+\exp\left(\frac{k_{Th} q_0 M}{Q} - k_{Th} C_0 t\right)} \qquad (5.1)$$

And linearized form is:

$$\ln\left(\frac{C_0}{C_t} - 1\right) = \frac{k_{Th} q_0 M}{Q} - k_{Th} C_0 t \qquad (5.2)$$

Where C_t is the effluent concentration at a specific time (mg/L), C_0 is the influent concentration (mg/L), k_{Th} is the Thomas rate constant (L/ min mg), q_0 is the equilibrium uptake per g of the adsorbent (mg/g), M the amount of adsorbent in the column (g), t is the time(min) and Q is the flowrate (L min−1). The kinetic coefficient k_{Th} and the adsorption capacity of the column q_0 can be determined from a plot of (C_0/C_t-1) against time (t) at a given flow rate using linear regression.

5.6.1.1 Application of Thomas Model to Modified Sand

The values of the model parameters for modified sand, i.e. k_{Th} (Thomas rate constant) and q_0 (adsorption capacity of column) were calculated from the slope and intercept of the graphs of ln (C_0/C_t-1) versus time with regard to bed depth, initial arsenic concentration and flow rate. The results are summarized in Table 5.12 whereas the linear forms of the graphs are presented in the appendices. Coefficients of determination values indicated that Thomas model fitted to the experimental data and R^2 values ranging from 0.707-0.940. As can be seen from Table 5.12, maximum adsorption capacity, q_o increased with increasing initial arsenic concentration for different bed depths. Adsorption capacity, q_0, obtained 2.961 µg/g and 6.637 µg/g for 115 and 620 µg/L initial arsenic concentrations at 10 cm bed depth.1.680 µg/g and 3.877 µg/g adsorption capacities were calculated for 115 and 620 µg/L at 20 cm bed depth. Besides, when initial arsenic concentration increased, adsorption capacity, q_0, *also* increased, however, Thomas rate constant, k_{Th}, decreased. However, increasing in flow rate from 3 ml/min to 6 ml/min did not considerably affect the adsorption capacity of modified sand, although Thomas rate constant, k_{Th}, increased from 0.180 to 0.282 L/min mg.

Table 5.12 Thomas model constants for arsenic adsorption by modified sand for varied bed depths, influent arsenic concentrations and flow rates

h (cm)	**Q (ml/min)**	**C_0 (mg/L)**	**k_{Th} (L/min.mg)**	**q_0 (mg/g)**	**R^2**
10	3	0.115	0.343	0.00296	0.9127
10	3	0.620	0.155	0.00637	0.7074
20	3	0.115	0.342	0.00168	0.9352
20	3	0.620	0.180	0.00387	0.9408
20	6	0.523	0.282	0.00330	0.9292

Breakthrough curves obtained experimental data and predicted values using Thomas model at different initial arsenic concentrations, bed depths, and flow rates are illustrated in Figures from 5.77 to 5.79. Figure 5.76 show that the differences between the experimental and predicted values were negligible especially for low initial As (T) concentrations. Thus, lower coefficient of determination value (i.e. 0.704) was obtained for higher initial As (T) concentration of 620 µg/L.

The differences between the e 0.0 nental and predicted values are shown in Figures 5.78 for bed depths of 10 and 20 cm. The Thomas model results fitted well with experimental data yielding high coefficient of determination values ranged in 0.9127-0.9352.

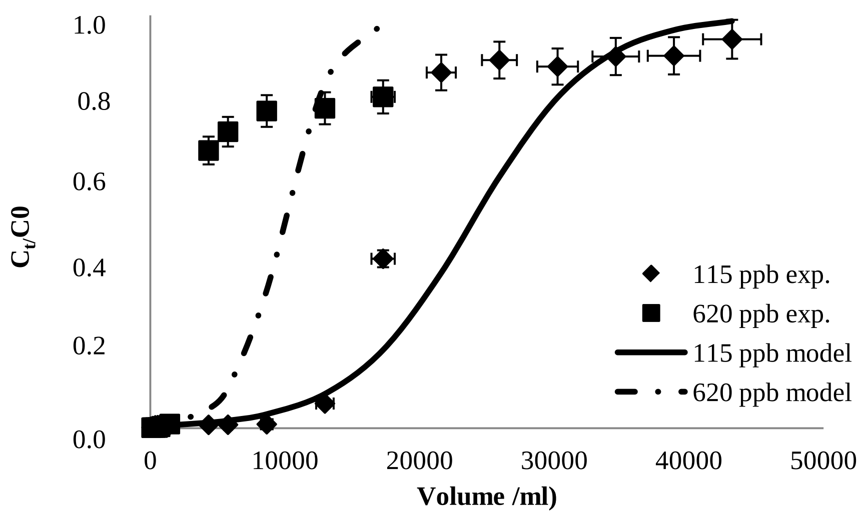

Figure 5.77 Experimental and simulating breakthrough curves for different initial concentrations (modified sand-Thomas model)

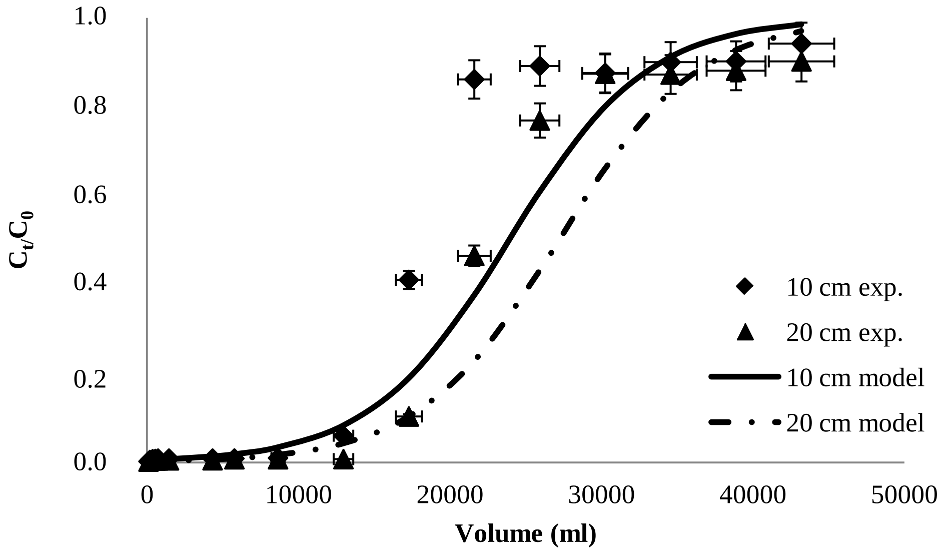

Figure 5.78 Experimental and simulating breakthrough curves for different bed depths (modified sand-Thomas model)

Finally, regarding to different flow rates, the Thomas model results fitted well with experimental data yielding high coefficient of determination values ranged in 0.9292-0.9408. The adsorption capacity did not change with increasing flow rates.

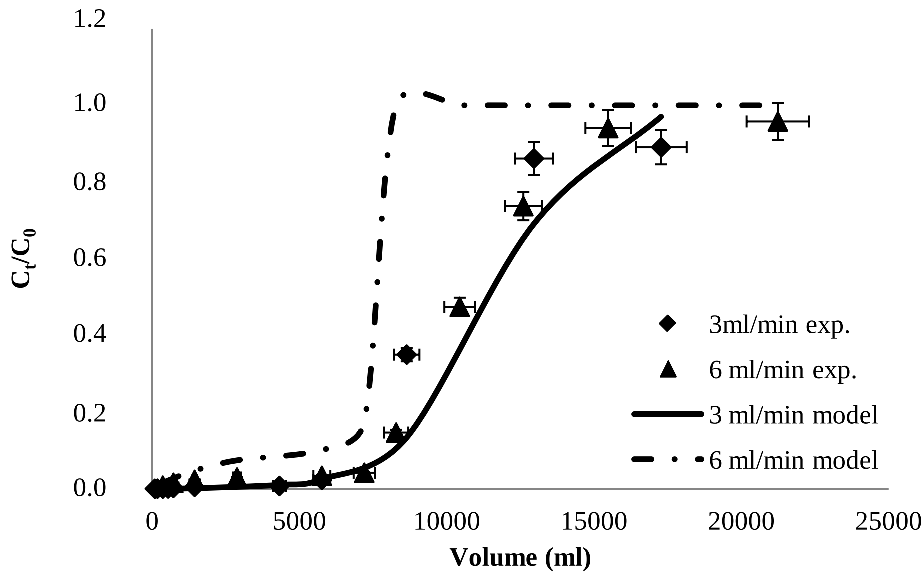

Figure 5.79 Experimental and simulating breakthrough curves for different flow rates (modified sand-Thomas model)

5.6.1.2 Application of Thomas Model to Modified Sepiolite

The values of the model parameters for modified sepiolite, i.e. k_{Th} (Thomas rate constant) and q_0 (adsorption capacity) were also determined from the graph of linearized form of the Thomas equation. The results are summarized in Table 5.13 whereas the linear forms of the graphs are presented in the Appendices. In general, adsorption capacities determined from the intercept of straight line were much higher than the modified sand column. In general, lower influent arsenic concentrations resulted with a reduction in the adsorption capacities. In other words, results revealed that adsorption capacity of the column increased with the increased initial As (T) concentration, while k_{Th} decreased.

Table 5.13 Thomas model constants for arsenic adsorption by modified sepiolite for varied bed depths, influent arsenic concentrations and flow rates

h (cm)	**Q (ml/min)**	**C_0 (mg/L)**	**k_{Th} (L/minmg)**	**q_0 (mg/g)**	**R^2**
10	3	0.104	0.306	0.013	0.8492
10	3	0.514	0.096	0.050	0.9365
20	3	0.104	0.176	0.010	0.6852
20	3	0.514	0.066	0.041	0.8686
20	6	0.523	0.153	0.0071	0.9165

As can be seen from the breakthrough curves, the differences between the experimental and predicted data were insignificant for all operating parameters (i.e. initial As (T) concentrations bed depth and flow rate). The experimental data of modified sepiolite fitted well with the Thomas model for varied initial arsenic concentrations and coefficient o determination values were ranging from 0.8492-0.9365. Adsorption capacities relatively decreased for increased bed depths. When bed depth increased as two folds (i.e. 20 cm), adsorption capacities were reduced to 0.013 and 0.010 mg/g for 10 and 20 cm bed depths respectively. In contrast to modified sand, adsorption capacity, q_o, decreased by increasing in flow rate from 3 ml/min to 6ml/min and obtained 0.041 and 0.007 mg/g, respectively. It could be a result of porous structure of modified sepiolite and arsenic could not be trapped efficiently on pores at high flow rates.

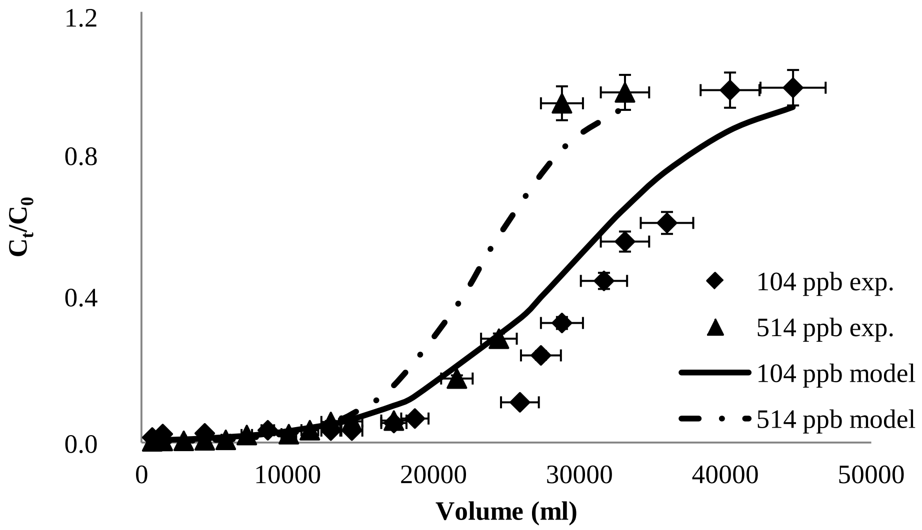

Figure 5.80 Experimental and simulating breakthrough curves for different initial concentrations (modified sepiolite-Thomas model)

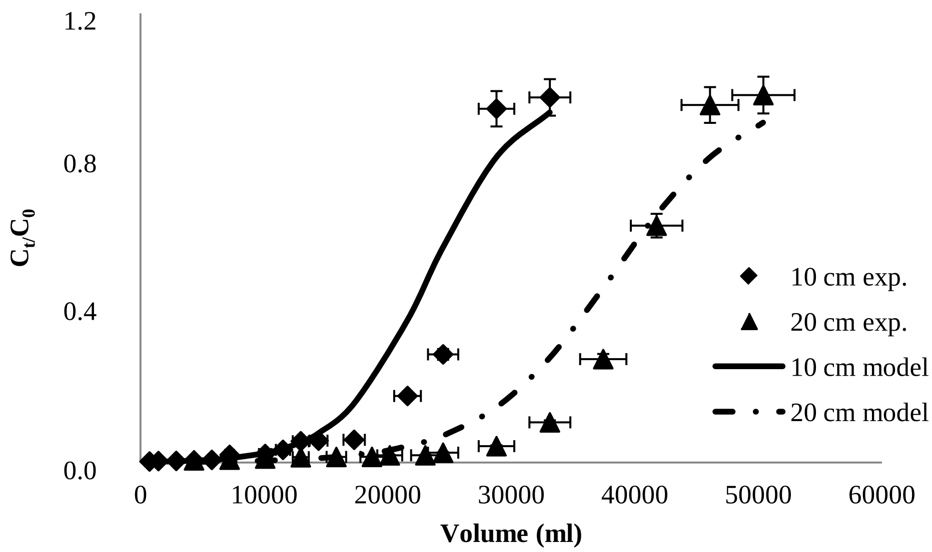

Figure 5.81 Experimental and simulating breakthrough curves for different bed depths (modified sepiolite-Thomas model)

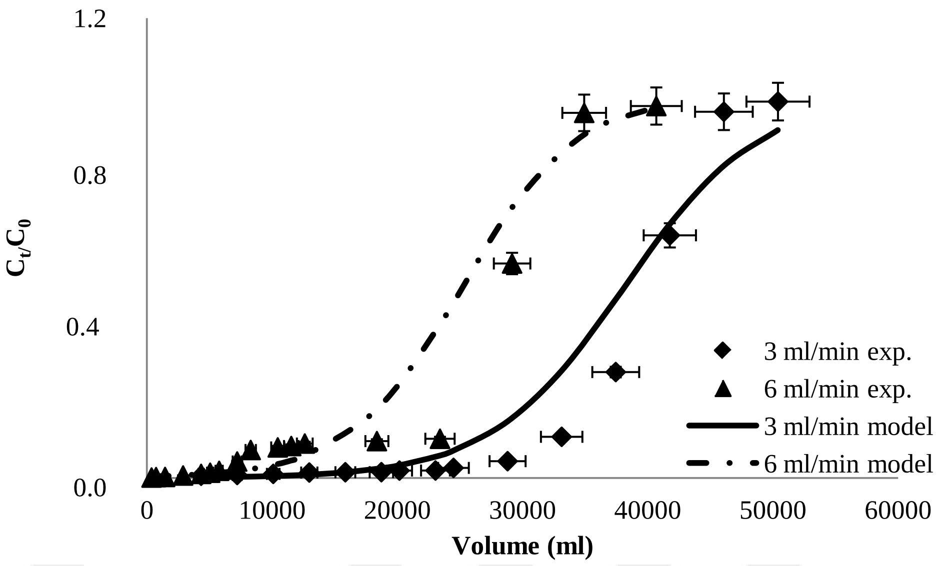

Figure 5.82 Experimental and simulating breakthrough curves for different flow rates (modified sepiolite-Thomas model)

5.6.2 Bohart&Adams (B&A) Model

Bohart&Adams model (Bohart and Adams, 1920) is based on the surface reaction theory assuming that equilibrium is not instantaneous; so, the rate of the adsorption is proportional to the adsorption capacity which still remains on the sorbent. This model established the fundamental equations describing the relationship between C_t/C_0 and t in a continuous system. Bohart&Adams model is used for the description of the initial part of the breakthrough curve. The model is expressed as:

$$\frac{C_t}{C_0} = \exp\left(k_{BA}C_0 t - \frac{k_{BA}NZ}{u}\right) \tag{5.3}$$

A linearized version of the Bohart&Adams analytical solution is given by:

$$ln\left(\frac{C_t}{C_0}\right) = k_{BA}C_0 t - \frac{k_{BA}NZ}{u} \tag{5.4}$$

Where C_t is the solution concentration at the fixed bed outlet at time t, C_0 is the feed concentration, k_{BA} is the Bohart&Adams rate constant(l/mg min), N is the sorption capacity of the sorbent per unit volume of the bed(mg/l), Z is the total bed depth(cm), u is the linear flow rate (ml/min) and t is time (t). In Equation (4.5), k_{BA} and N are fitting parameters. With known C_0, Z and u, the two parameters N and k_{BA} are given by the y-intercept and slope of the plot, respectively.

5.6.2.1 Application of B&A Model for Modified Sand

The values of the B&A model parameters for modified sand were determined from the slope and intercept of the graphs of ln (C_0/C_t-1) versus time with regard to bed depth, initial arsenic concentration and flow rate. The results are summarized in Table 5.13 whereas the linear forms of the graphs are presented in the Appendices. B&A model described initial part of the breakthrough curve, up to breakthrough point. It is shown from the Table 5.14 that coefficient of determination values, R^2, was in the range of 0.733 to 0.926 for varying influent arsenic concentrations. The k_{BA} values decreased from 0.233 to 0.165 L/mgmin when the inlet As (T) concentration increased from 115 to 620 µg/L. From Table 5.13, saturation concentration, *N*, increased with increasing initial arsenic concentration for both bed depths. Saturation concentration obtained as 6.872 mg/L for 112 µg/L initial arsenic concentrations at 10 cm bed was increased to 10.75 mg/L for 620 µg/L initial arsenic concentrations. Similar results were observed when bed depth increased to 20 cm. 3.615 and 7.852 mg/L adsorption capacities were calculated for 115 and 620 µg/L at 20 cm bed depth. Besides, when initial As (T) concentration increased, the adsorption capacities also increased, however, rate constant, $k_{BA,}$ decreased. Increasing in flow rate from 3 ml/min to 6 ml/min did not affect saturation concentration of modified sand so much; however, B&A rate constant, k_{BA}, increased from 0.141 to 0.214 L/mgmin.

Table 5.14 B&A model constants for arsenic adsorption by modified sand for varied bed depths, influent arsenic concentrations and flow rates

h (cm)	Q (ml/min)	C_0 (mg/L)	k_{BA} (L/mgmin)	N (mg/L)	R^2
10	3	0.115	0.233	6.872	0.8674
10	3	0.620	0.165	10.75	0.7336
20	3	0.115	0.250	3.615	0.9050
20	3	0.620	0.141	7.852	0.8886
20	6	0.523	0.214	6.793	0.9260

Breakthrough curves obtained experimental data and predicted values using B&A model at different initial As (T) concentrations, bed depths, and flow rates are illustrated in Figures from 5.83 to 5.85. Until the breakthrough point, B&A model agreed well for varying initial As (T) concentrations with coefficient of determination values ranged between 0.733 and 0.926. Experimental and predicted values were compared in Figure 5.83 for different initial arsenic concentrations.

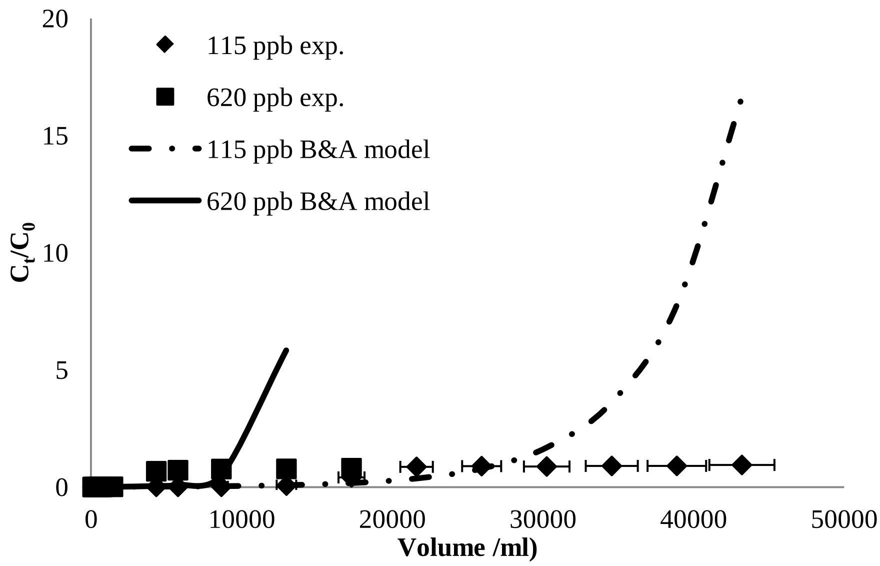

Figure 5.83 Experimental and simulating breakthrough curves for different initial concentrations (modified sand-B&A model)

Application of B&A model for modified sand for different bed depths (10 and 20 cm) are given in Figure 5.84. B&A agreed well with 10 cm and 20 cm bed depths by modified sand with 0.8674 and 0.9050 coefficient of determination, respectively. Experimental and predicted values were also compared in Figure 5.85 for different flow rates. For different flow rates, B&A model fitted well for modified sand. Coefficient of determination values obtained 0.8886 and 0.9292 at 3 ml/min and 6 ml/min flow rates, respectively.

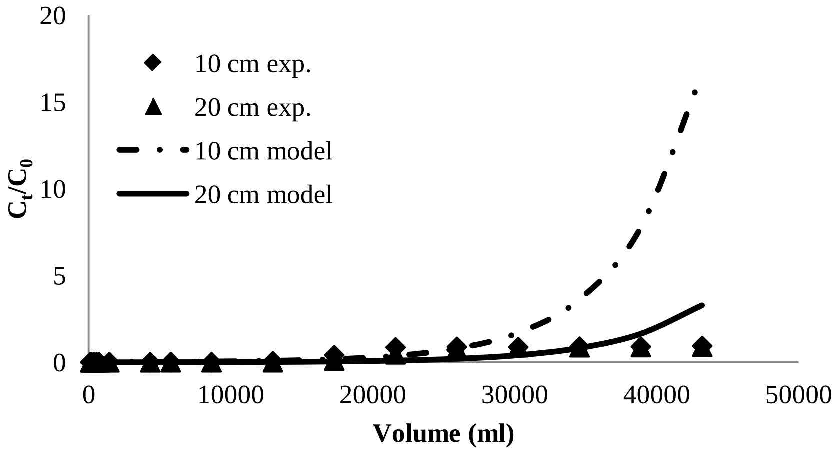

Figure 5.84 Experimental and simulating breakthrough curves for different bed depths (modified sand-B&A model)

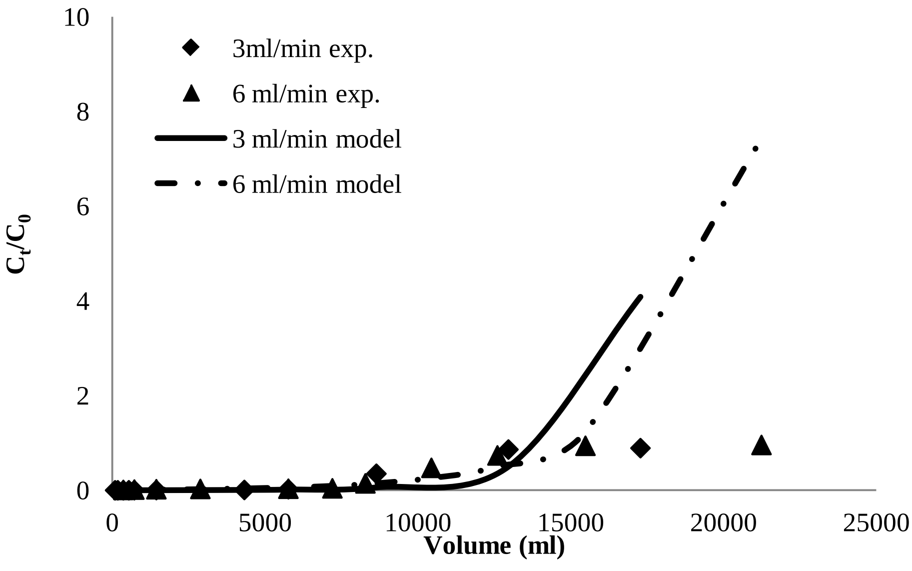

Figure 5.85 Experimental and simulating breakthrough curves for different flow rates (modified sand-B&A model)

5.6.2.2 Application of B&A Model for Modified Sepiolite

The values of the B&A model parameters for modified sepiolite were calculated from the slope and intercept of the graphs of ln (C_0/C_t-1) versus time with regard to bed depth, initial arsenic) concentration and flow rate. Table 5.15 shows the values of kinetic constants and saturated concentrations calculated using B&A model at different bed heights, flow rates and influent concentrations in the column. The linear forms of the graphs are presented in the Appendices. It is shown from the Table 5.15 that coefficient of determination values were in the range of 0.8173 to 0.9759 for 514 and 104 μg/L inlet arsenic concentrations. The k_{BA} values decreased from 0.18 to 0.066 L/mgmin when the inlet As (T) concentrations increased from 104 to 514 μg/L.

As given in Table 5.15, saturation concentration obtained 7.68 mg/L and 27.78 mg/L for 104 and 514 μg/L initial arsenic concentrations at 10 cm bed for modified sepiolite. At 20 cm bed depth 6.264 mg/L and 22.57 mg/L saturation concentrations were obtained for 104 and 514 μg/L, respectively. Increasing in initial arsenic concentration resulted by increasing in saturation concentrations as observed in modified sand. In contrast to modified sand, saturation concentration, *N*, decreased by increasing in flow rate from 3 ml/min to 6 ml/min and obtained 22.57 and 14.066 mg/L, respectively. Similar results were also obtained for modified sand. It can be a result of porous structure of modified sepiolite and arsenic could not be trapped efficiently on pores at high flow rate. It also indicates that contact time is not sufficient at higher flow rate.

Table 5.15 B&A model constants for arsenic adsorption by modified sepiolite for varied bed depths, influent arsenic concentrations and flow rates

h (cm)	Q (ml/min)	C_0 (mg/L)	k_{BA} (L/mgmin)	N (mg/L)	R^2
10	3	0.104	0.18	7.679	0.9518
10	3	0.514	0.066	27.78	0.9759
20	3	0.104	0.105	6.264	0.8173
20	3	0.514	0.043	22.57	0.9482
20	6	0.523	0.11	14.066	0.8253

Breakthrough curves obtained from experimental data and predicted values using B&A model at different initial As (T) concentrations, bed depths, and flow rates are illustrated in Figures from 5.86 to 5.88. The breakthrough curves showed that the superposition of experimental results (points) and the theoretical calculated points (lines) for varying initial As (T) concentrations with high coefficient of determination values ranged between 0.9518 and 0.9759. Experimental and predicted values were compared in Figure 5.86 for different initial arsenic concentrations. Similarly, experimental data and model values were fitted well yielding high coefficient of determination values for different bed depths. However, from the Figure 5.88, it is apparent that B&A model predicted the initial portion of the breakthrough for different flow rates and deviated significantly thereafter.

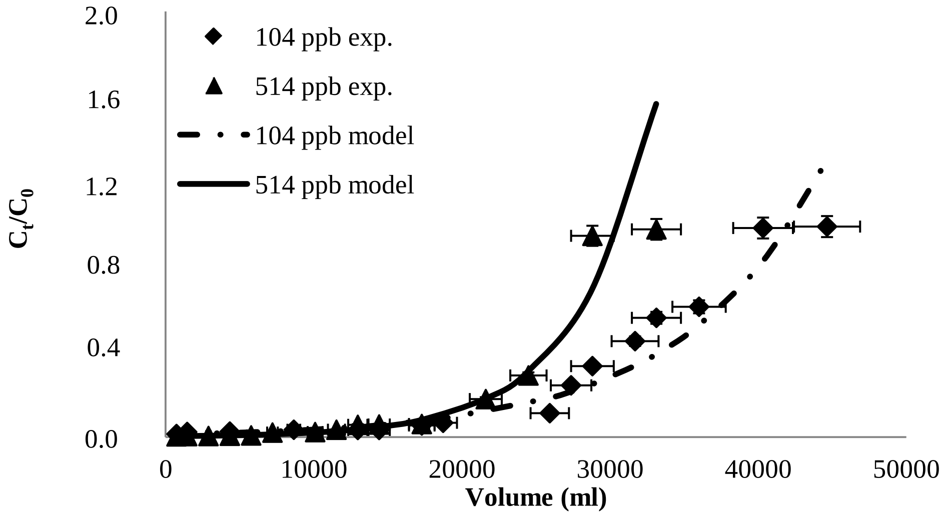

Figure 5.86 Experimental and simulating breakthrough curves for different initial concentrations (modified sepiolite-B&A model)

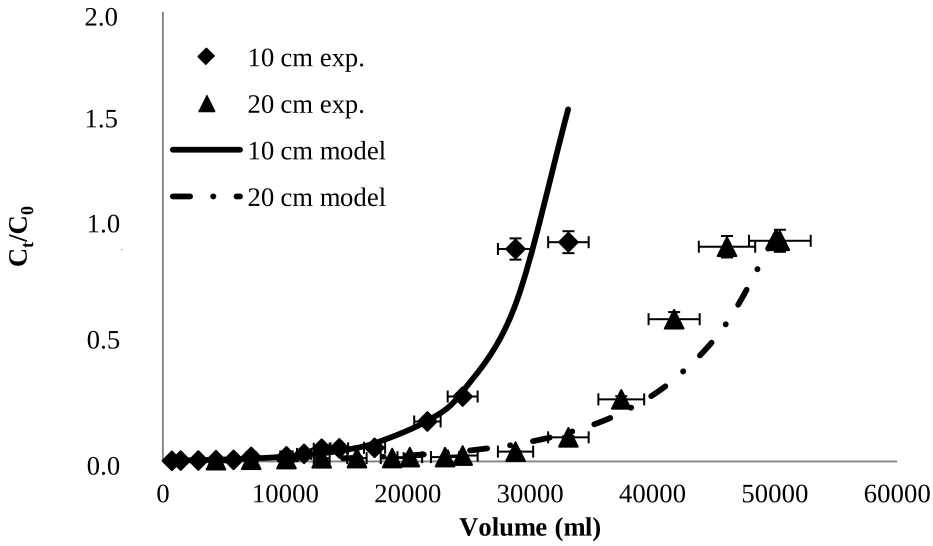

Figure 5.87 Experimental and simulating breakthrough curves for different bed depths (modified sepiolite-B&A model)

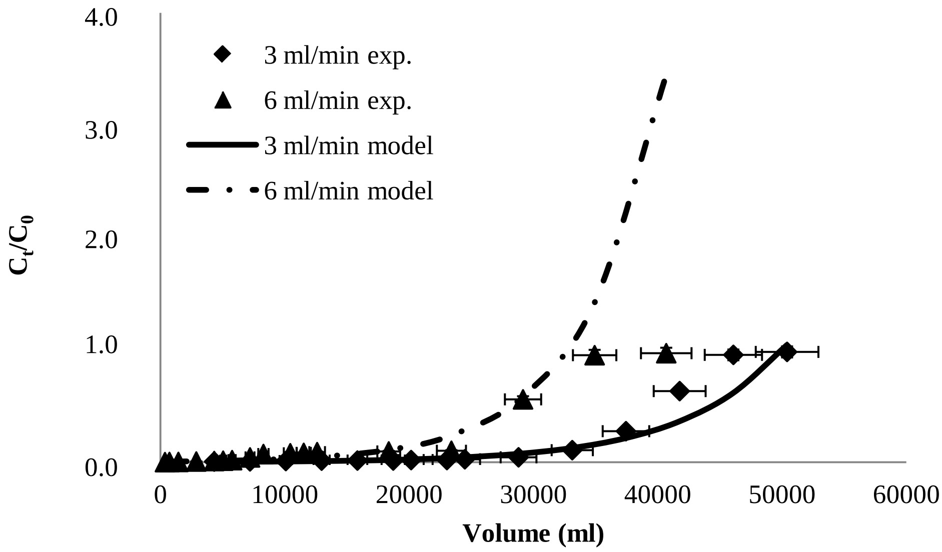

Figure 5.88 Experimental and simulating breakthrough curves for different flow rates (modified sepiolite-B&A model)

5.7 Effect of Column Regeneration on Adsorption Performance

For any adsorption process, regeneration capacity of the adsorbent is one of the most important factors. Desorption studies were carried out by alkaline solution, i.e. NaOH was used. After the regeneration process, the column was fed with arsenic solution at same conditions (3 ml/min flow rate and approximately 550 µg/L initial arsenic concentration) in order to determine its reuse potential. Figure 5.89 shows variation of effluent arsenic concentrations for regenerated sand column after the first use. The results revealed that approximately 1.4 L water could be treated below 10 µg/L after first regeneration. Then, effluent concentration rapidly increased and reached to 440 µg/L. Therefore, the column exhausted at 4.3 L of treated water volume; and effluent concentrations were nearly reached to influent concentration. The volume of the treated water after first regeneration was almost equal to former use of sand column. The breakthrough curve of sand column after first regeneration is depicted in Figure 5.90.

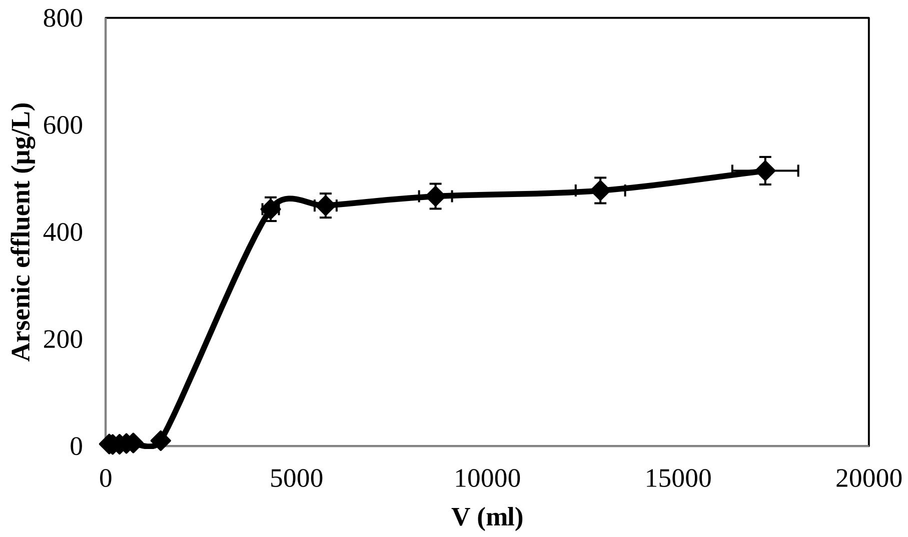

Figure 5.89 Arsenic effluent concentrations of regenerated sand column for first use (As_{in}=560µg/L, 10 cm column height)

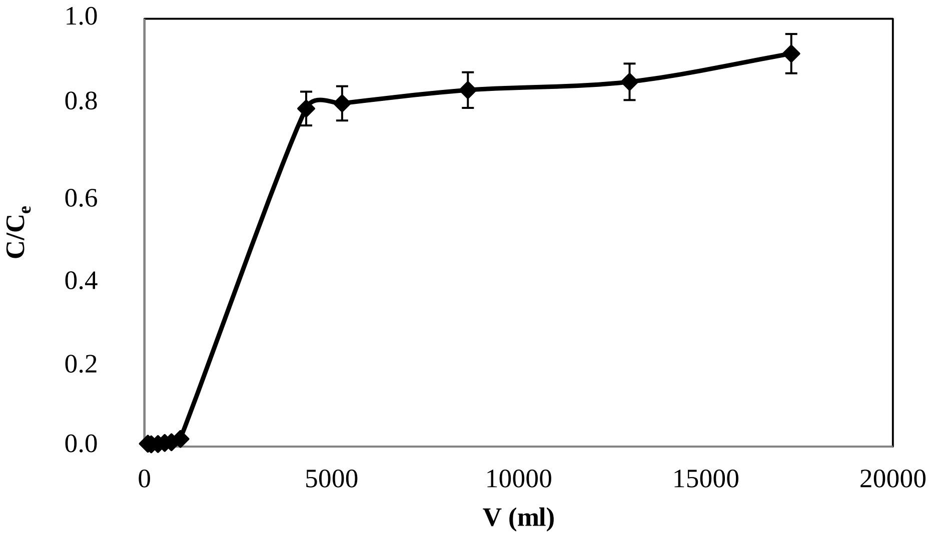

Figure 5.90 The breakthrough curve of sand column after first regeneration

Following to first regeneration, desorption studies were repeated; and column was fed with arsenic containing water. Regeneration and operation processes were the same as first regeneration at same conditions. Figure 5.91 shows variation of arsenic effluent for modified sand column after second regeneration. The volume of the water decreased significantly and 200 ml of feed water could be treated to desired limit. At exhausted point, the amount of water passing through the column was 13 L.

Figure 5.92 shows breakthrough curve of sand column after second regeneration. As seen in Figure 5.92, breakthrough point of (C/C_e) was 0.02 at 200 ml water volume. Approximately, 13 L water treated before exhausting point of C/C_e=0.95.

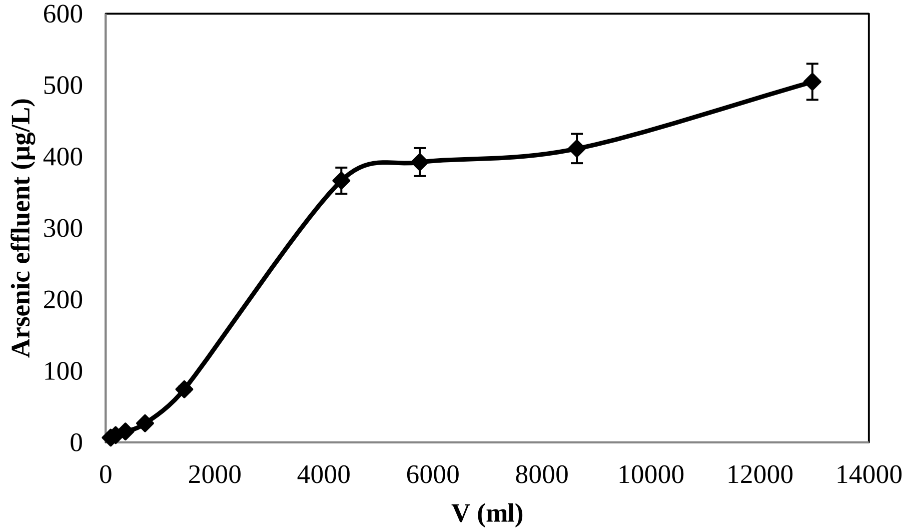

Figure 5.90 Arsenic effluent concentrations of regenerated sand column for second use (As_{in}=530µg/L, 10 cm column height)

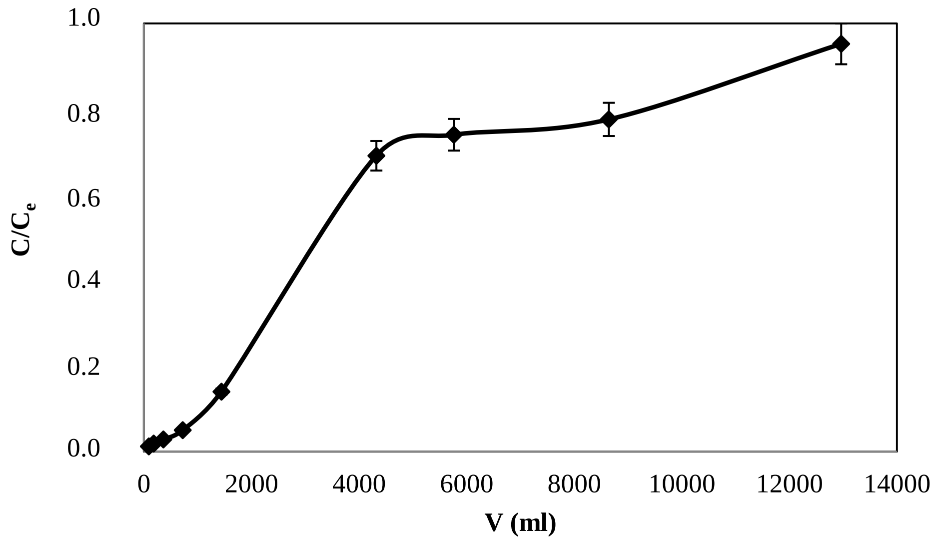

Figure 5.91 The breakthrough curve of sand column after second regeneration

On the other hand, modified sepiolite column could not be regenerated by same process like modified sand. Acid regeneration caused fouling due to decay of sepiolite structure. Therefore, modified sepiolite column could not be reused for arsenic adsorption.

CHAPTER SIX
CONCLUSIONS

In this thesis, arsenic adsorption performance of two natural materials via iron modification and also two commercial adsorbents were investigated and compared. In this scope, batch experiments were performed in order to obtain optimum adsorption parameters like pH, contact time, initial concentration, adsorbent dose and adsorbent size and existing ions in water. In this way, isotherm studies were conducted and adsorption capacities of the adsorbents calculated. Adsorption rates of adsorbents were obtained by kinetic studies. Column studies were performed for modified sand and modified sepiolite and critical operation parameters like flow rate, initial concentration and bed depth were investigated. Kinetic models which can describe the dynamics of adsorption in column were applied in order to design and operate column successfully.

From batch experiment results, it was observed that optimum pH is 7 for all the adsorbents, i.e. modified sand, modified sepiolite and commercial adsorbents. Over 90% removal rate was obtained for approximately 100 µg/L initial arsenic concentration for 2 hours contact time and 5 g/L dose of adsorbent.

Optimum contact time was found 4 hours operation at pH 7 and 5 g/L dose of adsorbent to obtain effluent concentration below 10 µg/L for 100 µg/L initial arsenic concentration. For commercial adsorbents, optimum contact times were 15 minutes for I1 and 2 hours for I2.

Approximately 100 µg/L initial arsenic concentration was optimum concentration to remove arsenic with desired level (<10 µg/L) at pH 7, 4 hours of contact time and 5 g/L dose of adsorbent for modified sand and modified sepiolite, however commercial adsorbents were less sensitive to initial concentration and about 1500 µg/L and 250 µg/L initial concentrations could be treated below <10 µg/L at same conditions by I1 and I2, respectively.

Optimum dose was 5 g/L for modified sand, modified sepiolite and commercial adsorbent (I2) at pH 7, 4 hours of contact time and 100 µg/L initial arsenic concentration. Whereas, 1 g/L dose of adsorbent was capable to remove arsenic for commercial adsorbent (I1) at same conditions.

In the range of 710-1000 µm particle size of adsorbents were successfully remove arsenic at pH 7, for 4 hours of contact time and 100 µg/L initial arsenic concentration for modified sand and modified sepiolite.

Arsenic removal rates, in case of existing competing ions (using groundwater) were obtained 41.9% and 77.4% for modified sand and modified sepiolite, respectively, at pH 7, for 4 hours of contact time and 100 µg/L initial arsenic concentration. Especially bicarbonate ions in groundwater affected arsenic removal significantly for both modified materials.

Adsorption mechanisms were best described by Freundlich isotherm for modified sand and by Langmuir isotherm for modified sepiolite. Adsorption capacities were calculated through these isotherms and obtained 0.117 mg/g and 0.501 mg/g for modified sand and modified sepiolite, respectively. Adsorption rate of adsorbents fitted well with pseudo second order reaction kinetic model for both modified sand and modified sepiolite.

Column experiments were performed using optimum parameters in batch experiments; pH of the solution (pH 7) and particle size of the adsorbents (710-1000 µm). Column experiments indicated that column utilization is more effective at low initial concentration (~100 µg/L) and low flow rate (3 ml/min), and higher bed height (20 cm) for modified sand and modified sepiolite. For modified sand, at 20 cm bed depth and for 115 µg/L initial arsenic concentration, approximately 13 L water could be treated at breakthrough point with desired levels (<10 µg/L). At same conditions, 43 L water could be effectively treated below10 µg/L by modified sepiolite.

Column design parameters were evaluated for initial concentration, depth and flow rate parameters by applying Thomas model and Bohart&Adams model to experimental data. Both of the models fitted well with approximately 90% coefficient of determination for modified sand and modified sepiolite. At 3ml/min flow rate and 20 cm bed depth with an initial concentration about 100 µg/L, Thomas model parameters; Thomas rate constants, k_{Th} and adsorption capacities, $q_{0,}$ obtained 0.342 L/min mg and 0.0017 mg/g for modified sand, and 0.176 L/min mg and 0.010 mg/g for modified sepiolite, respectively. At same conditions, Bohart&Adams model parameters, Bohart&Adams rate constants, k_{BA} and adsorption capacities, N, obtained 0.250 L/mg min and 3.615 mg/L for modified sand and 0.105 L/mg min and 6.264 mg/L for modified sepiolite, respectively.

Acid regeneration and then reuse of the modified sand column could be possible one more time with negligible efficiency loss. However, second reuse after regeneration caused 85% less water was treated with desired levels. Modified sepiolite could not be regenerated by same method because of the column clogging due to destroying structure of the material; therefore, reuse of the column was not possible.

Experimental results show that iron modified sand and sepiolite are high-performance materials to remove arsenic from water by adsorption with recommended values by WHO. Adsorption is a simple method and its ease of operation makes it favourable treatment option especially for rural remote areas where used highly arsenic contaminated groundwater. Sand is naturally available and can be supplied from rivers, seas or quarries from all over the world, so it is also cost efficient. Sepiolite has quite much more adsorption capacity then sand due to its porous structure; therefore, it is lightweight contrast to sand and also high-strength material for column operation. Most of the sepiolite reserves are in Turkey in the world, thus, modified sepiolite as an adsorbent can be produced with our country’s sources and will be a cost efficient adsorbent, as well.

Recommendations for future studies:

- Different modification methods, like thermal process or thin film processes can be tried in order to increase adsorption capacity of materials.
- Different porous materials which have high surface area can be modified and used for adsorption.
- Lab-scale column studies may conduct with larger column diameter to evaluate surface hydraulic loading and can be carried out pilot scale operation.
- Column studies may perform using groundwater in order to determine effect of competing ions.
- Columns can be operated in series and in this wise, utilization of column can be compared.

REFERENCES

Alpaslan, M.N., Dölgen, D., Boyacıoğlu H., & Sarptaş, H. (2010). İçme suyundan kimyasal yöntemlerle arsenik giderimi. *Su Kirlenmesi Kontrolü, İTÜ Dergisi, 20* (1): 15-25.

Ansari, R. & Sadegh, M. (2007). Application of activated carbon for removal of arsenic ions from aqueous solutions. *Journal of Chemistry, 4*, 103-108.

ATSDR (2007). *Public health statement for arsenic*. Retrieved August 21, 2016 from https://www.atsdr.cdc.gov/phs/phs.asp?id=18&tid=3.

Attinti, R., Sarkar, D., Barrett, K.R.,& Datta, R. (2015). Adsorption of arsenic(V) from aqueous solutions by goethite/silica nanocomposite. *International Journal of Environmental Science and Technology, 12,* 3905–3914.

Baba, A. & Sozbilir H. (2012). Source of arsenic based on geological and hydrogeochemical properties of geothermal systems in Western Turkey. *Chemical Geology, 334,* 364–377.

Bailey, R. P., Bennett, T., & Benjamin, M. M. (1992). Sorption onto and recovery of Cr(VI) using iron-oxide-coated sand. *Water Science and Technology, 26*(5-6), 1239-1244.

Bohart, G.S.,& Adam, E.Q. (1920). Some aspects of the behavior of charcoal with respect to chlorine. *Journal of the American Chemical Society, 42* (3), 523–544.

Boparai, H., Joseph, M., & O'carroll, D. (2011). Kinetics and thermodynamics of cadmium ion removal by adsorption onto nano zerovalent iron particles. *Journal of Hazardous Materials, 186,* 458–465.

Chen, A.S., Sorg, T.J., & Wang, L. (2015). Regeneration of iron-based adsorptive media used for removing arsenic from groundwater. *Water Research 77*, 85-97.

Clifford D.A., Sorg T.J., & Ghurye G.L. (2011). *Ion exchange and adsorption of inorganics contaminants water quality and treatment, a handbook on drinking water*. Denver: AWWA.

Devi, R.R., Umlong, I.M., Das, B. Borah K., Thakur A.J., Raul P.K., Banerjee S., & Singh L.(2014). Removal of iron and arsenic (III) from drinking water using iron oxide-coated sand and limestone. *Applied Water Science, 4*, 175.

Dixit, S., & Hering, J. G. (2003). Comparison of arsenic(V) and arsenic(III) sorption onto iron oxide minerals: Implications for arsenic mobility. *Environmental Science & Technology, 37*(18), 4182-4189.

Edwards, M. (1994). Chemistry of arsenic removal during coagulation and Fe-Mn oxidation. *Journal American Water Works Association, 86*(9), 64-78.

Edwards, M., & Benjamin, M. M. (1989). Adsorptive Filtration Using Coated Sand - a New Approach for Treatment of Metal-Bearing Wastes. *Research Journal of the Water Pollution Control Federation, 61*(9-10), 1523-1533.

Essington, M.E. (2015). *Soil and water chemistry: An integrative approach*, (2nd ed.). Florida: CRC Press.

Feenstra, L., van Erkel, J. & Vasak, L. (2007). *Arsenic in groundwater: Overview and evaluation of removal methods.* Retrieved July 10, 2016, from www.un-igrac.org/download/file/fid/272.

Fendorf, S., Eick, M.J., Gross P., & Sparks, D.L. (1997). Arsenate and chromate retention mechanisms on goethite. 1. surface structure. *Environmental Science & Technology , 31* (2), 315–320.

Gang, D.D., Deng, B.L., & Lin, L.S. (2010). As(III) removal using an iron-impregnated chitosan sorbent. *Journal of Hazardous Materials*, *182*, 156-161.

Goldberg, S., & Johnston, C. T. (2001). Mechanisms of arsenic adsorption on amorphous oxides evaluated using macroscopic measurements, vibrational spectroscopy, and surface complexation modeling. *Journal of Colloid and Interface Science. 234*(1), 204-216.

Goldberg, S. (2002). Competitive adsorption of arsenate and arsenite on oxides and clay minerals. *Soil Science Society of America Journal*, *66*, 413–421.

Ghosh, D., & Gupta A. (2012). Economic justification and eco-friendly approach for regeneration of spent activated alumina for arsenic contaminated groundwater treatment *Resources, Conservation and Recycling*, *61* (1), 118–124.

Guo, X. J., Du, Y. H., Chen, F. H., Park, H. S., & Xie, Y. N. (2007). Mechanism of removal of arsenic by bead cellulose loaded with iron oxyhydroxide (beta-FeOOH): EXAFS study. *Journal of Colloid and Interface Science*, *314*(2), 427-433.

Gupta, V. K., Saini, V. K., & Jain, N. (2005). Adsorption of As(III) from aqueous solutions by iron oxide-coated sand. *Journal of Colloid and Interface Science, 288*(1), 55-60.

Jeon, C. S., Baek, K., Park, J. K., Oh, Y. K., & Lee, S. D. (2009). Adsorption characteristics of As(V) on iron-coated zeolite. *Journal of Hazardous Materials, 163*(2-3), 804-808.

Johnston, R., Heijnen H. & Wurzel P. (2001). *Chapter 6: safe water technology*. Retrieved July 10, 2016 from http://www.who.int/water_sanitation_health/dwq/arsenicun6.pdf.

Joshi, A., & M.Chaudhuri, (1996). Removal of arsenic from ground water by iron oxidecoated sand. *ASCE Journal of Environmental Engineering, 122*(8), 769-771.

IARC (n.d.). *Arsenic and arsenic compounds.* Retrieved July 30, 2016 from http://monographs.iarc.fr/ENG/Monographs/vol100C/mono100C-6.pdf.

Isa, M. H., Lang, L. S., Asaari, F. A. H., Aziz, H. A., Ramli, N. A.,& Dhas, J. P. A.(2007). Low cost removal of disperse dyes from aqueous solution using palm ash [J]. *Dyes and Pigments, 74*(2), 446–453.

Kundu, S., & Gupta, A. K. (2007). Adsorption characteristics of As(III) from aqueous solution on iron oxide coated cement (IOCC). *Journal of Hazardous Materials, 142*(1-2), 97-104.

Li, Y. R., Wang, J., Luan, Z. K., & Liang, Z. (2010). Arsenic removal from aqueous solution using ferrous based red mud sludge. *Journal of Hazardous Materials, 177*(1-3), 131-137.

Li, Z. H., Jean, J. S., Jiang, W. T., Chang, P. H., Chen, C. J., & Liao, L. B. (2011). Removal of arsenic from water using Fe-exchanged natural zeolite. *Journal of Hazardous Materials, 187*(1-3), 318-323.

Maji, S. K., Kao, Y. H., & Liu, C. W. (2011). Arsenic removal from real arsenic-bearing groundwater by adsorption on iron-oxide-coated natural rock (IOCNR). *Desalination, 280* (1-3), 72-79.

Maji, S. K., Kao, Y. H., Wang, C. J., Lu, G. S., Wu, J. J., & Liu, C. W. (2012). Fixed bed adsorption of As(III) on iron-oxide-coated natural rock (IOCNR) and application to real arsenic-bearing groundwater. *Chemical Engineering Journal, 203*, 285-293.

Maliyekkal, S.M.& Philip, L. (2011). Fixed-bed adsorption of arsenite (As(III)) from drinking water: breakthrough studies and modeling; *Proceedings of the 3rd International CEMEPE & SECOTOX Conference.* Skiathos.

Martinez-Cabanas, M., Carro, L., Lopez-Garcia, M., Herrero, R., Barriada, J. L., & de Vicente, M. E. S. (2015). Achieving sub-10 ppb arsenic levels with iron based biomass-silica gel composites. *Chemical Engineering Journal, 279*, 1-8.

Mercado-Borrayo, B.M., Schouwenaars, R., Litter, M.I., Montoya-Bautista, C.V. , & Ramírez-Zamora, R.M.(2014). *Metallurgical Slag as an Efficient and Economical Adsorbent of Arsenic.* S. Ahuja, (Ed.) Water Reclamation and Sustainability (95-114). Boston: Elsevier.

Mohan D. & Pittman C.U. (2007). Arsenic removal from water/wastewater using adsorbents – A critical review. *Journal of Hazardous Materials, 142* (1–2), 1–53.

Mondal, P., Majumder, C. B., & Mohanty, B. (2008). Effects of adsorbent dose, its particle size and initial arsenic concentration on the removal of arsenic, iron and manganese from simulated ground water by Fe3+ impregnated activated carbon. *Journal of Hazardous Materials, 150*(3), 695-702.

Mostafa, M. G., Chen, Y. H., Jean, J. S., Liu, C. C., & Lee, Y. C. (2011). Kinetics and mechanism of arsenate removal by nanosized iron oxide-coated perlite. *Journal of Hazardous Materials, 187*(1-3), 89-95.

Nguyen, T. V., Vigneswaran, S., Ngo, H. H., & Kandasamy, J. (2010). Arsenic removal by iron oxide coated sponge: Experimental performance and mathematical models. *Journal of Hazardous Materials, 182*(1-3), 723-729.

Odesola, I. F. & Adebayo J.(2010). Solar adsorption technologies for ice – making and recent developments in solar technologies: A review. *International Journal of Advanced Engineering Technology,1* (3), 284-303.

Satpathy, J. K., & Chaudhuri, M. (1995). Treatment of Cadmium-Plating and Chromium-Plating Wastes by Iron Oxide-Coated Sand. *Water Environment Research, 67*(5), 788-790.

Sengupta research (n.d.). *Regeneration and reuse of sorbent media*. Retrieved July 20, 2016 from https://senguptaresearch.web.lehigh.edu/sites/senguptaresearch.web.lehigh.edu/files/REGENERATION.pdf.

Tchobanoglous, G. and Burton, F. L.(1991). *Wastewater engineering: treatment, disposal and reuse* (3rd ed.). New York: Metcalf & Eddy, Inc., McGraw-Hill.

Thakur, J.K., Thakur, R.K., Ramanathan, A., Kumar, M. & Singh, S.K. (2011). Arsenic contamination of groundwater in Nepal—An overview. *Water*, *3* (1), 1-20.

Thirunavukkarasu, O. S., Viraraghavan, T., & Subramanian, K. S. (2001). Removal of arsenic in drinking water by iron-oxide coated sand and ferrihydrite – Batch studies. *Water Quality Research Journal of Canada, 36* (1), 55–70.

Thomas, H.C. (1944).Heterogeneous ion exchange in a flowing system. *Journal of the American Chemical Society*, *66* (10), 1664–1666.

Vitela-Rodriguez, A. V., & Rangel-Mendez, J. R. (2013). Arsenic removal by modified activated carbons with iron hydro(oxide) nanoparticles. *Journal of Environmental Management*, *114*, 225-231.

US EPA (1997). *Exposure factors handbook (1997 final report)*. EPA/600/P-95/002F a-c. Washington, DC: US Environmental Protection Agency.

US EPA (2000). *Technologies and costs for removal of arsenic from drinking water*. Washington DC: US EPA Office of Water.

US EPA (2001) *Technical fact sheet: final rule for arsenic in drinking water.* Retrieved July 11, 2016, from http://nepis.epa.gov/Exe/ZyPdf.cgi?Dockey=20001XXE.txt.

US EPA (2002). *Arsenic treatment technology design manual for small systems.* Retrieved May 14, 2016 from https://frtr.gov/pdf/arsenicdesignmanualpeerreviewdraft.pdf.

US EPA (2003). *Design manuel, Removal of arsenic from drinking water by ion exchange*. EPA/600/R-03/080. Washington DC: US Environmental Protection Agency.

US EPA (2003). *Design manuel, Removal of arsenic from drinking water by adsorptive media*. EPA/600/R-03/019. Arizona: US Environmental Protection Agency.

US EPA (n.d). *Drinking water treatability database*. Retrieved July 19, 2016, from https://iaspub.epa.gov/tdb/pages/general/home.do.

US OSHA (2001). *Occupational safety and health guidelines for arsenic, organic compounds.* Washington DC: US Occupational Safety and Health Administration.

Watts, H.D., Tribe, L., & Kubicki, J.D. (2014). Arsenic adsorption onto minerals: connecting experimental observations with density functional theory calculations, *Minerals*, *4*, 208-240.

WHO (1993). *Guidelines for drinking-water quality. Vol. 1. Recommendations* (2nd ed.). Switzerland: World Health Organization.

WHO (2001). *Arsenic and arsenic compounds (Environmental health criteria ; 224)*. Retrieved June 30, 2016, from http://www.inchem.org/documents/ehc/ehc/ehc224.htm.

WHO (2004). *Guidelines for drinking-water quality. Vol. 1. Recommendations*. (3rd ed.). Switzerland: World Health Organization.

WHO (2010). *Exposure to arsenic: a major public health concern*. Retrieved 10.05.2016, from http://www.who.int/ipcs/features/arsenic.pdf.

WHO (2011*). Arsenic in drinking water, background document for development of WHO guidelines for drinking-water quality*. Retrieved June 25, 2016, from http://www.who.int/water_sanitation_health/dwq/chemicals/arsenic.pdf.

World Bank Group (1998). *Pollution prevention and abatement handbook-toward cleaner production*. Washington DC: World Bank Group.

Wilkie, J.A. & Hering, J.G. (1996). Adsorption of arsenic onto ferric hydroxide: effects of adsorbate/adsorbent ratios and co-occurring solutes. *Colloids and Surfaces A, 107*, 97–110.

Yang, C.H. (1998). Statistical mechanical study on the freundlich isotherm equation. *Journal of Colloid Interface Science, 208*, 379–387.

APPENDICES

APPENDICE 1: THOMAS MODEL (MODIFIED SAND)

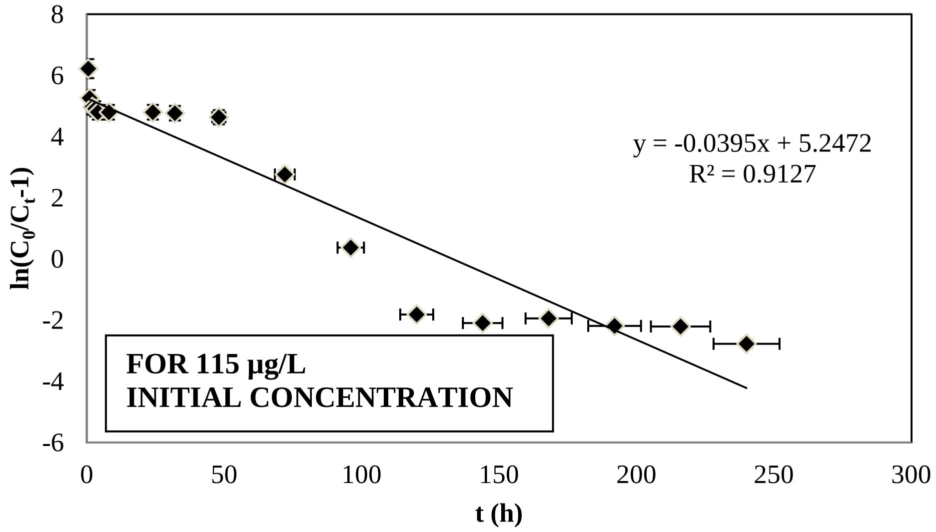

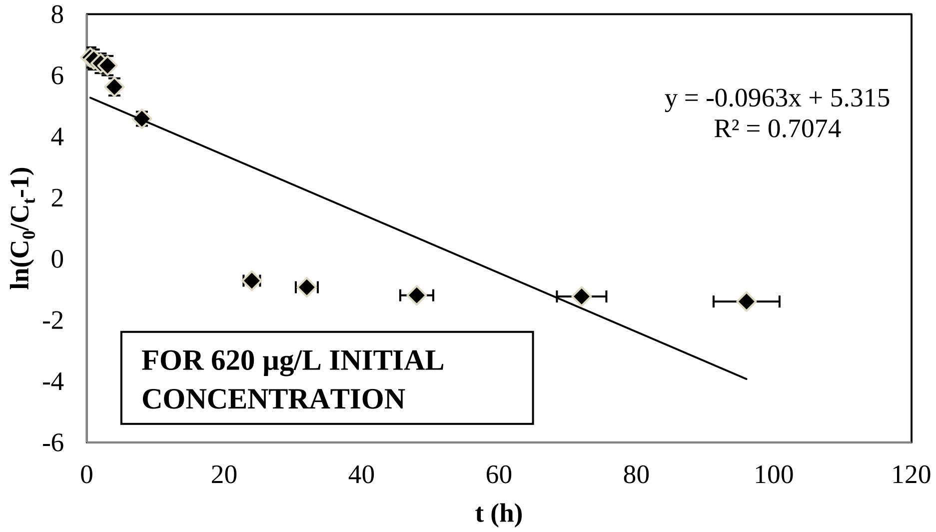

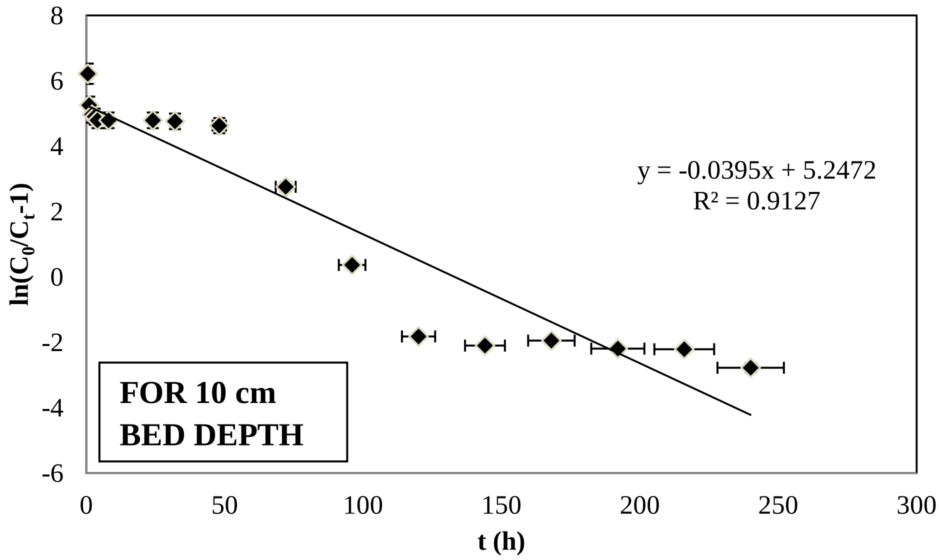
y = -0.0395x + 5.2472
R² = 0.9127
FOR 10 cm
BED DEPTH
ln(C0/Ct-1)
t (h)

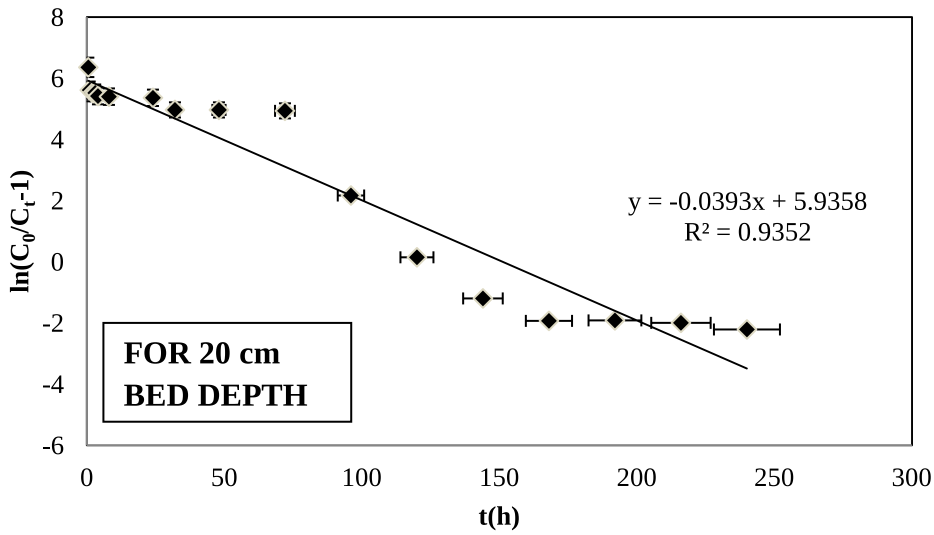
y = -0.0393x + 5.9358
R² = 0.9352
FOR 20 cm
BED DEPTH
ln(C0/Ct-1)
t(h)

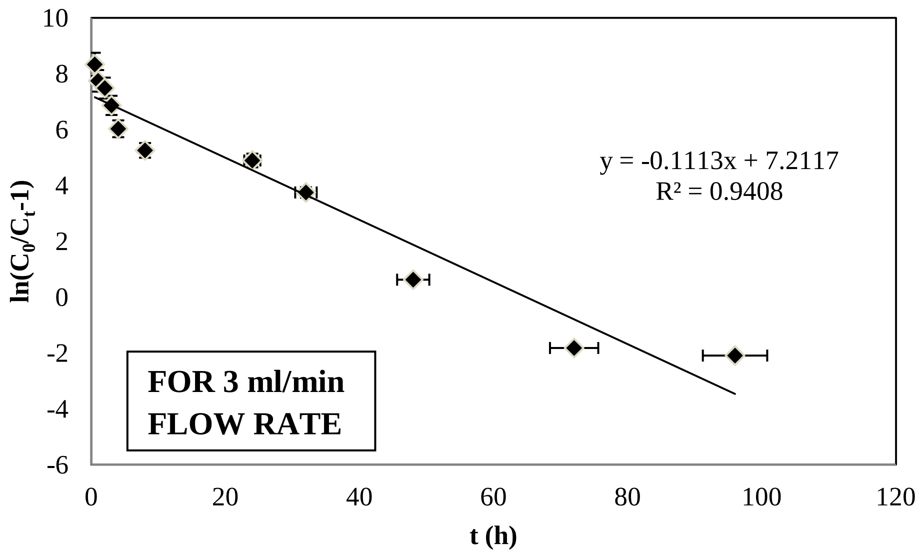

10
8
6
4
2
0
-2
-4
-6
0
20
40
60
80
100
120
ln(C0/Ct-1)
t (h)
y = -0.1113x + 7.2117
R² = 0.9408
FOR 3 ml/min
FLOW RATE

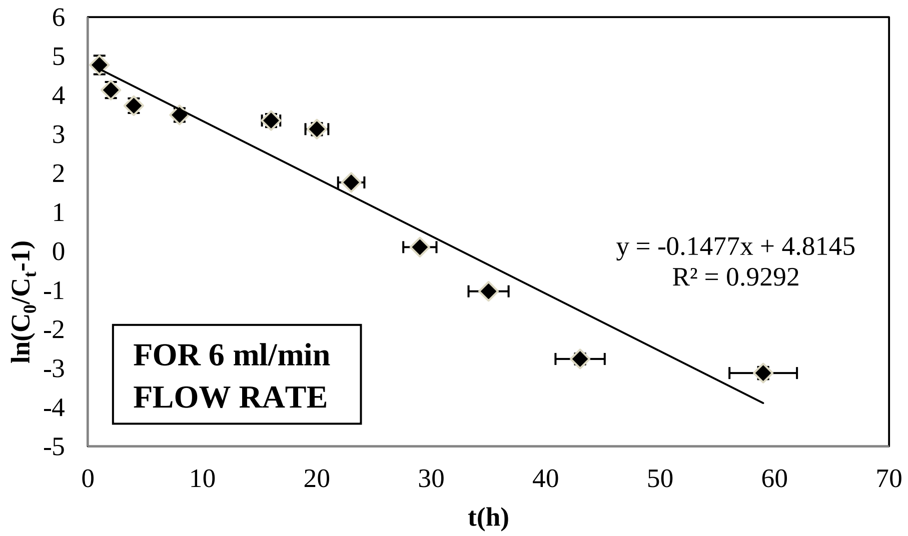

6
5
4
3
2
1
0
-1
-2
-3
-4
-5
0
10
20
30
40
50
60
70
ln(C0/Ct-1)
t(h)
y = -0.1477x + 4.8145
R² = 0.9292
FOR 6 ml/min
FLOW RATE

APPENDICE 2: THOMAS MODEL (MODIFIED SEPIOLITE)

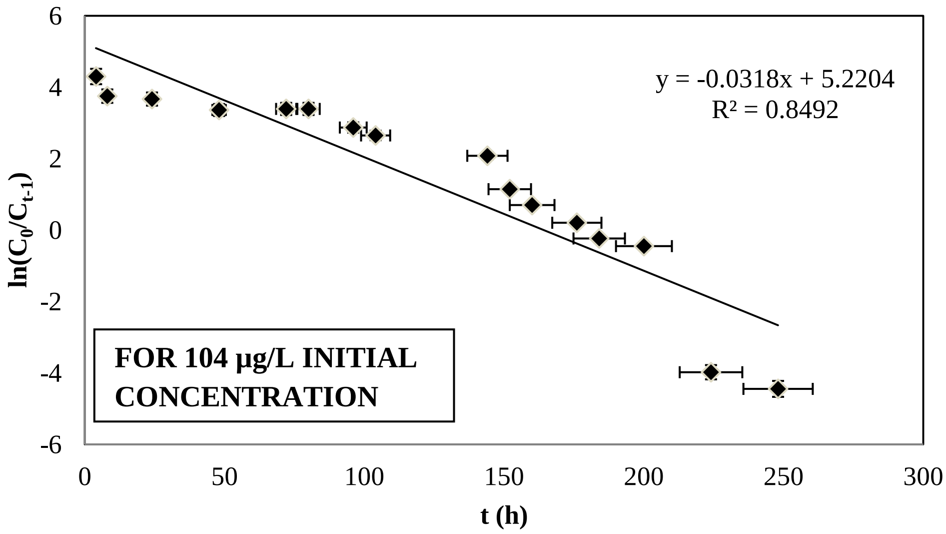

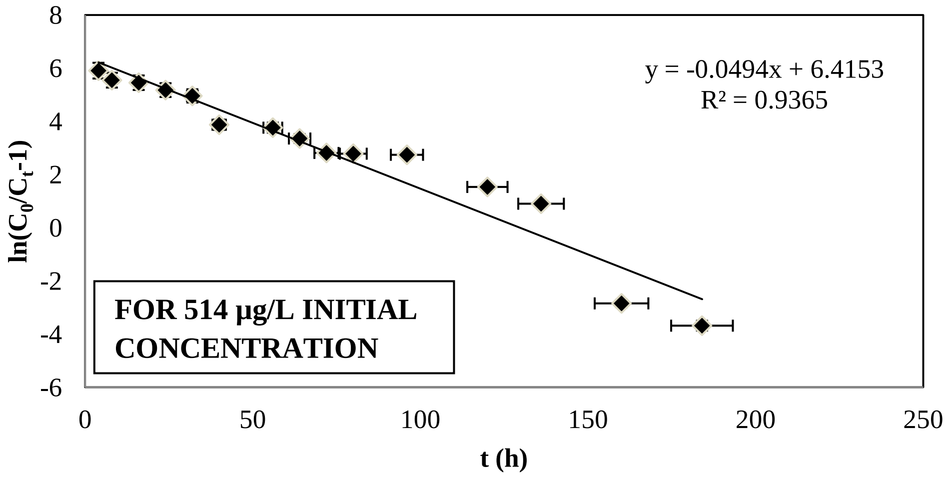

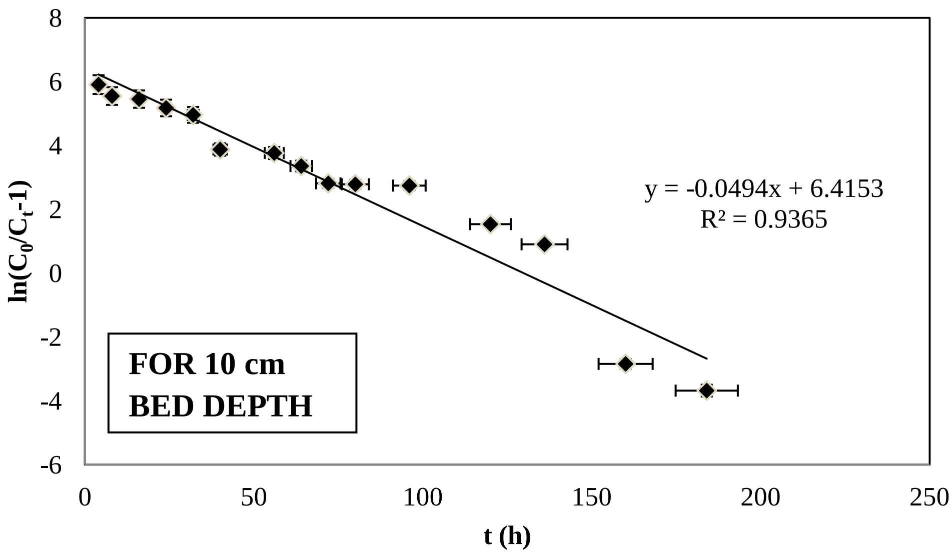

y = -0.0494x + 6.4153
R² = 0.9365
FOR 10 cm
BED DEPTH
ln(C0/Ct-1)
t (h)

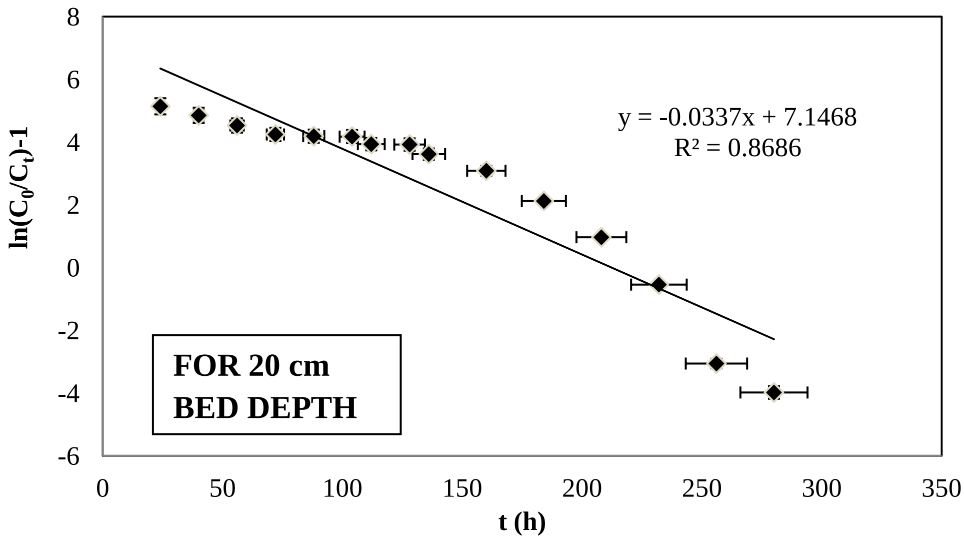

y = -0.0337x + 7.1468
R² = 0.8686
FOR 20 cm
BED DEPTH
ln(C0/Ct)-1
t (h)

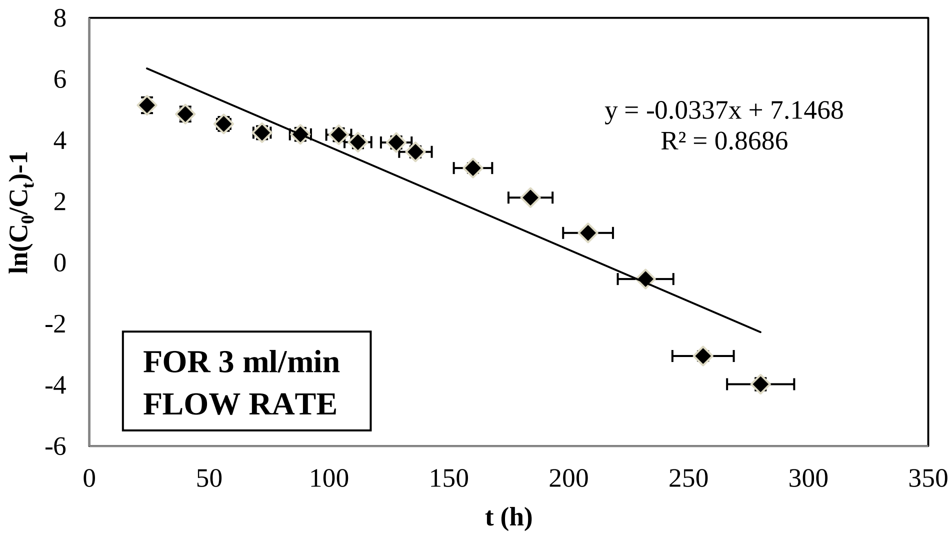
y = -0.0337x + 7.1468
R² = 0.8686
FOR 3 ml/min
FLOW RATE
ln(C0/Ct)-1
t (h)

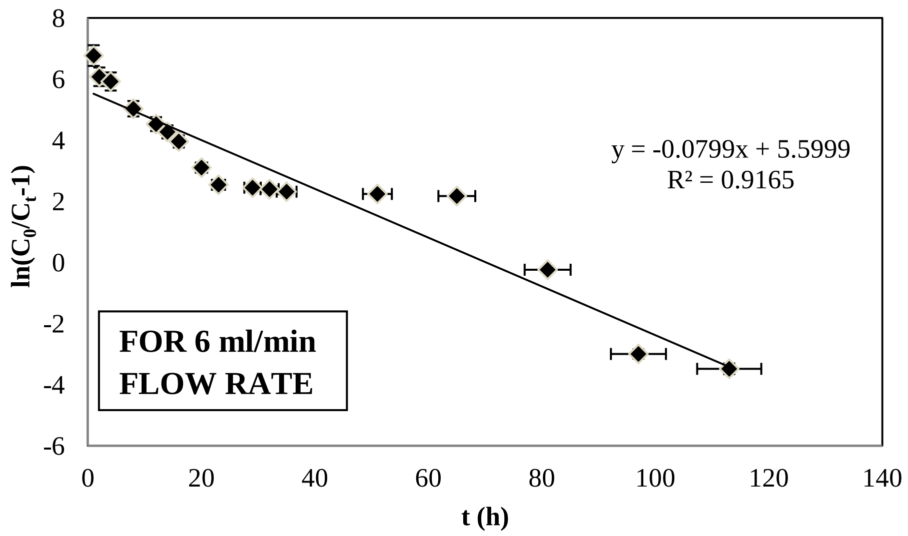
y = -0.0799x + 5.5999
R² = 0.9165
FOR 6 ml/min
FLOW RATE
ln(C0/Ct-1)
t (h)

APPENDICE 3: B&AMODEL (MODIFIED SAND)

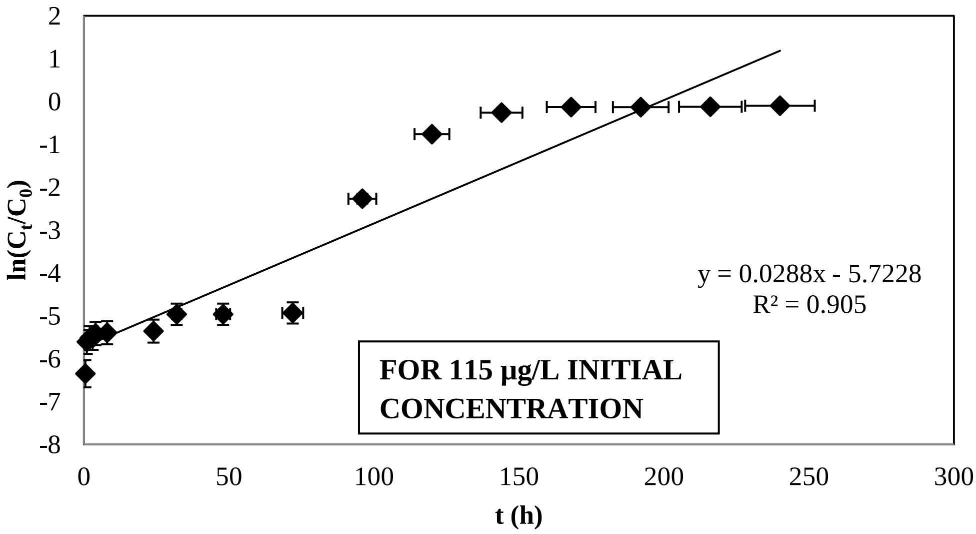

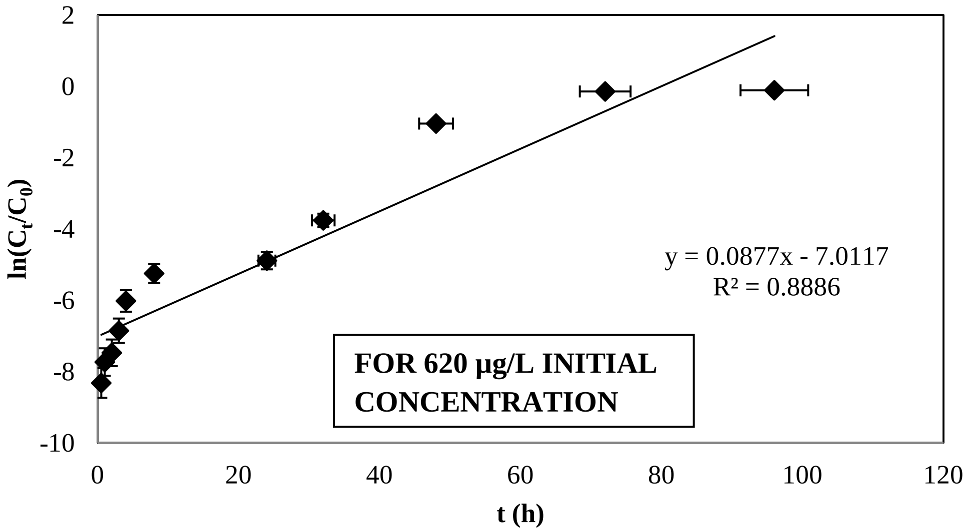

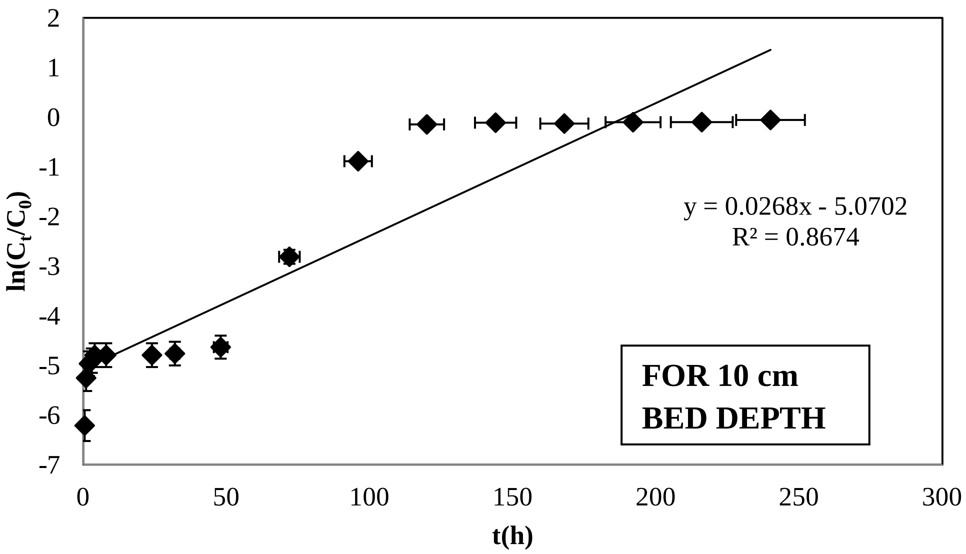

y = 0.0268x - 5.0702
R² = 0.8674
FOR 10 cm
BED DEPTH
ln(Ct/C0)
t(h)

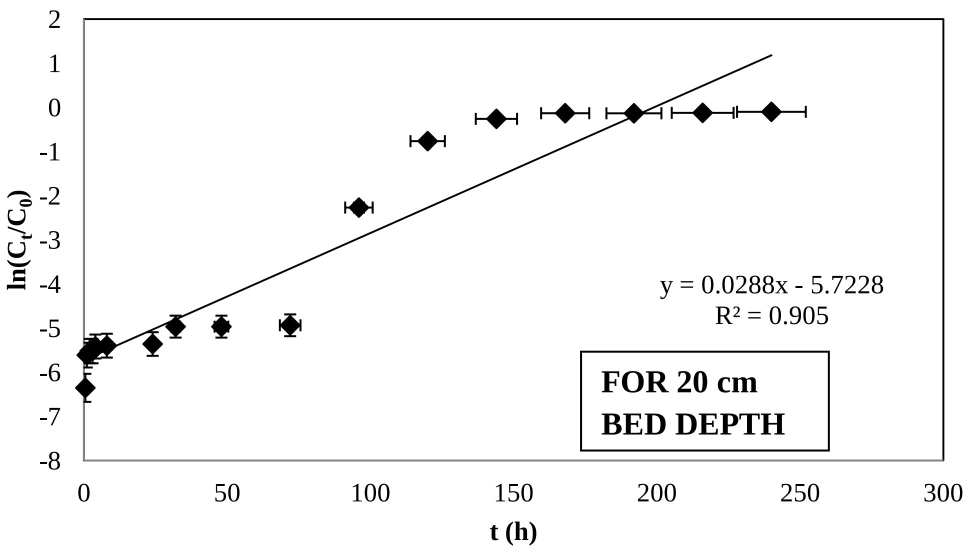

y = 0.0288x - 5.7228
R² = 0.905
FOR 20 cm
BED DEPTH
ln(Ct/C0)
t (h)

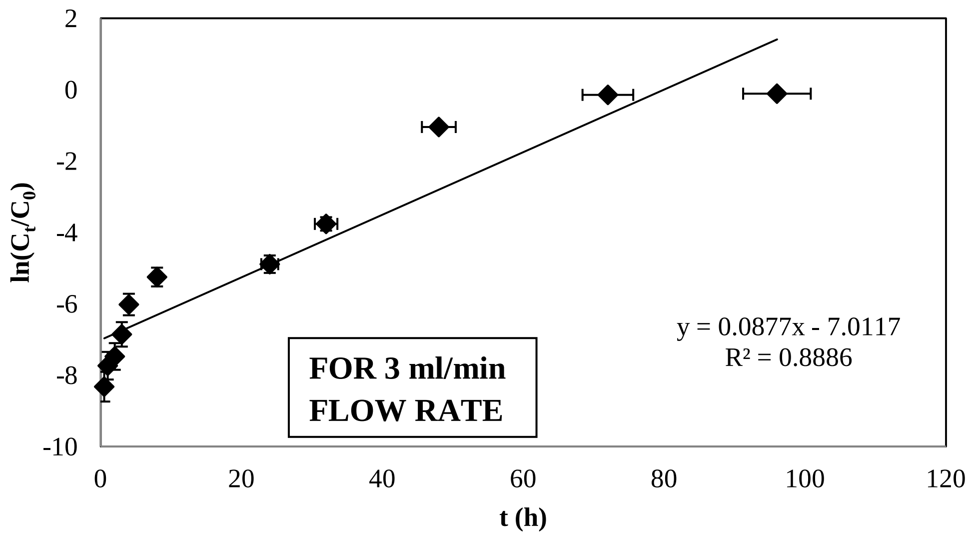

ln(Ct/C0)
t (h)
y = 0.0877x - 7.0117
R² = 0.8886
FOR 3 ml/min
FLOW RATE
2
0
-2
-4
-6
-8
-10
0
20
40
60
80
100
120

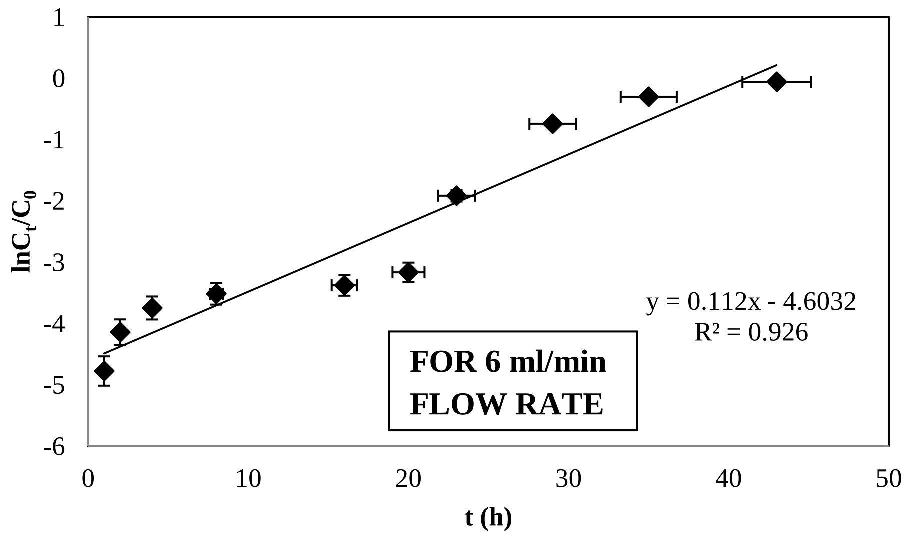

lnCt/C0
t (h)
y = 0.112x - 4.6032
R² = 0.926
FOR 6 ml/min
FLOW RATE
1
0
-1
-2
-3
-4
-5
-6
0
10
20
30
40
50

APPENDICE 4: B&AMODEL (MODIFIED SEPIOLITE)

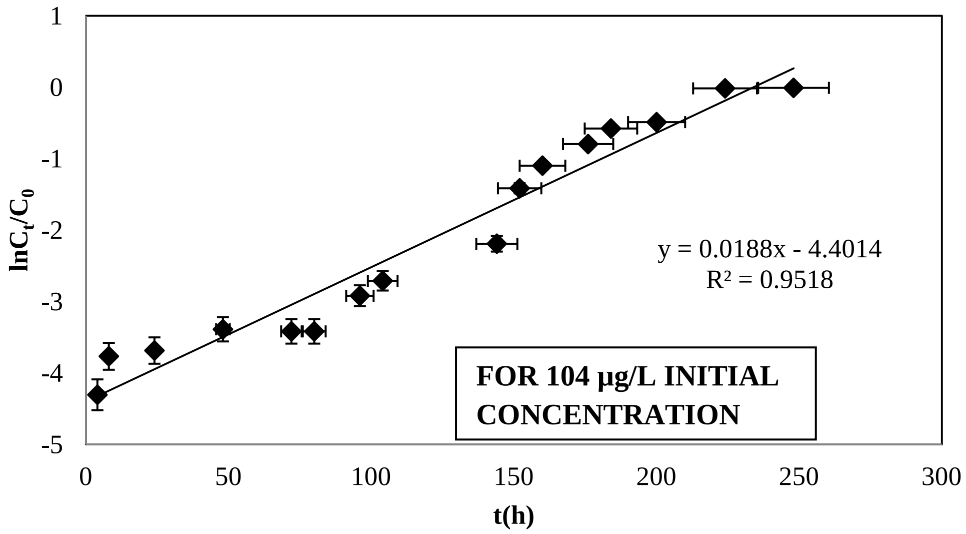

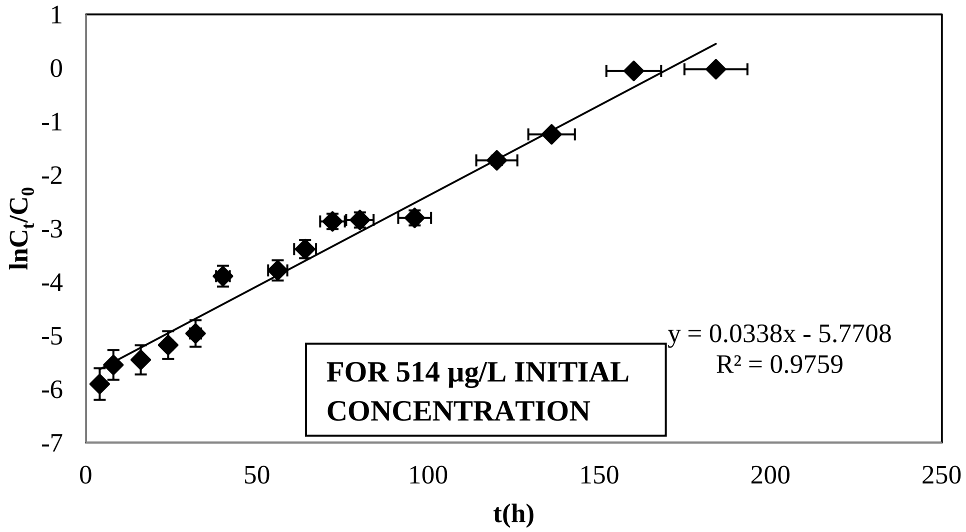

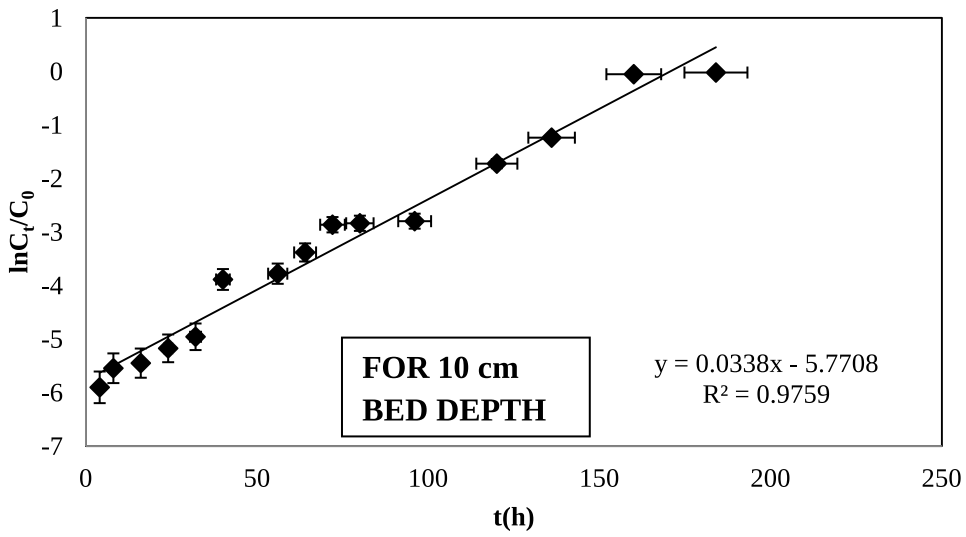

FOR 10 cm
BED DEPTH
y = 0.0338x - 5.7708
R² = 0.9759
lnCt/C0
t(h)

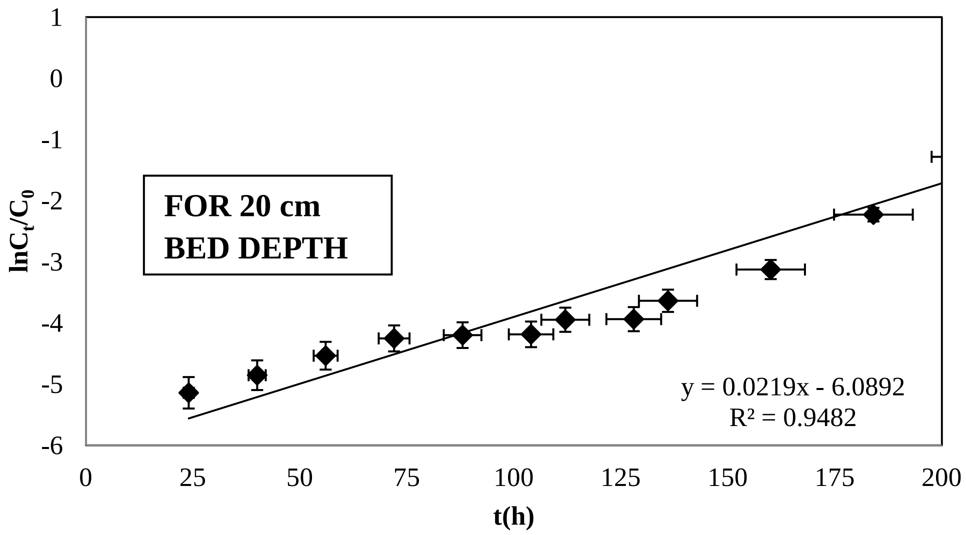

FOR 20 cm
BED DEPTH
y = 0.0219x - 6.0892
R² = 0.9482
lnCt/C0
t(h)

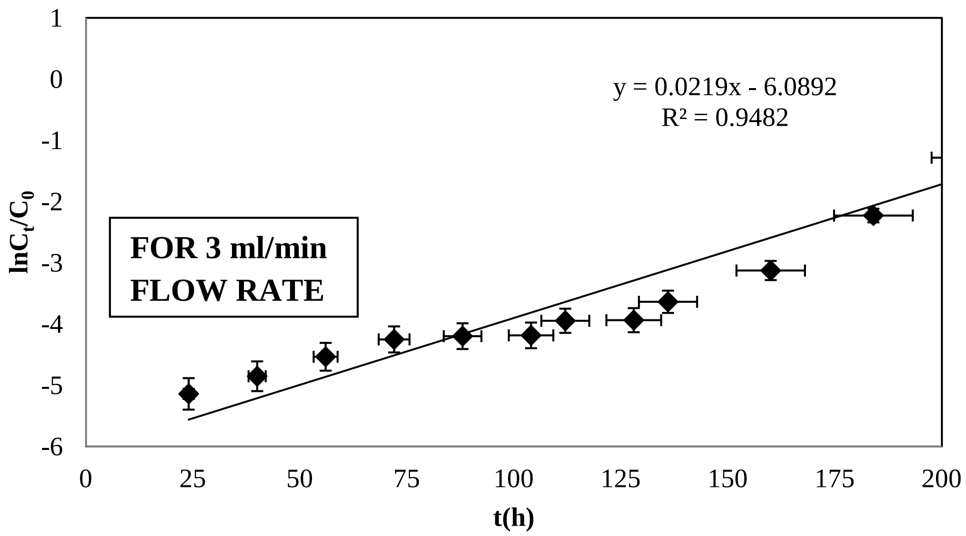
y = 0.0219x - 6.0892
R² = 0.9482
FOR 3 ml/min
FLOW RATE
lnCt/C0
t(h)

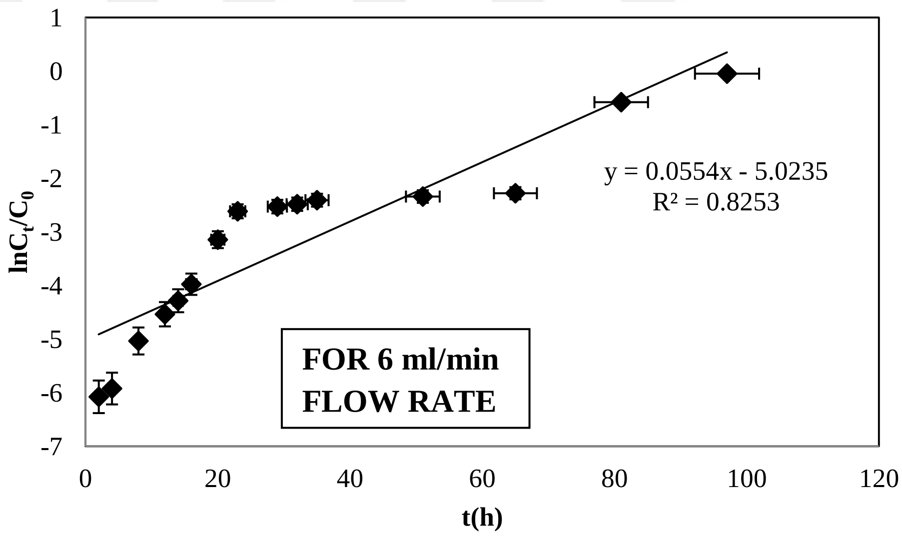
y = 0.0554x - 5.0235
R² = 0.8253
FOR 6 ml/min
FLOW RATE
lnCt/C0
t(h)